

ISSN 1881-7831 Online ISSN 1881-784X

DD & T

Drug Discoveries & Therapeutics

Volume 5 • Number 3 • 2011



www.ddtjournal.com

DD & T

Drug Discoveries & Therapeutics



ISSN: 1881-7831
Online ISSN: 1881-784X
CODEN: DDTRBX
Issues/Year: 6
Language: English
Publisher: IACMHR Co., Ltd.

Drug Discoveries & Therapeutics is one of a series of peer-reviewed journals of the International Research and Cooperation Association for Bio & Socio-Sciences Advancement (IRCA-BSSA) Group and is published bimonthly by the International Advancement Center for Medicine & Health Research Co., Ltd. (IACMHR Co., Ltd.) and supported by the IRCA-BSSA and Shandong University China-Japan Cooperation Center for Drug Discovery & Screening (SDU-DDSC).

Drug Discoveries & Therapeutics publishes contributions in all fields of pharmaceutical and therapeutic research such as medicinal chemistry, pharmacology, pharmaceutical analysis, pharmaceuticals, pharmaceutical administration, and experimental and clinical studies of effects, mechanisms, or uses of various treatments. Studies in drug-related fields such as biology, biochemistry, physiology, microbiology, and immunology are also within the scope of this journal.

Drug Discoveries & Therapeutics publishes Original Articles, Brief Reports, Reviews, Policy Forum articles, Case Reports, News, and Letters on all aspects of the field of pharmaceutical research. All contributions should seek to promote international collaboration in pharmaceutical science.

Editorial Board

Editor-in-Chief:

Kazuhisa SEKIMIZU
The University of Tokyo, Tokyo, Japan

Co-Editors-in-Chief:

Xishan HAO
Tianjin Medical University, Tianjin, China
Norihiro KOKUDO
The University of Tokyo, Tokyo, Japan
Yun YEN
City of Hope National Medical Center, Duarte, CA, USA

Chief Director & Executive Editor:

Wei TANG
The University of Tokyo, Tokyo, Japan

Managing Editor:

Hiroshi HAMAMOTO
The University of Tokyo, Tokyo, Japan
Munehiro NAKATA
Tokai University, Hiratsuka, Japan

Senior Editors:

Guanhua DU
Chinese Academy of Medical Science and Peking Union Medical College, Beijing, China
Xiao-Kang LI
National Research Institute for Child Health and Development, Tokyo, Japan

Masahiro MURAKAMI
Osaka Ohtani University, Osaka, Japan
Yutaka ORIHARA
The University of Tokyo, Tokyo, Japan
Tomofumi SANTA
The University of Tokyo, Tokyo, Japan
Wenfang XU
Shandong University, Ji'nan, China

Web Editor:

Yu CHEN
The University of Tokyo, Tokyo, Japan

Proofreaders

Curtis BENTLEY
Roswell, GA, USA
Thomas R. LEBON
Los Angeles, CA, USA

Editorial Office

Pearl City Koishikawa 603,
2-4-5 Kasuga, Bunkyo-ku,
Tokyo 112-0003, Japan
Tel: 03-5840-9697
Fax: 03-5840-9698
E-mail: office@ddtjournal.com

Drug Discoveries & Therapeutics

Editorial and Head Office

Pearl City Koishikawa 603, 2-4-5 Kasuga, Bunkyo-ku,
Tokyo 112-0003, Japan

Tel: 03-5840-9697, Fax: 03-5840-9698
E-mail: office@ddtjournal.com
URL: www.ddtjournal.com

Editorial Board Members

Alex ALMASAN
(Cleveland, OH)
John K. BUOLAMWINI
(Memphis, TN)
Shousong CAO
(Buffalo, NY)
Jang-Yang CHANG
(Tainan)
Fen-Er CHEN
(Shanghai)
Zhe-Sheng CHEN
(Queens, NY)
Zilin CHEN
(Wuhan, Hubei)
Chandradhar DWIVEDI
(Brookings, SD)
Mohamed F. EL-MILIGI
(6th of October City)
Hao FANG
(Ji'nan, Shandong)
Marcus L. FORREST
(Lawrence, KS)
Takeshi FUKUSHIMA
(Funabashi, Chiba)
Harald HAMACHER
(Tübingen, Baden-Württemberg)
Kenji HAMASE
(Fukuoka, Fukuoka)
Xiaojiang HAO
(Kunming, Yunnan)
Waseem HASSAN
(Rio de Janeiro)
Langchong HE
(Xi'an, Shaanxi)
Rodney J. Y. HO
(Seattle, WA)
Hsing-Pang HSIEH
(Zhunan, Miaoli)
Yongzhou HU
(Hangzhou, Zhejiang)
Yu HUANG
(Hong Kong)
Hans E. JUNGINGER
(Marburg, Hesse)
Amrit B. KARMARKAR
(Karad, Maharashtra)
Toshiaki KATADA
(Tokyo)

Gagan KAUSHAL
(Charleston, WV)
Ibrahim S. KHATTAB
(Kuwait)
Shiroh KISHIOKA
(Wakayama, Wakayama)
Robert Kam-Ming KO
(Hong Kong)
Nobuyuki KOBAYASHI
(Nagasaki, Nagasaki)
Toshiro KONISHI
(Tokyo)
Chun-Guang LI
(Melbourne)
Minyong LI
(Ji'nan, Shandong)
Jikai LIU
(Kunming, Yunnan)
Xinyong LIU
(Ji'nan, Shandong)
Yuxiu LIU
(Nanjing, Jiangsu)
Hongxiang LOU
(Ji'nan, Shandong)
Ken-ichi MAFUNE
(Tokyo)
Sridhar MANI
(Bronx, NY)
Tohru MIZUSHIMA
(Tokyo)
Abdulla M. MOLOKHIA
(Alexandria)
Yoshinobu NAKANISHI
(Kanazawa, Ishikawa)
Xiao-Ming OU
(Jackson, MS)
Weisan PAN
(Shenyang, Liaoning)
Rakesh P. PATEL
(Mehsana, Gujarat)
Shivanand P. PUTHLI
(Mumbai, Maharashtra)
Shafiqur RAHMAN
(Brookings, SD)
Adel SAKR
(Cairo)
Gary K. SCHWARTZ
(New York, NY)

Brahma N. SINGH
(New York, NY)
Tianqiang SONG
(Tianjin)
Sanjay K. SRIVASTAVA
(Amarillo, TX)
Hongbin SUN
(Nanjing, Jiangsu)
Chandan M. THOMAS
(Bradenton, FL)
Murat TURKOGLU
(Istanbul)
Fengshan WANG
(Ji'nan, Shandong)
Hui WANG
(Shanghai)
Quanxing WANG
(Shanghai)
Stephen G. WARD
(Bath)
Bing YAN
(Ji'nan, Shandong)
Yasuko YOKOTA
(Tokyo)
Takako YOKOZAWA
(Toyama, Toyama)
Rongmin YU
(Guangzhou, Guangdong)
Guangxi ZHAI
(Ji'nan, Shandong)
Liangren ZHANG
(Beijing)
Lining ZHANG
(Ji'nan, Shandong)
Na ZHANG
(Ji'nan, Shandong)
Ruiwen ZHANG
(Amarillo, TX)
Xiu-Mei ZHANG
(Ji'nan, Shandong)
Yongxiang ZHANG
(Beijing)

(As of June 2011)

Editorial

- 107 - 108 **Prospects of cancer biotherapy.**
Xishan Hao

Review

- 109 - 118 **Anti-aging effects of oligomeric proanthocyanidins isolated from persimmon fruits.**
Takako Yokozawa, Young A Lee, Eun Ju Cho, Qi Zhao, Kinzo Matsumoto, Chan Hum Park, Naotoshi Shibahara

Brief Report

- 119 - 124 **A low-dose combination of valsartan and low molecular weight heparin better improved glomerular permeability than did high-dose monotherapy in rats with diabetic nephropathy.**
Bo Jiao, Yahui Zhang, Yanna Cheng, Jianjun Gao, Qingzhu Zhang

Original Articles

- 125 - 129 **Hemocytes and humoral factors in silkworm blood are cooperatively involved in sheep erythrocyte aggregation.**
Katsutoshi Imamura, Kenichi Ishii, Hiroshi Hamamoto, Kazuhisa Sekimizu
- 130 - 135 **Arabino-mycolates derived from cell-wall skeleton of *Mycobacterium bovis* BCG as a prominent structure for recognition by host immunity.**
Masanori Miyauchi, Masashi Murata, Keiko Shibuya, Erina Koga-Yamakawa, Yuko Uenishi, Naoto Kusunose, Makoto Sunagawa, Ikuya Yano, Yasuo Kashiwazaki
- 136 - 143 **Mechanisms of vincristine-induced neurotoxicity: Possible reversal by erythropoietin.**
Lobna A. Kassem, Maha M. Gamal El-Din, Nadia A. Yassin
- 144 - 149 **Antityrosinase and antioxidant activities of essential oils of edible Thai plants.**
Kiattisak Saeio, Wantida Chaiyana, Siriporn Okonogi

CONTENTS

(Continued)

- 150 - 156** **Emulsions and rectal formulations containing myrrh essential oil for better patient compliance.**
*Mohamed Etman, Mohamed Amin, Aly H. Nada, Mohamed Shams-Eldin,
Osama Salama*

Guide for Authors

Copyright

Prospects of cancer biotherapy

Xishan Hao

Co-Editor-in-Chief, Drug Discoveries & Therapeutics



Xishan Hao M.D., FACS

Member, Chinese Academy of Engineering;

President and Professor, Tianjin Medical University;

President and Professor, Tianjin Medical University Cancer Institute and Hospital; President, China Anti-Cancer Association

Biotherapy became recognized as the fourth modality of cancer treatment applied after surgical treatment, radiotherapy and chemotherapy since the Biological Response Modifier (BRM) theory was proposed by Dr. Oldham in the 1980s (1). Cancer biotherapy is a therapeutic method that could prohibit the growth of tumors through mobilizing the host's immune system or *via* the effect of biological agents, thereby regulating the body's biological responses (2). Biotherapy is regarded as the most vigorous and promising strategy among the cancer multimodality treatments in this century due to its advantages of high safety and effectiveness as well as low side-effects (2-4). Treatment methods of biotherapy are emerging with the development of such subjects as immunology, cell biology and molecular biology. Currently, the main approaches of biotherapy include molecule targeted therapy, gene therapy and cell therapy.

Molecule targeted therapy: Targeted therapy is a type of medication that aims at signature molecules over-expressed in tumor cells or unusual molecules in the tumor microenvironment. It interferes with regulation of these molecules or signal transduction pathways closely related with tumor development using selective inhibitors, thereby blocking tumor growth, progression or metastasis (5,6). Targeted drugs include small molecule compounds, monoclonal antibodies, polypeptides, *etc.* Molecule targeted therapy enhances treatment specificity and reduces drug resistance since it targets key molecules or signal transduction pathways involved in tumor development and progression (7). The targeted therapy has achieved important progress and pointed a new way forward, and is one of the most popular fields in anticancer research at present.

Since the approvals of two monoclonal antibody drugs trastuzumab (Herceptin) and rituximab (Rituxan) for treatment of metastatic breast carcinoma and diffuse large-B-cell lymphoma, respectively, in 1997, the period of history of molecule targeted therapy is less than 15 years.

Thus far, more than 10 molecule targeted drugs applied in solid tumor treatment and several such drugs employed in hematological malignancy remedies have been approved for cancer therapy (8).

Research and development of novel molecule targeted drugs is extensively carried out nowadays. Drugs with startling efficacy have continuously sprung up in the recent two years. As the survival time of patients is the gold standard for evaluating drug efficacy, the value of molecule targeted therapy has two components. On the one side, the five-year survival or cure rate of cancer patients may be raised by using the targeted drugs to reduce tumor cell differentiation or in combination with conventional surgical treatment, radiotherapy and chemotherapy. This category of drugs includes: *all-trans* retinoic acid (for acute promyelocytic leukemia), trastuzumab (for breast carcinoma), rituximab (for lymphoma) and imatinib (for gastrointestinal stromal tumors and chronic myeloid leukemia). On the other side, the targeted therapy may delay tumor progression, thus improving life quality and prolonging the lifetime of patients. Along with the advancing research, the clinical value of molecule targeted therapy will be enriched and expanded.

Gene therapy: Gene therapy is a biomedical technique that overcomes genetic defects or exerts therapeutic effects *via* transduction of normal or therapeutic genes into targeted cells in certain ways, thus achieving the purpose of treatment of diseases (9). The limitations of conventional cancer therapies such as surgical treatment, radiotherapy and chemotherapy have prompted searching for novel treatments. With the in-depth understanding of molecular mechanisms involving in tumor development and progression, it was realized that tumors are genopathies from the viewpoint of genetics. Correcting genetic defects may offer a new hope for cancer management.

There are two key issues that should be resolved in gene therapy. First comes the screening of the potential

genes and subsequent is the control of the safety of vectors. Based on the therapeutic strategies, the targeted genes could be proto-oncogenes or antisense nucleic acid of genes that encode tumor cell autocrine growth factors and their receptors, tumor suppressor genes, immune regulatory factor genes, anti-angiogenesis factor genes, tumor cell suicide genes, antitumor antibody genes, etc. According to the types of vectors, gene therapy has experienced a developing process from naked DNA, non-viral gene delivery systems, to viral gene delivery systems. Up to the present, clinical treatment schemes that use adenovirus as a gene transfer vector are most widely used in gene therapy.

The number of clinical gene therapy programs provided by the journal *J Gene Med* reached 1,537 in May 2009, in which the number of gene therapies for cancer treatment is 993, making up about 2/3 of all projects (10). However, such therapies are mainly in phase I/II clinical trials so far.

Cell therapy: Tumor cellular immunotherapy is a therapeutic method that utilizes biotechnologies and biological agents to separate *in vitro*, activate and reintroduce tumor specific or non-specific effector cells, either autologous or allogenic, into cancer patients (11). Compared with traditional tumor therapies, it mainly focuses on improving the status of low cellular immune function and strengthening the host's antitumor immune response.

Adoptive cellular immunotherapy could be classified into two categories based on the antigen-specificity of the infused cells: non-specific cellular immunotherapy in which the infused cells include lymphokine activated killer cells (LAK), cytokine induced killer cells (CIK) and dendritic cells (DC), and specific cellular immunotherapy in which the infused cells mainly comprise cytotoxic T cells (CTL) and helper T cells (Th).

Up to now, many clinical studies of non-specific adoptive cellular immunotherapy have been performed and achieved some prospective results (12). Sipuleucel-T (Provenge), the first therapeutic cancer vaccine, was approved to treat advanced prostate cancer by the Food and Drug Administration (FDA) on April 29, 2010. The successful development of this drug which took over 20 years opened a new era of cancer immunotherapy. In addition, several phase I/II clinical studies of adoptive cellular immunotherapy based on CIK and DC have attained preliminary results in treatment of metastatic melanoma, liver cancer, metastatic renal cancer, and gastric cancer (13-15).

Specific adoptive cellular immunotherapy based on CTL has been the focus in immunotherapy of solid tumors such as melanoma, gastric cancer, colorectal cancer and liver cancer. Several phase I studies of such therapy have been accomplished (12). However, operative treatment schemes that can be applied in the clinic for cancer treatment are rare so far because of the low inducing efficiency of CTL *in vitro*, the complicated operation, and the long period and quantity limitation of amplification that often defeat the desired results.

Outlook: Biotherapy will be a main direction in cancer therapy in the future. In order to further increase its therapeutic effect in cancer treatment, efforts should be directed to the following aspects. First is the development

of novel approaches of biotherapy to enhance the efficacy. Second is deeply and objectively evaluating the therapeutic effect of biotherapy through making randomized control studies in a large number of patients. Third, since biotherapy is largely adjuvant therapy and demonstrated to have a synergistic effect with conventional radiotherapy or chemotherapy, how to combine biotherapy with these traditional methods to achieve a better therapeutic effect in individualized cancer treatment should be explored in the future. Last, due to large individual differences in the efficacy of biotherapy, searching for biomarkers that could validly predict treatment outcome plays an important role in its clinical application. With the advancement of biotechnology, the means and efficacy of biotherapy will be improved constantly, which may make biotherapy occupy an increasingly important position in a comprehensive cancer treatment system.

References

1. Oldham RK. Biologicals and biological response modifiers: Fourth modality of cancer treatment. *Cancer Treat Rep.* 1984; 68:221-232.
2. Principles of Cancer Biotherapy. 5 ed., Springer Dordrecht Heidelberg London New York, 2009.
3. Song P, Tang W, Tamura S, Hasegawa K, Sugawara Y, Dong J, Kokudo N. The management of hepatocellular carcinoma in Asia: A guideline combining quantitative and qualitative evaluation. *BioSci Trends.* 2010; 4:283-287.
4. Hao XS. Biological therapy: New hope for cancer treatment. *Chinese Medicinal Biotechnology.* 2008; 3:401.
5. Barros Costa RL. Targeted therapy: Comprehensive review. *Am J Hosp Palliat Care.* 2009; 26:137-146.
6. Gao JJ, Xue X, Qu XJ, Tang W. c-Met: A potential therapeutic target for hepatocellular carcinoma. *Drug Discov Ther.* 2011; 5:2-11.
7. Phay JE, Shah MH. Targeting RET receptor tyrosine kinase activation in cancer. *Clin Cancer Res.* 2010; 16:5936-5941.
8. U.S. Food and Drug Administration. <http://www.fda.gov> (accessed April 2011).
9. Zhao Y, Lam DH, Yang J, Lin J, Tham CK, Ng WH, Wang S. Targeted suicide gene therapy for glioma using human embryonic stem cell-derived neural stem cells genetically modified by baculoviral vectors. *Gene Ther.* 2011.
10. In this issue. Gene therapy. *J Gene Med.* 2009; 11:1075-1076.
11. Chow KK, Gottschalk S. Cellular immunotherapy for high-grade glioma. *Immunotherapy.* 2011; 3:423-434.
12. U.S. National Institutes of Health. <http://clinicaltrials.gov> (accessed April 2011).
13. Hui D, Qiang L, Jian W, Ti Z, Da-Lu K. A randomized, controlled trial of postoperative adjuvant cytokine-induced killer cells immunotherapy after radical resection of hepatocellular carcinoma. *Dig Liver Dis.* 2009; 41:36-41.
14. Su X, Zhang L, Jin L, Ye J, Guan Z, Chen R, Guo T. Immunotherapy with cytokine-induced killer cells in metastatic renal cell carcinoma. *Cancer Biother Radiopharm.* 2010; 25:465-470.
15. Jiang JT, Shen YP, Wu CP, Zhu YB, Wei WX, Chen LJ, Zheng X, Sun J, Lu BF, Zhang XG. Increasing the frequency of CIK cells adoptive immunotherapy may decrease risk of death in gastric cancer patients. *World J Gastroenterol.* 2010; 16:6155-6162.

(May 06, 2011)

Review

DOI: 10.5582/ddt.2011.v5.3.109

Anti-aging effects of oligomeric proanthocyanidins isolated from persimmon fruits

Takako Yokozawa^{1,2,*}, Young A Lee¹, Eun Ju Cho³, Kinzo Matsumoto¹, Chan Hum Park¹, Naotoshi Shibahara¹

¹ Institute of Natural Medicine, University of Toyama, Toyama, Japan;

² Organization for Promotion of Regional Collaboration, University of Toyama, Toyama, Japan;

³ Department of Food Science and Nutrition, Pusan National University, Busan, Korea.

ABSTRACT: Senescence-accelerated mouse prone/8 (SAMP8), a murine model of accelerated senescence, shows age-related deficits in learning and memory. The oral administration of oligomers improved spatial and object recognition impairment in SAMP8. The expression of phosphorylated neurofilament-H was significantly elevated in the hippocampal CA1. This indicates that oligomers induce an increase in the density of axons. To investigate the protective mechanisms of oligomers against brain dysfunction with aging, we carried out a receptor tyrosine kinase phosphorylation antibody array, and clarified that the administration of oligomers led to an increase in the phosphorylation of vascular endothelial growth factor receptor (VEGFR)-2, suggesting the neuroprotective role of oligomers. The phosphorylation of VEGFR-2 was more markedly increased in the hypothalamus and choroid plexus than in other brain regions of SAMP8. Memory in oligomer-treated mice was impaired by SU1498, a VEGFR-2-specific antagonist. Elucidating the relationship between memory impairment with aging and VEGFR-2 signaling may provide new suggestions for protection against memory deficit in the aging brain. In addition, we revealed that the administration of oligomers extended the life span of SAMP8. Oligomers elevated SIRT1 expression, which is recognized as an essential factor for life span extension in the brain. However, the administration of oligomers did not induce stereotypical behaviors such as rearing, jumping, or hanging from the lid of a cage, while food restriction increased these frequencies without a significant change in motor function. The present study suggests the promising role of oligomers as an anti-aging agent to extend life span.

Keywords: Oligomer, SAMP8, memory, VEGFR-2, life span, stereotypical behavior

1. Introduction

The senescence-accelerated mouse (SAM), a murine model of accelerated senescence, was developed by Takeda *et al.* (1). The phenotype shows a shortened life span with an acceleration of several distinctive disease processes such as osteoporosis (P6), degenerative joint disease (P3), cataract (P9), hyperinflammation of the lungs (P1), and hearing impairment (P1) (2). One of these strains, SAMP8, was found to have age-related deficits in learning and memory. Numerous age-dependent alterations have been found in the brain of SAMP8, such as cortical atrophy in the pyriform cortex, increased axonal dystrophy in the gracile nucleus, spongiform degeneration in the brainstem reticular formation, periodic acid Schiff-positive granular structures in the hippocampus, β A4 protein-like immunoreactive granular structures in various regions, and blood-brain barrier dysfunction (3). There is increasing evidence showing that SAMP8 has a similar pathology to the human brain in regard to Alzheimer's disease as well as normal aging (2,4). Acetyl-L-carnitine (5), α -lipoic acid (6), and caloric restriction (7) ameliorated memory impairment in SAMP8. Anti-oxidative activity limited to the cerebral cortex was suggested as the underlying mechanism of those treatments (8). Considering neuronal degeneration in various brain regions of SAMP8, amelioration of injury in the cerebral cortex may not be sufficient. Therefore, identifying compounds which improve memory deficits in SAMP8 and analyzing the underlying mechanism other than the anti-oxidative effect are important.

Proanthocyanidins are known as condensed tannins, members of a specific group of polyphenolic compounds, and they have been reported to exhibit powerful antioxidant activity (9,10). Although proanthocyanidin is the most abundant dietary polyphenol, its high-level

*Address correspondence to:

Dr. Takako Yokozawa, Institute of Natural Medicine, University of Toyama, 2630 Sugitani, Toyama 930-0194, Japan.

e-mail: yokozawa@inm.u-toyama.ac.jp

polymerization results in limited absorption *in vivo* (11). We previously isolated oligomeric proanthocyanidins from persimmon peel, which is usually discarded even though it is rich in phenolic compounds (12). The amount of proanthocyanidin in the peel is higher than in the rest of the fruit. It was reported that oligomeric proanthocyanidins (oligomers) isolated from persimmon peel increased the expression of silent information regulator two ortholog 1 (SIRT1), which is recognized as an essential factor in life span extension, in an H₂O₂-induced cellular senescence model. Oligomer treatment also decreased the expression level of 8-hydroxy-2'-deoxyguanosine (8-OHdG), a marker of oxidation in the model (13). In the present study, we hypothesized that the oligomeric form of proanthocyanidins exerts a beneficial effect on memory dysfunction and neuroprotection in the aged brain. Using the SAMP8 model, we investigated the effect of oligomers on spatial and object recognition memory, and the densities of axons, dendrites, and synapses were observed. Furthermore, to evaluate the neuroprotective effect, vascular endothelial growth factor receptor (VEGFR)-2 and its phosphorylation were also investigated. Moreover, we investigated the possibility of oligomers extending the life span of SAMP8 mice. Since dietary restriction extends the life span of rodents, we compared food-restricted with oligomer-treated mice regarding longevity and behavioral characters.

2. Oligomeric proanthocyanidins improve memory and enhance phosphorylation of VEGFR-2 in SAMP8

SAMP8 developed age-related cognitive deficits as early as 4 months and had a short life span relative to SAMR1. SAMP8 show decreased release of acetylcholine and noradrenaline in comparison with age-matched SAMR1 (14,15). Many age-dependent alterations in various brain regions such as the cerebral cortex and hippocampus at an early stage in SAMP8 were suggested as causes of memory deficits (16,17). In the hippocampus, an increase of glial fibrillary acidic protein as an astrocyte marker was observed in the CA1-CA3 regions of SAMP8 compared to age-matched SAMR1, indicating enhanced reactive gliosis in aged SAMP8 (18). Tanaka *et al.* (19) reported severe loss of oligodendrocytes in the hippocampal CA1 of SAMP8 mice. Moreover, neuronal loss and lower expression of glial cell line-derived neurotrophic factor in the hippocampal CA1 associated with memory impairment of SAMP8 were reported (20). Therefore, hippocampal dysfunction of SAMP8 has been considered as a major cause of age-dependent memory impairment in the brain. Various candidate therapeutic agents for memory dysfunction in SAMP8 were reported, such as acetyl-L-carnitine, α -lipoic acid, and Choto-san (a herbal formula), along with caloric restriction (5-7,21). In those studies, oxidative stress was focused on as a cause

of memory impairment of SAMP8, although change of oxidative stress was limited to the cerebral cortex. Additionally, neuronal morphological evaluations were insufficient in those studies.

We previously reported that oligomers attenuated the expression level of 8-OHdG as a DNA damage maker and increased the expression level of SIRT1, which is recognized as an essential factor in lifespan extension in an H₂O₂-induced cellular senescence model (13). These bioactivities were stronger in the oligomer-treated group than the group treated with non-oligomerized proanthocyanidins showing a high-level of polymerization. Aging is a progressive physiological change in an organism that leads to senescence, or a decline in biological functions and the organism's ability to adapt to metabolic stress. The process decreases the prevalence of learning and increases memory deficits. For example, in aged rats, a loss of synapses in the dentate gyrus and an alteration of Ca²⁺ regulation in the CA1 area lead to a decline of synaptic plasticity, resulting in a change in interactions among hippocampal networks and deficits in the storage and retrieval of information regarding spatial organization of the environment (22). Therefore, we expected the anti-aging effect of oligomers to improve age-associated memory impairment. In the present study, oligomers improved spatial memory and object recognition memory in SAMP8. The memory improvements seen in 18-week-old and 38-week-old SAMP8 led to memory levels almost the same as those of SAMR1 (Figures 1 and 2). To investigate neurological changes brought about by the oral administration of oligomers, we carried out an immunohistological analysis in the brain of 59-week-old SAMP8. The oral administration of oligomers increased expression levels of phosphorylated neurofilament-H (p-NF-H), microtubule-associated protein 2 (MAP2), and synaptophysin in the hippocampus, but this was not observed in regions of the cerebral cortex and striatum of SAMP8. In particular, expression of p-NF-H significantly increased in the hippocampal CA1 with oligomer administration (Figure 3). p-NF-H is used as a marker of axons, since the phosphorylated form of NF-H is translocated into axons (23). In the hippocampus of aged mice, fragments of degenerated axons were also increased, although reductions of neuronal numbers were small in this region (24). Axonal termination to the spine is a necessary step for synaptogenesis. Considering synaptic losses in the hippocampal CA1 and CA3 and the parietal cortex in SAMP8 (25), as well as in the hippocampal CA1, CA3, and dentate gyrus in aged rats (26), axonal regeneration is important for improving hippocampal function. Therefore, the increased density of axons in the hippocampal CA1 was suggested to perform a protective role against memory deficit with aging.

Other previous studies suggested that oxidative stress is a major cause of memory impairment in SAMP8. Hippocampus-specific modulation by oligomers is

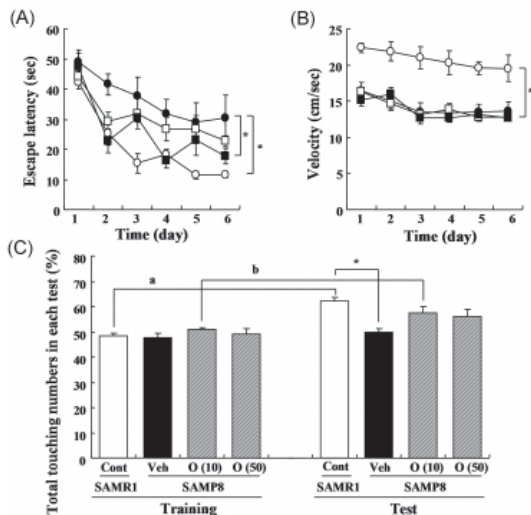


Figure 1. Effects of oligomers on spatial memory deficit in SAMP8. Eighteen-week-old SAMP8 were administered vehicle (Veh, water *p.o.*, $n = 6$; closed circles) or oligomers (10 mg/kg body weight/day, *p.o.*, $n = 6$; open squares) or 100 mg/kg body weight/day, *p.o.*, $n = 5$; closed squares) for 5 weeks. SAMR1 were used as a control (Cont, $n = 5$; open circles). Fifteen days after administration started, memory acquisition tests were continued for 6 days in a Morris water maze. Administration was continued during the tests. Escape latencies to a hidden platform were measured (A). Swimming velocities of mice in the memory acquisition test are shown (B). Thirty-eight-week-old SAMP8 were administered vehicle (Veh, water *p.o.*, $n = 7$) or oligomers (O (10), 10 mg/kg body weight/day, *p.o.*, $n = 7$ or O (50), 50 mg/kg body weight/day, *p.o.*, $n = 7$). Age-matched SAMR1 were used as a control (Cont, $n = 7$). Twenty eight days after administration started, an object location test was performed. The preference index was defined as the number of times a mouse made contact with any one of the objects (training session) or the moved object (test session) out of the total number of times the mouse made contact with both objects (%) (C). * $p < 0.05$ vs. Veh. (A and B: Repeated measures two-way ANOVA followed by Dunnett's or Bonferroni's *post-hoc* test); * $p < 0.05$ (C: One-way ANOVA followed by Bonferroni's *post-hoc* test); ^a $p = 0.0005$; ^b $p = 0.0213$ (C: paired *t*-test).

not explained by an antioxidative effect, since only the cerebral cortex is susceptible to oxidative stress in SAMP8 and not the hippocampus (8). Therefore, to investigate target molecules following the oral administration of oligomers in the brain of SAMP8, we performed a receptor tyrosine kinase phosphorylation antibody array, and clarified that oligomer treatment increased phosphorylation of VEGFR-2 (Figure 4). Expression of VEGFR-2 was identified in the cerebral cortex, hippocampus, and choroid plexus of adults as well as neonatal rodents (27,28). However, the localization of VEGFR-2 in the brain of SAMP8 has yet to be clarified. In the present study, VEGFR-2 expression was also detected in the striatum and hypothalamus of SAMP8, as well as the cerebral cortex, hippocampus, and choroid plexus. In neurons, stimulation by VEGFR-2 among protein tyrosine kinase receptors of VEGF is linked to Akt/protein kinase B activation and neuronal protection in hypoxic preconditioning (29). Moreover, VEGFR-2 mediated a protective effect through phosphatidylinositol-3-kinase/Akt- and mitogen-activated protein/extracellular signal-regulated kinase-signalling pathways in glutamate-

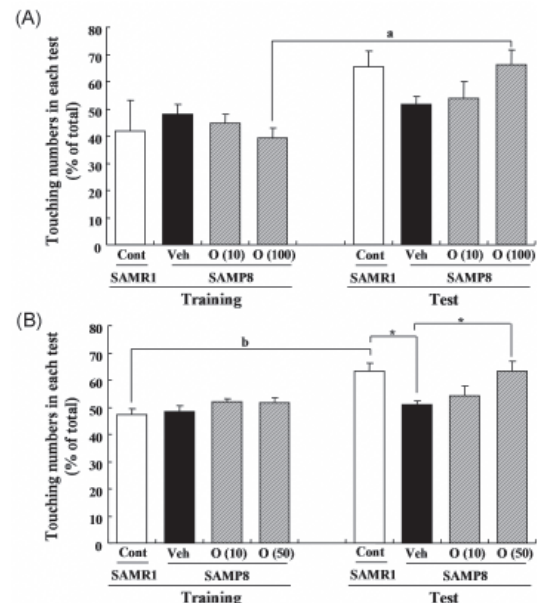


Figure 2. Effects of oligomers on object recognition memory deficit in SAMP8. Eighteen-week-old SAMP8 were administered vehicle (Veh, water *p.o.*, $n = 6$) or oligomers (O (10), 10 mg/kg body weight/day, *p.o.*, $n = 6$ or O (100), 100 mg/kg body weight/day, *p.o.*, $n = 5$). Age-matched SAMR1 were used as a control (Cont, $n = 5$). Twenty four days after administration started, a novel object recognition test was performed (A). Thirty-eight-week-old SAMP8 were administered vehicle (Veh, water *p.o.*, $n = 7$) or oligomers (O (10), 10 mg/kg body weight/day, *p.o.*, $n = 7$ or O (50), 50 mg/kg body weight/day, *p.o.*, $n = 7$). Age-matched SAMR1 were used as a control (Cont, $n = 7$). Twenty three days after administration started, a novel object recognition test was performed (B). The preference index was defined as the number of times a mouse made contact with any one of the objects (training session) or the novel object (test session) out of the total number of times the mouse made contact with both objects (%). * $p < 0.05$ (One-way ANOVA followed by Bonferroni's *post-hoc* test); ^a $p = 0.0174$; ^b $p = 0.0014$ (paired *t*-test).

induced toxicity (30). In particular, the memory enhancement shown by mice injected with recombinant adeno-associated viral vectors expressing human VEGF was inhibited by injection of dominant-negative mutant VEGFR-2 (31). This indicates that VEGF/VEGFR-2 is directly associated with neuronal signaling. VEGF also exerts indirect effects on neurons. Moreover, the topical administration of VEGF to the surface of the brain reduces the infarct size, and intraventricular VEGF enhanced the survival of newly generated neurons in the dentate gyrus and subventricular zones after focal cerebral ischemia (32). In this study, we first showed that memory enhancement through oligomer treatment was eliminated by SU1498 (Figure 5). Considering that VEGF-E-induced memory was also inhibited by SU1498, oligomers or their metabolites may regulate memory by activation of VEGFR-2.

We elucidated that administration of oligomers increased phosphorylation of VEGFR-2 in the hippocampal CA3 regions (Figure 6), suggesting that oligomeric metabolites directly affect the hippocampus, like the VEGFR-2 ligand. It has been reported that

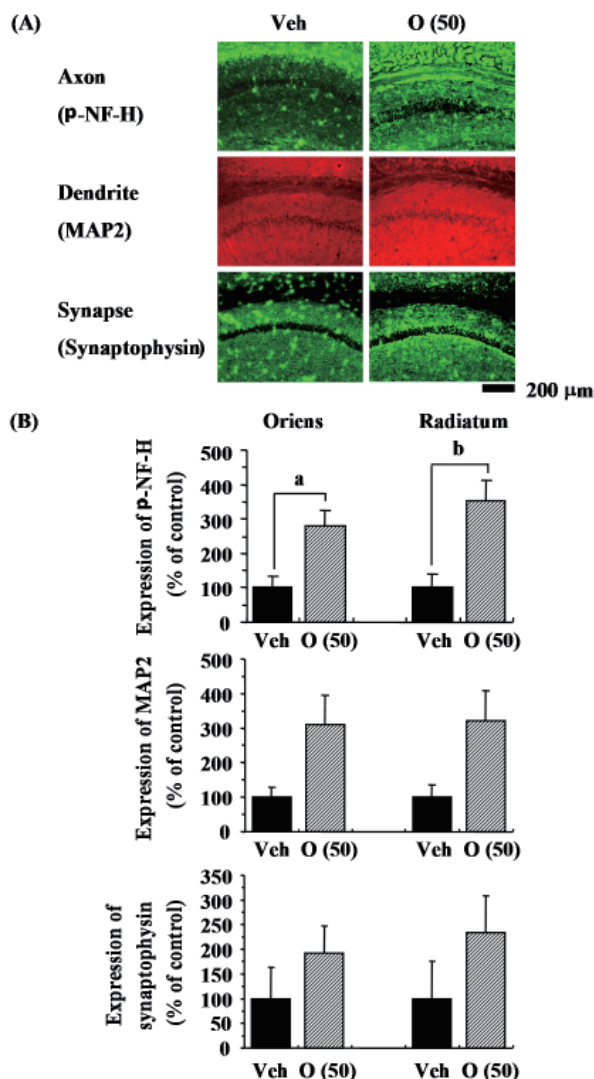


Figure 3. Effects of oligomers on the decrease of axons, dendrites, and synapses in the hippocampal CA1. Fifty-nine-week-old SAMP8 were administered vehicle (Veh, water *p.o.*, $n = 3$) or oligomers (O (50), 50 mg/kg body weight/day, *p.o.*, $n = 3$). After seven days of administration, brain slices were immunostained with p-NF-H, MAP2, and synaptophysin antibodies (A). Intensities of immuno-positive areas in the stratum oriens and stratum radiatum in CA1 were quantified (B). ^a $p = 0.0243$; ^b $p = 0.0344$ (Student's *t*-test).

Ca²⁺ influx and synaptic transmission by VEGF in the hippocampus influences generation of long-term changes in synaptic efficacy (33). VEGF also stimulates neurite outgrowth *via* Rho/Rho kinase signaling in cerebral cortical neurons (34). Interestingly, changes in the synapses and neurites induced by VEGF are caused by activation of VEGFR-2 rather than VEGFR-1. Therefore, we speculated that phosphorylation of VEGFR-2 induced by administration of oligomers within the hippocampus may be related to an increase in densities of neurites and synapses in the hippocampus.

Administration of oligomers increased phosphorylation of VEGFR-2 in the hypothalamus and choroid plexus as well as hippocampus. The hypothalamus is contained in the Papez circuit. The Papez circuit is a sensory circuit involving the thalamus, sensory cortex

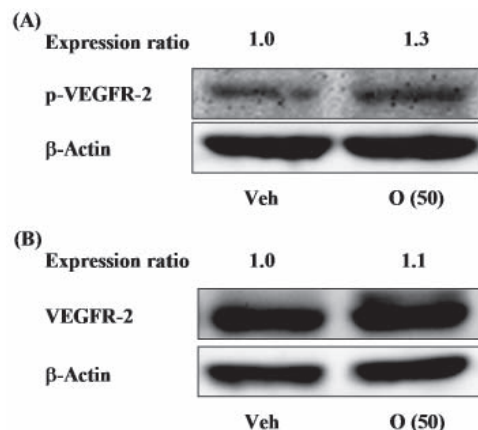


Figure 4. Effects of oligomers on p-VEGFR-2 and VEGFR-2 expressions. Fifty-nine-week-old SAMP8 were administered vehicle (Veh, water *p.o.*) or oligomers (O (50), 50 mg/kg body weight/day, *p.o.*). After seven days of administration, brain lysates were immunoblotted with antibodies for p-VEGFR-2 (A) or VEGFR-2 (B). Expression intensities were divided by β -actin expression to generate ratios.

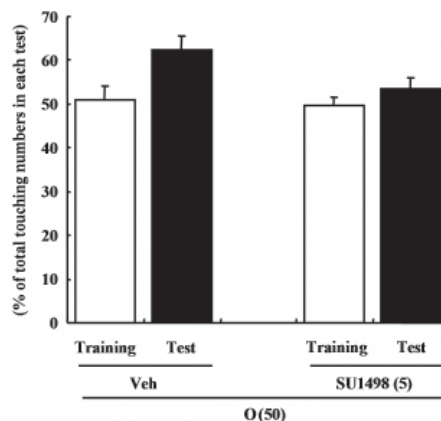


Figure 5. Effects of oligomers and VEGFR-2 on memory. Male ddY mice (6 weeks old) were administered oligomers (O (50), 50 mg/kg body weight/day, *p.o.*, $n = 4$) for 7 days. Then, the vehicle (Veh, 5% DMSO in 0.9% NaCl) was injected intracerebroventricularly at 60 min after the final administration of oligomers. Five days after vehicle injection, SU1498 (5 nmol/ μ L, solution is 5% DMSO in 0.9% NaCl) injected intracerebroventricularly at 60 min after the final administration of oligomers.

(especially the cingulate region), hippocampus, and mammillary body of the hypothalamus (35). It has been reported that lesions in the Papez circuit are associated with amnesia and impairment of recognition memory (36). Therefore, we speculate that the hypothalamus is activated by phosphorylation of VEGFR-2, which may affect the hippocampus through the Papez circuit.

The choroid plexus is made up of numerous villi that project into the ventricles of the brain. Each villus is composed of a single layer of epithelial cells overlying a core of connective tissue and blood capillaries (37). The choroid plexus is involved in the most basic aspects of neural function, including maintaining the extracellular milieu of the brain by actively modulating chemical exchange between the cerebrospinal fluid and brain parenchyma, surveying the chemical and immunological

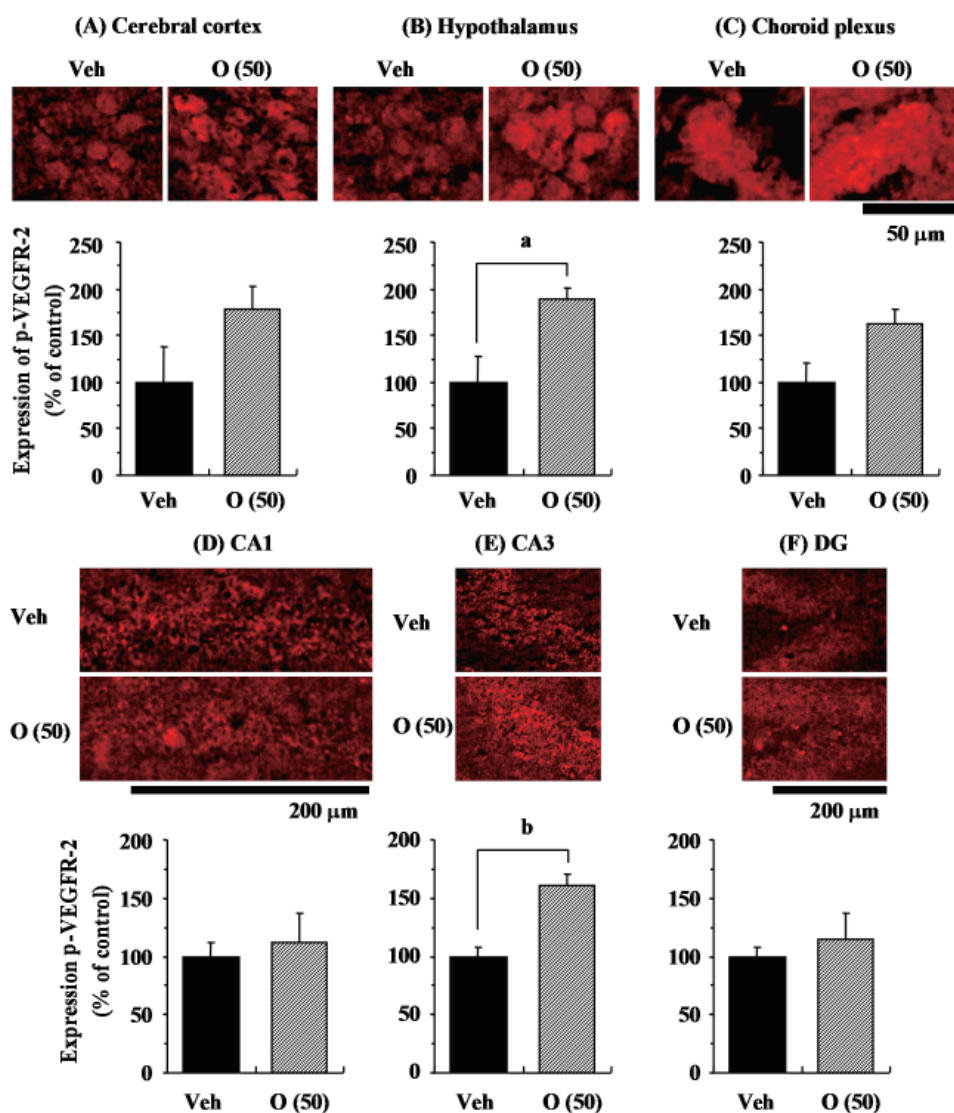


Figure 6. Effects of oligomers on p-VEGFR-2 expression in various brain regions. Fifty-nine-week-old SAMP8 were administered vehicle (Veh, water *p.o.*, $n = 3$) or oligomers (O (50), 50 mg/kg body weight/day, *p.o.*, $n = 3$). After seven days of administration, brain slices were immunostained with p-VEGFR-2 antibody. Intensities of p-VEGFR-2-positive areas were quantified in the cerebral cortex (A), hypothalamus (B), and choroid plexus (C), and CA1 (D), CA3 (E), and dentate gyrus (F) of the hippocampus. ^a $p = 0.0429$; ^b $p = 0.0076$ (Student's *t*-test).

status of the brain, detoxifying the brain, secreting a nutritive cocktail of polypeptides, and participating in repair processes following trauma. This diversity of functions may mean that even modest changes in the choroid plexus can have far-reaching effects (38). Actually, a host of growth factors and other neuroprotective agents supplied by the cerebrospinal fluid can minimize the adverse effects of stroke on the rat hippocampus. Multiple functional failures including a decrease of cerebrospinal fluid as well as atrophy of choroidal epithelial cells shown in normal aging as well as advanced Alzheimer's disease indicate that the maintenance of cerebrospinal fluid through the choroid plexus may have beneficial effects against neurodegenerative diseases (39). Moreover, it was reported that the intracerebroventricular injection of nerve growth factor or insulin-like growth factor-1 improved memory deficit and hippocampal deterioration (40,41). Therefore, we speculate that oligomers induce the

secretion of some peptides after the phosphorylation of VEGFR-2 in the choroid plexus, and then these peptides induce changes in the hippocampus.

We previously elucidated that the oligomers consisted of various combinations of 4 types of monomer: epigallocatechin (EGC), epicatechin (EC), epigallocatechin 3-*O*-gallate (EGCg), and epicatechin 3-*O*-gallate (ECg). Oligomers containing dimers, trimers, and tetramers of EGC, EC, EGCg, and ECg are considered to exert a stronger activity than polymers. de Boer *et al.* (42) demonstrated that ECg and EGCg stimulated SIRT1 more effectively than EC and EGC, since galloyl and catechol groups are essential for the repair of DNA damage. Therefore, the structural difference between oligomers and polymers is considered to be an important factor regarding proanthocyanidin's action, and it also affects utilization in biological systems. It is absorbed through the gut barrier, and its absorption

depends on the degree of polymerization. Low-molecular-weight proanthocyanidins are known as sustained-release antioxidants; on the contrary, high-molecular-weight proanthocyanidins can exert their anti-oxidant activity in the digestive tract and protect lipids, proteins, and carbohydrates from oxidative damage during digestion and spare soluble antioxidants (43). Furthermore, EC and EGCg are distributed in the brain by their absorption into plasma after oral administration, and these monomeric forms may act as potential therapeutic agents in neurodegenerative diseases (44). This suggests that those monomeric forms can act as potential therapeutic agents against neurodegenerative diseases in the brain. In addition, it has been reported that dimers and trimers of proanthocyanidins can be absorbed into epithelial cells such as Caco-2 cells (45), suggesting that oligomers act both oligomerically and monomerically. We must elucidate the similarities and differences in activities and functional mechanisms between oligomers and metabolites including monomers *in vivo*.

3. Oligomeric proanthocyanidins extend life span of SAMP8

Increased longevity is one of the most common desires of human beings. Therefore, research on anti-aging is ultimately focused on life span extension. However, no convincing strategy based on scientific evidence has been suggested, except for dietary restriction (46). Life span extension by dietary restriction has been observed over the years in many species, including rats, mice, hamsters, dogs, fish, invertebrates, and yeast. The inhibition of reactive oxygen molecule formation in isolated mitochondria and microsomes was considered an important mechanism for life span extension in food-restricted rodents (47). In particular, it has been reported that the attenuation of oxidative stress by dietary restriction is involved in the protective role against degenerative diseases related to the aging process such as diabetes, cardiovascular diseases, and neurodegenerative diseases (48). Despite these very encouraging results, clinical application is complex and limited. Regarding this point, although various dietary restriction mimetics, such as glycolytic inhibitors and antioxidants, have been suggested, scientific evidence must be accumulated to support their application (46). For this reason, the search for novel anti-aging agents to elicit the same beneficial effects as caloric restriction without side effects and toxicity has attracted much attention. Recently, we showed that oligomers have more effective anti-aging activities than polymers in a cellular senescence model (13). Although polymers structurally contain many more phenolic groups compared to free radical scavengers than oligomers, oligomers are more easily absorbed than polymers, which is associated with their bioactivity (43).

The administration of oligomers extended life span, as shown in Figure 7. On the other hand, life span does

not extend in response to an increase in oral dose of oligomers. Probably, absorption of proanthocyanidins is related to the effect on life span. Bioactivity of catechin derivatives is related to their structural phenolic groups. Increase in the level of polymerization means a rise in phenolic group content. Previously, we demonstrated that proanthocyanidins showed strong antioxidative activities compared with monomeric catechin derivatives *in vitro* (49). Many researchers have suggested that antioxidative activities are associated with a delay in the aging process and extension of life span in various organisms (50). Actually, we demonstrated that oligomers increased SIRT1 expression, associated with extended longevity, in a cellular senescence model (13). Therefore, we expected oligomeric proanthocyanidins to exert stronger activity to extend life span, compared with monomeric forms such as catechin derivatives. Further study has to be carried out to elucidate differences between monomeric and oligomeric forms.

To elucidate related mechanisms, expression of SIRT1 was observed. Sir2 is an NAD⁺-dependent deacetylase implicated in regulation of lifespan in species as diverse as yeast, worms, and flies (51). Yeast Sir2 is a heterochromatin component that silences transcription at the silent mating loci, telomeres, and ribosomal DNA (52). In addition, it suppresses recombination in rDNA and modulates longevity of most organisms including mammals (53,54). Therefore, the enzymatic activity of Sir2 may indicate its usefulness as an effective

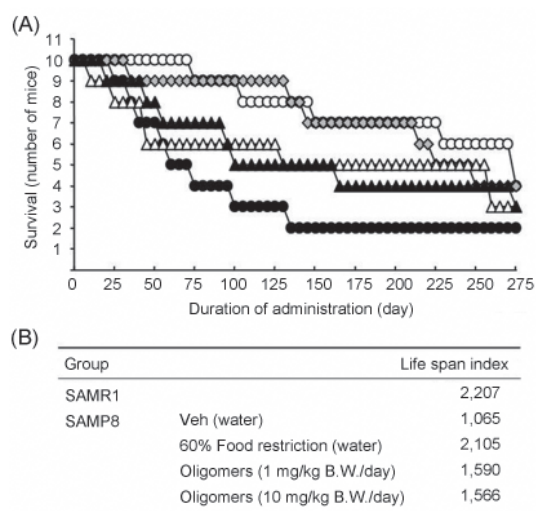


Figure 7. Effects of oligomers on the life span of SAMP8. Forty-five- or forty-six-week-old SAMP8 mice were administered vehicle (Veh, water *p.o.*, $n = 10$), while another two groups were administered oligomers orally at doses of 1 or 10 mg/kg body weight/day ($n = 10$) using a stomach tube until death. For the remaining group of mice, the mean food intake was restricted to 60% until death ($n = 10$). SAMR1 mice (45-46 weeks old, $n = 10$) were used as a control group. (A) Effect of oligomers on survival of SAMP8. (B) Life span index based on survival data. Open circle: SAMR1; Closed circle: SAMP8 (Veh); Open triangle: SAMP8 (oligomers at 1 mg/kg body weight/day); Closed triangle: SAMP8 (oligomers at 10 mg/kg body weight/day); Gray square: SAMP8 (60% food restriction).

caloric restriction mimetic (55). Among the seven mammalian homologues of Sir2, SIRT1 is the human orthologue of yeast Sir2, and the best-characterized member of mammalian sirtuins. Recently, we showed that pretreatment with oligomers significantly increased SIRT1 expression in a cellular senescence model (13). Therefore, in the present study, we investigated the effect of oligomers on the expression of SIRT1 in the SAM model.

Resveratrol, as an activator of SIRT1, has been reported to extend the fitness and survival of simple organisms such as *Saccharomyces cerevisiae* (56,57) as well as mice fed high-calorie diets (58,59). Moreover, we previously clarified that oligomers increased SIRT1 expression in a cellular senescence model (13). Therefore, the effect of oligomers on SIRT1 was compared with resveratrol *in vivo*. We expected administration of oligomers to also increase expression and activation of SIRT1 in the brain to slow aging-related deteriorations of SAMP8. In this study, the administration of oligomers slightly elevated SIRT1 expression in the brain of SAMP8, whereas resveratrol did not show a significant effect (Figure 8). On the other hand, another report demonstrated that acetylated p53, a well-characterized target of SIRT1 deacetylase activity, is decreased by resveratrol treatment (60).

We previously elucidated that oligomers reversed up-regulation of oxidative stress-related gene expression such as inducible nitric oxide synthase and cyclooxygenase-2 in type 1 and 2 diabetic rodent models (61,62). In addition to activation of SIRT1, attenuation of oxidative stress would play a crucial role in the anti-aging effect of oligomers. Since oxidative stress plays an important role in modulation of life span in SAMP8, the antioxidative

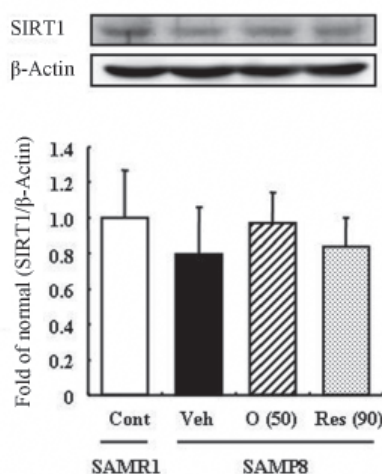


Figure 8. Effects of oligomers on SIRT1 expression in the brain of SAMP8. Forty-five-week-old SAMP8 were administered vehicle (Veh, water *p.o.*, $n = 5$), oligomers (O (50), 50 mg/kg body weight/day, *p.o.*, $n = 5$), or resveratrol (Res (90), 90 μ mol/kg body weight/day, *p.o.*, $n = 5$). Five weeks after administration, brain lysates were immunoblotted with antibodies for SIRT1. SIRT1 expression intensities were divided by β -actin expression. SAMR1 were used as a control (Cont, $n = 4$).

effects of oligomers may also be involved with life span extension in SAMP8.

Dietary restriction as an effective method for the extension of longevity has also been reported to induce stereotypical behaviors such as rearing and jumping independent of life span (63). In behavioral analyses, we showed that rearing, jumping, and hanging from the lid of the cage in 60% food-restricted SAMP8 markedly increased compared with vehicle-treated SAMP8. Surprisingly, oligomer-treated SAMP8 did not show an increase in these stereotypical behaviors (Figure 9). Moreover, in the inclined plane and voluntary running tests performed to observe differences in motor function, we found no significant difference in motor function among all SAMP8 groups (Figure 10). These results indicate that stereotypical behaviors shown in the 60% food-restricted group have no relation with motor function. It has been reported that dietary restriction may induce anxiety-like behavior by down-regulation of corticotrophin-releasing factor (64). Diet-restricted rats showed stereotypy by an increase of dopamine receptor signaling (65). Chen *et al.* (63) demonstrated that stereotypical behaviors brought about by caloric restriction were eliminated in SIRT1-knockout mice, indicating that SIRT1 activation may cause stereotypical behaviors with dietary restriction. In our study, although life span was extended by oligomers as well as 60% food restriction, mice administered oligomers did not

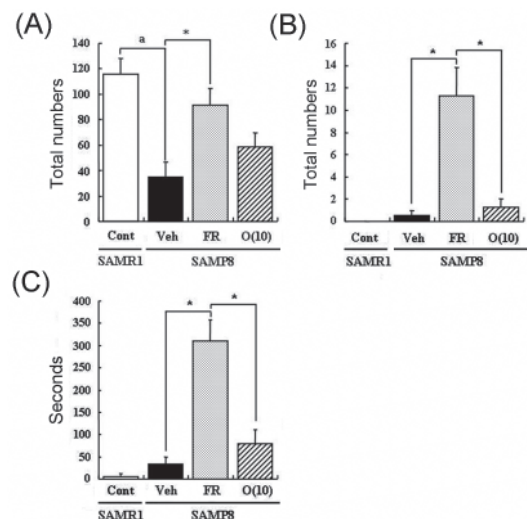


Figure 9. Effects of oligomers on stereotypical behaviors. Forty-five- or forty-six-week-old SAMP8 were administered vehicle (Veh, water *p.o.*, $n = 4$), while another two groups were administered oligomers orally at doses of 10 mg/kg body weight/day (O (10), $n = 4$) using a stomach tube until death. For the remaining group of mice, the mean food intake was restricted to 60% until death (FR, $n = 4$). SAMR1 mice (Cont, 45-46 weeks old, $n = 4$) were used as a control group. One hundred and thirty nine days after administration, actions of rearing up on the hindlimbs and jumping from the bottom of the cage were counted for 15 min (A, B). The time spent hanging from the lid was measured for 10 min (C). Administration was continued during the tests. * $p < 0.05$ (One-way ANOVA, *post-hoc* Bonferroni's test); ^a $p = 0.0034$ (Student's *t*-test).

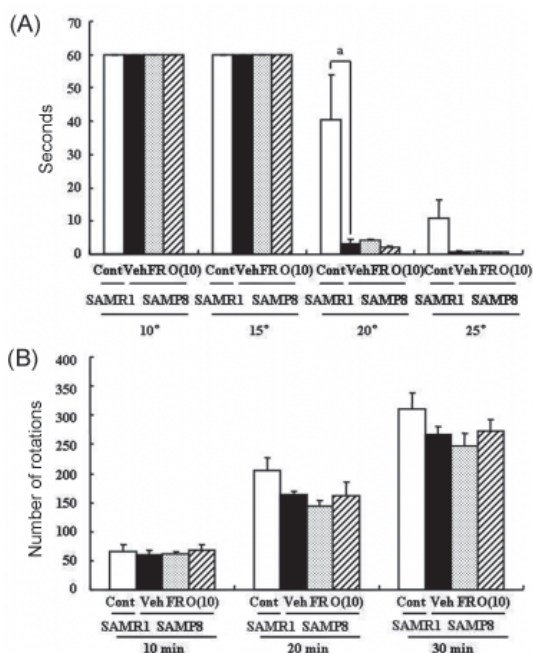


Figure 10. Effects of oligomers on motor function. Forty-five- or forty-six-week-old SAMP8 were administered vehicle (Veh, water *p.o.*, $n = 4$), while another two groups were administered oligomers orally at doses of 10 mg/kg body weight/day (O (10), $n = 4$) using a stomach tube until death. For the remaining group of mice, the mean food intake was restricted to 60% until death (FR, $n = 4$). SAMR1 (Cont, 45-46 weeks old, $n = 4$) were used as a control group. One hundred and thirty nine days after administration, the time spent on the inclined surface without dropping was measured (A). The number of rotations was measured for 30 min (B). Administration was continued during the tests. ^a $p = 0.0159$ (A: Student's *t*-test).

show stereotypical behaviors, like SIRT1-knockout mice undergoing food restriction. We revealed that oligomers consist of various combinations of 4 types of monomer: EGC, EC, EGCg, and ECg. Their absorption rates and bioactivities were distinguished by their types (44). Therefore, composition of oligomers may play an important role in neuronal signaling.

We also carried out an investigation of side effects or toxicity of oligomers. The results showed normal ranges of hematological data such as alanine aminotransaminase, aspartate aminotransaminase, and blood urea nitrogen as well as changes in body and tissue weights, although the maximum concentration for oral administration was at a higher level (500 mg/kg body weight/day) than the average dietary intake of proanthocyanidins of 58 mg/day of humans in the United States (66). Therefore, we suggest that oligomeric proanthocyanidins are safe and novel anti-aging agents associated with life span extension. Further studies are needed to elucidate molecular mechanisms associated with extension of life span by oligomers, as well as to clarify the contribution of SIRT1 to the aging process of SAM.

4. Conclusion and perspectives

The present study indicated that oral administration of

oligomers improved memory impairment in SAMP8. In particular, the density of axons in the hippocampal CA1 was significantly increased by oligomer administration. Moreover, the administration of oligomers increased phosphorylation of VEGFR-2 in the hippocampal CA3, hypothalamus, and choroid plexus. We speculate that memory improvement accompanied with histological changes may be induced directly in the hippocampus and indirectly in the hypothalamus and choroid plexus through VEGFR-2 signaling. In the present study, we elucidated the protective effect of oligomers against memory impairment with aging. VEGFR-2 signaling may provide new insight into ways to protect against memory deficit in the aging brain. The present study also indicated that the oral administration of oligomers extended the life span of SAMP8 with a slight up-regulation of SIRT1 in the brain. On the other hand, oligomer-treated SAMP8 did not show stereotypical behavior.

Proanthocyanidin is known as a condensed tannin, a member of a specific group of polyphenolic compounds, and it has been reported to exhibit powerful antioxidant activity (67,68). Although this is the most abundant dietary polyphenol, its marked polymerization leads to limited absorption *in vivo* (69). Many researchers have focused on the oligomeric form with its lower level of polymerization in foodstuffs such as grape seeds and blackberry (70). In this study, oligomers are suggested to be novel anti-aging agents.

Acknowledgements

The present study was supported in part by Grant-in-Aid (C) from the Ministry of Education, Culture, Sports, Science and Technology (No. 1950066) and by the Ministry of Economy, Trade and Industry (2006-2007), Japan.

References

1. Takeda T, Matsushita T, Kurozumi M, Takemura K, Higuchi K, Hosokawa M. Pathobiology of the senescence-accelerated mouse (SAM). *Exp Gerontol.* 1997; 32:117-127.
2. Markowska AL, Spangler EL, Ingram DK. Behavioral assessment of the senescence-accelerated mouse (SAM P8 and R1). *Physiol Behav.* 1998; 64:15-26.
3. Kawamata T, Akiguchi I, Yagi H, Irino M, Sugiyama H, Akiyama H, Shimada A, Takemura M, Ueno M, Kitabayashi T, Ohnishi K, Seriu N, Higuchi K, Hosokawa M, Takeda T. Neuropathological studies on strains of senescence-accelerated mice (SAM) with age-related deficits in learning and memory. *Exp Gerontol.* 1997; 32:161-169.
4. Flood JF, Morley JE. Learning and memory in the SAMP8 mouse. *Neurosci Biobehav Rev.* 1998; 22:1-20.
5. Yasui F, Matsugo S, Ishibashi M, Kajita T, Ezashi Y, Oomura Y, Kojo S, Sasaki K. Effects of chronic acetyl-L-carnitine treatment on brain lipid hydroperoxide level and

- passive avoidance learning in senescence-accelerated mice. *Neurosci Lett.* 2002; 334:177-180.
6. Farr SA, Poon HF, Dogrukol-Ak D, Drake J, Banks WA, Eyerman E, Butterfield DA, Morley JE. The antioxidants α -lipoic acid and *N*-acetylcysteine reverse memory impairment and brain oxidative stress in aged SAMP8 mice. *J Neurochem.* 2003; 84:1173-1183.
 7. Komatsu T, Chiba T, Yamaza H, Yamashita K, Shimada A, Hoshiyama Y, Henmi T, Ohtani H, Higami Y, de Cabo R, Ingram DK, Shimokawa I. Manipulation of caloric content but not diet composition, attenuates the deficit in learning and memory of senescence-accelerated mouse strain P8. *Exp Gerontol.* 2008; 43:339-346.
 8. Sato E, Kurokawa T, Oda N, Ishibashi S. Early appearance of abnormality of microperoxisomal enzymes in the cerebral cortex of senescence-accelerated mouse. *Mech Ageing Dev.* 1996; 92:175-184.
 9. Dixon RA, Xie DY, Sharma SB. Proanthocyanidins – a final frontier in flavonoid research? *New Phytol.* 2005; 165:9-28.
 10. Xie DY, Dixon RA. Proanthocyanidin biosynthesis – still more questions than answers? *Phytochemistry.* 2005; 66:2127-2144.
 11. Manach C, Williamson G, Morand C, Scalbert A, Rémésy C. Bioavailability and bioefficacy of polyphenols in humans. I. Review of 97 bioavailability studies. *Am J Clin Nutr.* 2005; 81:230S-242S.
 12. Gorinstein S, Zachwieja Z, Folta M, Barton H, Piotrowicz J, Zemsler M, Weisz M, Trakhtenberg S, Martín-Belloso O. Comparative contents of dietary fiber, total phenolics, and minerals in persimmons and apples. *J Agric Food Chem.* 2001; 49:952-957.
 13. Lee YA, Cho EJ, Yokozawa T. Protective effect of persimmon (*Diospyros kaki*) peel proanthocyanidin against oxidative damage under H₂O₂-induced cellular senescence. *Biol Pharm Bull.* 2008; 31:1265-1269.
 14. Zhao XH, Nomura Y. Age-related changes in uptake and release on L-[³H]noradrenaline in brain slices of senescence accelerated mouse. *Int J Dev Neurosci.* 1990; 8:267-272.
 15. Zhao XH, Kitamura Y, Nomura Y. Age-related changes in NMDA-induced [³H]acetylcholine release from brain slices of senescence-accelerated mouse. *Int J Dev Neurosci.* 1992; 10:121-129.
 16. Kawamata T, Akiguchi I, Maeda K, Tanaka C, Higuchi K, Hosokawa M, Takeda T. Age-related changes in the brains of senescence-accelerated mice (SAM): Association with glial and endothelial reactions. *Microsc Res Tech.* 1998; 43:59-67.
 17. Sureda FX, Gutierrez-Cuesta J, Romeo M, Mulero M, Canudas AM, Camins A, Mallol J, Pallàs M. Changes in oxidative stress parameters and neurodegeneration markers in the brain of the senescence-accelerated mice SAMP-8. *Exp Gerontol.* 2006; 41:360-367.
 18. Wu Y, Zhang AQ, Yew DT. Age related changes of various markers of astrocytes in senescence-accelerated mice hippocampus. *Neurochem Int.* 2005; 46:565-574.
 19. Tanaka J, Okuma Y, Tomobe K, Nomura Y. The age-related degeneration of oligodendrocytes in the hippocampus of the senescence-accelerated mouse (SAM) P8: A quantitative immunohistochemical study. *Biol Pharm Bull.* 2005; 28:615-618.
 20. Miyazaki H, Okuma Y, Nomura J, Nagashima K, Nomura Y. Age-related alterations in the expression of glial cell line-derived neurotrophic factor in the senescence-accelerated mouse brain. *J Pharmacol Sci.* 2003; 92:28-34.
 21. Mizushima Y, Kan S, Yoshida S, Irie Y, Urata Y. Effect of Choto-san, a Kampo medicine, on impairment of passive avoidance performance in senescence accelerated mouse (SAM). *Phytother Res.* 2003; 17:542-545.
 22. Rosenzweig ES, Barnes CA. Impact of aging on hippocampal function: Plasticity, network dynamics, and cognition. *Prog Neurobiol.* 2003; 69:143-179.
 23. Dahl D, Labkovsky B, Bignami A. Neurofilament phosphorylation in axons and perikarya: Immunofluorescence study of the rat spinal cord and dorsal root ganglia with monoclonal antibodies. *J Comp Neurol.* 1988; 271:445-450.
 24. von Bohlen und Halbach O, Unsicker K. Morphological alterations in the amygdala and hippocampus of mice during ageing. *Eur J Neurosci.* 2002; 16:2434-2440.
 25. Yamamoto T, Hirayama A. Effects of soft-diet feeding on synaptic density in the hippocampus and parietal cortex of senescence-accelerated mice. *Brain Res.* 2001; 902:255-263.
 26. Smith TD, Adams MM, Gallagher M, Morrison JH, Rapp PR. Circuit-specific alterations in hippocampal synaptophysin immunoreactivity predict spatial learning impairment in aged rats. *J Neurosci.* 2000; 20:6587-6593.
 27. Yang SZ, Zhang LM, Huang YL, Sun FY. Distribution of Flk-1 and Flt-1 receptors in neonatal and adult rat brains. *Anat Rec A Discov Mol Cell Evol Biol.* 2003; 274:851-856.
 28. Nico B, Mangieri D, Corsi P, De Giorgis M, Vacca A, Roncali L, Ribatti D. Vascular endothelial growth factor-A, vascular endothelial growth factor receptor-2 and angiopoietin-2 expression in the mouse choroid plexuses. *Brain Res.* 2004; 1013:256-259.
 29. Wick A, Wick W, Waltenberger J, Weller M, Dichgans J, Schulz JB. Neuroprotection by hypoxic preconditioning requires sequential activation of vascular endothelial growth factor receptor and Akt. *J Neurosci.* 2002; 22:6401-6407.
 30. Matsuzaki H, Tamatani M, Yamaguchi A, Namikawa K, Kiyama H, Vitek MP, Mitsuda N, Tohyama M. Vascular endothelial growth factor rescues hippocampal neurons from glutamate-induced toxicity: Signal transduction cascades. *FASEB J.* 2001; 15:1218-1220.
 31. Cao L, Jiao X, Zuzga DS, Liu Y, Fong DM, Young D, During MJ. VEGF links hippocampal activity with neurogenesis, learning and memory. *Nat Genet.* 2004; 36:827-835.
 32. Sun Y, Jin K, Xie L, Childs J, Mao XO, Logvinova A, Greenberg DA. VEGF-induced neuroprotection, neurogenesis, and angiogenesis after focal cerebral ischemia. *J Clin Invest.* 2003; 111:1843-1851.
 33. Kim BW, Choi M, Kim YS, Park H, Lee HR, Yun CO, Kim EJ, Choi JS, Kim S, Rhim H, Kaang BK, Son H. Vascular endothelial growth factor (VEGF) signaling regulates hippocampal neurons by elevation of intracellular calcium and activation of calcium/calmodulin protein kinase II and mammalian target of rapamycin. *Cell Signal.* 2008; 20:714-725.
 34. Jin K, Mao XO, Greenberg DA. Vascular endothelial growth factor stimulates neurite outgrowth from cerebral cortical neurons *via* Rho kinase signaling. *J Neurobiol.* 2006; 66:236-242.
 35. Dalgleish T. The emotional brain. *Nat Rev Neurosci.* 2004; 5:583-589.
 36. Aggleton JP, Shaw C. Amnesia and recognition memory: A re-analysis of psychometric data. *Neuropsychologia.* 1996; 34:51-62.
 37. Brown PD, Davies SL, Speake T, Millar ID. Molecular

- mechanisms of cerebrospinal fluid production. *Neuroscience*. 2004; 129:957-970.
38. Emerich DF, Skinner SJ, Borlongan CV, Vasconcellos AV, Thanos CG. The choroid plexus in the rise, fall and repair of the brain. *Bioessays*. 2005; 27:262-274.
 39. Johanson CE, Duncan JA, Stopa EG, Baird A. Enhanced prospects for drug delivery and brain targeting by the choroid plexus-CSF route. *Pharm Res*. 2005; 22:1011-1037.
 40. Jakubowska-Doğru E, Gümüşbaş U. Chronic intracerebroventricular NGF administration improves working memory in young adult memory deficient rats. *Neurosci Lett*. 2005; 382:45-50.
 41. Shi L, Linville MC, Tucker EW, Sonntag WE, Brunso-Bechtold JK. Differential effects of aging and insulin-like growth factor-1 on synapses in CA1 of rat hippocampus. *Cereb Cortex*. 2005; 15:571-577.
 42. de Boer VC, de Goffau MC, Arts IC, Hollman PC, Keijer J. SIRT1 stimulation by polyphenols is affected by their stability and metabolism. *Mech Ageing Dev*. 2006; 127:618-627.
 43. Bagchi D, Bagchi M, Stohs SJ, Das DK, Ray SD, Kuszynski CA, Joshi SS, Pruess HG. Free radicals and grape seed proanthocyanidin extract: Importance in human health and disease prevention. *Toxicology*. 2000; 148:187-197.
 44. Weinreb O, Mandel S, Amit T, Youdim MB. Neurological mechanisms of green tea polyphenols in Alzheimer's and Parkinson's diseases. *J Nutr Biochem*. 2004; 15:506-516.
 45. Deprez S, Mila I, Huneau JF, Tome D, Scalbert A. Transport of proanthocyanidin dimer, trimer, and polymer across monolayers of human intestinal epithelial Caco-2 cells. *Antioxid Redox Signal*. 2001; 3:957-967.
 46. Roth GS, Lane MA, Ingram DK. Caloric restriction mimetics: The next phase. *Ann N Y Acad Sci*. 2005; 1057:365-371.
 47. Masoro EJ. Overview of caloric restriction and ageing. *Mech Ageing Dev*. 2005; 126:913-922.
 48. Roth GS, Ingram DK, Lane MA. Caloric restriction in primates and relevance to humans. *Ann N Y Acad Sci*. 2001; 928:305-315.
 49. Nakagawa T, Yokozawa T. Direct scavenging of nitric oxide and superoxide by green tea. *Food Chem Toxicol*. 2002; 40:1745-1750.
 50. Finkel T, Holbrook NJ. Oxidants, oxidative stress and the biology of ageing. *Nature*. 2000; 408:239-247.
 51. Sasaki T, Maier B, Koclega KD, Chruszcz M, Gluba W, Stukenberg PT, Minor W, Scoble H. Phosphorylation regulates SIRT1 function. *PLoS One*. 2008; 3:e4020.
 52. Imai S, Armstrong CM, Kaeberlein M, Guarente L. Transcriptional silencing and longevity protein Sir2 is an NAD-dependent histone deacetylase. *Nature*. 2000; 403:795-800.
 53. Guarente L. Sir2 links chromatin silencing, metabolism, and aging. *Genes Dev*. 2000; 14:1021-1026.
 54. Michan S, Sinclair D. Sirtuins in mammals: Insights into their biological function. *Biochem J*. 2007; 404:1-13.
 55. Chen D, Guarente L. SIR2: A potential target for caloric restriction mimetics. *Trends Mol Med*. 2007; 13:64-71.
 56. Howitz KT, Bitterman KJ, Cohen HY, Lamming DW, Lavu S, Wood JG, Zipkin RE, Chung P, Kisilewski A, Zhang LL, Scherer B, Sinclair DA. Small molecule activators of sirtuins extend *Saccharomyces cerevisiae* lifespan. *Nature*. 2003; 425:191-196.
 57. Wood JG, Rogina B, Lavu S, Howitz K, Helfand SL, Tatar M, Sinclair D. Sirtuin activators mimic caloric restriction and delay ageing in metazoans. *Nature*. 2004; 430:686-689.
 58. Baur JA, Pearson KJ, Price NL, et al. Resveratrol improves health and survival of mice on a high-calorie diet. *Nature*. 2006; 444:337-342.
 59. Lagouge M, Argmann C, Gerhart-Hines Z, Meziane H, Lerin C, Daussin F, Messadeq N, Milne J, Lambert P, Elliott P, Geny B, Laakso M, Puigserver P, Auwerx J. Resveratrol improves mitochondrial function and protects against metabolic disease by activating SIRT1 and PGC-1 α . *Cell*. 2006; 127:1109-1122.
 60. Pearson KJ, Baur JA, Lewis KN, et al. Resveratrol delays age-related deterioration and mimics transcriptional aspects of dietary restriction without extending life span. *Cell Metab*. 2008; 8:157-168.
 61. Lee YA, Kim YJ, Cho EJ, Yokozawa T. Ameliorative effects of proanthocyanidin on oxidative stress and inflammation in streptozotocin-induced diabetic rats. *J Agric Food Chem*. 2007; 55:9395-9400.
 62. Lee YA, Cho EJ, Yokozawa T. Effects of proanthocyanidin preparations on hyperlipidemia and other biomarkers in mouse model of type 2 diabetes. *J Agric Food Chem*. 2008; 56:7781-7789.
 63. Chen D, Steele AD, Lindquist S, Guarente L. Increase in activity during caloric restriction requires Sirt1. *Science*. 2005; 310:1641.
 64. Levay EA, Govic A, Penman J, Paolini AG, Kent S. Effects of adult-onset caloric restriction on anxiety-like behavior in rats. *Physiol Behav*. 2007; 92:889-896.
 65. Carr KD, Tsimberg Y, Berman Y, Yamamoto N. Evidence of increased dopamine receptor signaling in food-restricted rats. *Neuroscience*. 2003; 119:1157-1167.
 66. Erdman JW Jr, Balentine D, Arab L, Beecher G, Dwyer JT, Fols J, Harnly J, Hollman P, Keen CL, Mazza G, Messina M, Scalbert A, Vita J, Williamson G, Burrowes J. Flavonoids and heart health: Proceedings of the ILSI North America Flavonoids Workshop, May 31-June 1, 2005, Washington, DC. *J Nutr*. 2007; 137:718S-737S.
 67. Dixon RA, Xie DY, Sharma SB. Proanthocyanidins – a final frontier in flavonoid research? *New Phytol*. 2005; 165:9-28.
 68. Xie DY, Dixon RA. Proanthocyanidin biosynthesis – still more questions than answers? *Phytochemistry*. 2005; 66:2127-2144.
 69. Manach C, Williamson G, Morand C, Scalbert A, Rémésy C. Bioavailability and bioefficacy of polyphenols in humans. I. Review of 97 bioavailability studies. *Am J Clin Nutr*. 2005; 81 (1 Suppl):230S-242S.
 70. Gu L, Kelm MA, Hammerstone JF, Beecher G, Holden J, Haytowitz D, Prior RL. Screening of foods containing proanthocyanidins and their structural characterization using LC-MS/MS and thiolytic degradation. *J Agric Food Chem*. 2003; 51:7513-7521.

(Received March 29, 2011; Revised June 02, 2011; Accepted June 13, 2011)

Brief Report

DOI: 10.5582/ddt.2011.v5.3.119

A low-dose combination of valsartan and low molecular weight heparin better improved glomerular permeability than did high-dose monotherapy in rats with diabetic nephropathyBo Jiao^{1,*}, Yahui Zhang^{1,2}, Yanna Cheng¹, Jianjun Gao¹, Qingzhu Zhang¹¹ Department of Pharmacology, School of Pharmaceutical Science, Shandong University, Ji'nan, Shandong, China;² Department of Pharmacy, Provincial Hospital Affiliated to Shandong University, Ji'nan, Shandong, China.

ABSTRACT: Diabetic nephropathy is the most common and severe renal complication of diabetes mellitus. The present study sought to investigate the renoprotective effects of a combination therapy of valsartan and low molecular weight heparin (LMWH) in rats with diabetic nephropathy induced by uninephrectomy and streptozotocin. The animals were divided into five groups as follows: sham-operated rats, diabetic control rats, diabetic rats treated with 20 mg/kg/day valsartan, diabetic rats treated with 600 IU/kg/day LMWH, diabetic rats treated with a combination of valsartan and LMWH (valsartan 10 mg/kg/day and LMWH 300 IU/kg/day). The treatment regimen was maintained for 8 weeks. Treatment with valsartan, LMWH, or a combination of the two had no significant effect on blood glucose levels. However, the urine protein excretion levels significantly decreased for the three drug treatment groups; the most dramatic decreases were observed in the combination treatment group. Kidney histology was examined using periodic acid-Schiff staining and immunohistochemical staining of extracellular matrix proteins. Results indicated that histopathology improved markedly in the three drug treatment groups; combination therapy had an equal or better effect than monotherapy in terms of decreasing the abnormal thickness of the glomerular basal membrane, the ratio of the area of the mesangial region with respect to the total area of renal glomeruli, and the accumulation of collagen IV and laminin in kidney tissue. In addition, serum levels of transforming growth factor- β_1 (TGF- β_1) also markedly decreased in the drug treatment groups according to ELISA. However, there were no significant differences between the combination therapy group and monotherapy group. These

results suggest that a combination of valsartan and LMWH at half the dose used in monotherapy is better at improving glomerular permeability in rats with diabetic nephropathy.

Keywords: Valsartan, low molecular weight heparin, transforming growth factor- β_1 (TGF- β_1), diabetic nephropathy

1. Introduction

Diabetic nephropathy is the most common complication of diabetes mellitus, often leading to end-stage kidney disease and a high risk of mortality (1). The condition is characterized by progressively increasing albuminuria and histopathological features including glomerular basement membrane (GBM) thickening and mesangial expansion due to accumulation of extracellular matrix (ECM) proteins (2). Previous studies suggested that the rennin-angiotensin system (RAS) plays an important role in progressive renal injury in diabetic nephropathy (3). Angiotensin II (Ang II), a member of the RAS family, is thought to act as a crucial mediator in this disease (4). It was indicated that Ang II induced the expression of TGF- β_1 , a key cytokine responsible for GBM thickening, mesangial expansion, and glomerulosclerosis after coupling to its receptors (5,6). Ang II type 1 receptor blockers (ARBs) were found to inhibit TGF- β_1 expression in kidney tissues and thus delay the progression of diabetic nephropathy (7).

Valsartan, a typical ARB, has been widely used in the clinical treatment of diabetic nephropathy. However, a major adverse effect of this drug is to induce a compensatory rise in renin due to the disruption of the Ang II feedback inhibition of renin production, potentially leading to renal and cardiovascular damage (8). Since the compensatory rise in renin paralleled the dosage of ARBs, reduction of the dosage of this drug may decrease the risk of its adverse effect (9).

Low molecular weight heparin (LMWH) has been

*Address correspondence to:

Dr. Bo Jiao, Department of Pharmacology, School of Pharmaceutical Science, Shandong University, Wenhua-xi Road No. 44, Ji'nan 250012, Shandong, China.
e-mail: jiaob@sdu.edu.cn

used clinically and has renoprotective action through inhibition of the alteration of the GBM, decreasing the accumulation of mesangial matrix and reducing the abnormal excretion of albumin (10-12). Further studies suggested that LMWH has a renoprotective effect by suppressing high glucose-induced TGF- β_1 expression (13). Because valsartan and LMWH have similar mechanisms of renoprotection, *i.e.* inhibiting the expression of TGF- β_1 in kidney tissue, the present study sought to investigate the renoprotective effects of a combination of valsartan and LMWH at low doses in rats with diabetic nephropathy induced by unilateral nephrectomy and streptozotocin (STZ) injection. In addition, the serum TGF- β_1 concentration was determined in order to elucidate the underlying mechanism of inhibited TGF- β_1 expression.

2. Materials and Methods

2.1. Chemicals

Valsartan was purchased from Changzhou Kony Pharm Co., Ltd. LMWH was obtained from Qilu Pharmaceutical Co., Ltd. Valsartan was suspended in 0.5% carboxy methyl cellulose solution and LMWH was dissolved in normal sodium before use.

2.2. Animal model

Male Wistar rats weighing 180-220 g were purchased from the Animal Experimental Center, Shandong University, Shandong, China. The research protocol was in accordance with the institutional guidelines of the Animal Care and Use Committee of Shandong University. Rats were kept in a 12 h light/dark cycle at 25°C and fed a standard rat chow and water *ad libitum*. Before unilateral nephrectomy, rats were anaesthetized by intraperitoneal injection of sodium pentobarbital at a dose of 45 mg/kg body weight. Under sterile conditions, a right dorsolateral laparotomy was performed and the right kidney was retracted to expose the renal vessels and ureter. The vessels and ureter were ligated with cotton thread and cut between the kidney hilus and ligated portion to remove the kidney. The adrenal gland was left in place. The skin was sutured and the rats were kept in regular cages. In sham-operated rats, the thread was passed around the vessels and ureter and then removed. The kidney was returned to the abdominal cavity and the incision was sutured. After surgery, the rats were administered 50 U/d penicillin for 3 days. The wound completely healed after 2 weeks.

The uninephrectomized rats were intraperitoneally injected with STZ (Sigma-Aldrich, USA) at a dose of 45 mg/kg body weight (14). The sham-operated rats were given an equal volume of citric acid buffer solution. After 72 h, blood glucose was determined and diabetes was confirmed by BG \geq 16.7 mmol/L. Rats were randomly

divided into 5 groups ($n = 8$ /group). Group 1 consisted of sham-operated rats, group 2 consisted of diabetic rats, group 3 consisted of diabetic rats intragastrically administered valsartan at a dose of 20 mg/kg/day, group 4 consisted of diabetic rats hypodermically injected with LMWH at a dose of 600 IU/kg/day, and group 5 consisted of diabetic rats simultaneously given half the dose of valsartan and LMWH, *i.e.* 10 mg/kg/day and 300 IU/kg/day, respectively. The treatment regimen was maintained for 8 weeks.

2.3. Blood glucose and urine protein assay

A blood glucose assay was performed by collecting blood samples from the tails of rats in each group at the beginning and the end of the study period, respectively. A urine protein assay was performed by collecting 24 hours of urine using metabolic cages on the day before the end of the experiment. Blood glucose and urine protein were measured with an Automatic Biochemistry Analyzer (AU2700; Olympus Optical Co., Mishima, Japan).

2.4. Enzyme-linked immunosorbent assay (ELISA)

Blood samples were collected from the abdominal aorta of rats at the end of the study period to measure the serum levels of TGF- β_1 . TGF- β_1 was determined with a commercially available ELISA kit (Bionewtrans Pharmaceutical Biotechnology Co. Ltd., USA). Analysis was performed according to the manufacturer's recommended protocol and the methods described previously (15,16). Concentrations are presented as the mean of two measurements.

2.5. Histologic examination

Kidneys were completely perfused with normal saline and then removed. Kidney samples were fixed in 4% paraformaldehyde solution for 24 hours and subsequently embedded in paraffin (17). Tissues were cut into 3- μ m-thick slices for the following studies. For an examination of histomorphological features, tissues were cut into 3- μ m-thick slices and stained with periodic acid-Schiff (PAS). To characterize the expression of ECM proteins, Col-IV and LN immunohistochemical staining was performed (18,19). After incubation with anti-Col-IV (Chemicon, California, USA) or anti-LN (abcam, Cambridge, UK) antibody at 4°C, the sections were washed and treated with biotinylated anti-immunoglobulin and then washed, reacted with avidin-conjugated horseradish peroxidase H complex, and incubated in diaminobenzidine and hydrogen peroxide. The slides were then rinsed in distilled water, counterstained with hematoxylin, and mounted. Images were captured and quantified by means of a computer-assisted image analyzer, Image Pro Plus 5.1 (Media Cybernetics, Inc., Bethesda, MD, USA). Ten glomeruli were analyzed in each section (20).

2.6. Statistical analysis

Data are expressed as mean \pm S.D. One-way ANOVA followed by LSD post hoc analysis was performed using SPSS/Win11.0 software (SPSS, Inc., Chicago, Illinois, USA); $p < 0.05$ was indicative of a significant difference.

3. Results and Discussion

3.1. Effect of valsartan, LMWH, and a combination of the two on blood glucose and urinary protein excretion

Blood glucose levels of rats in all groups at the beginning and the end of the study period were determined. There was no significant variation in the blood glucose for all of the diabetic rats (groups 2-5) before or after the experiment (Figure 1A, $p > 0.05$). Blood glucose did not change significantly before and after the experiment for any group, indicating that treatment with valsartan, LMWH, or a combination of the two did not affect blood glucose (Figure 1A, $p > 0.05$).

Figure 1B shows the amount of 24-h protein excretion in urine collected on the day before the end

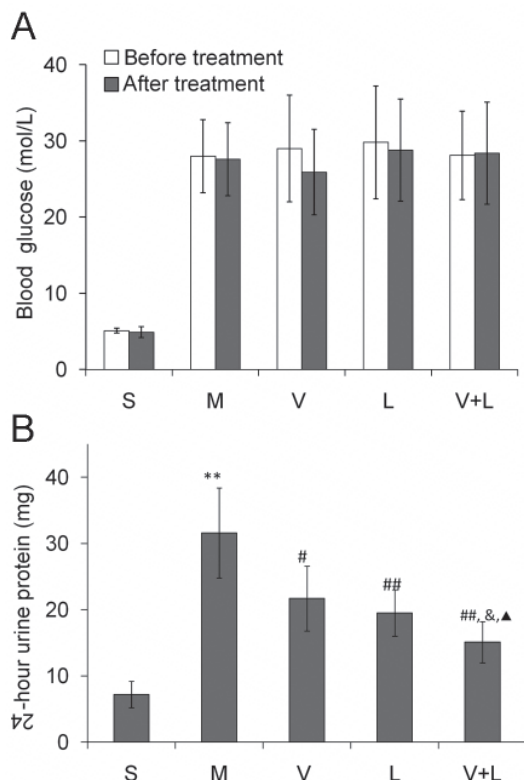


Figure 1. (A) Rat blood glucose levels determined at the beginning and the end of the study period; **(B)** The amount of 24 h protein excretion in urine collected during the day before the end of the study. S, sham-operated rats; M, model rats (diabetic control rats); V, valsartan-treated rats (20 mg/kg/day); L, LMWH-treated rats (600 IU/kg/day); V + L, combination (valsartan + LMWH)-treated rats (10 mg/kg/day and 300 IU/kg/day). ** $p < 0.01$ vs. sham-operated group. # $p < 0.05$, ## $p < 0.01$ vs. model group. & $p < 0.05$ vs. valsartan group. & $p < 0.05$ vs. LMWH group.

of the study. The mean amount of protein excretion in diabetic control rats was 31.6 mg, which was significantly higher than that (7.2 mg) in sham-operated control rats ($p < 0.01$). The amount of protein excretion was 21.7 and 19.5 mg, respectively, in groups treated with valsartan at a dose of 20 mg/kg/d and LMWH at a dose of 600 IU/kg/day ($p < 0.05$, valsartan group vs. diabetic control; $p < 0.01$, LMWH group vs. diabetic control). Diabetic rats that received a combination of valsartan and LMWH at half the dose used in monotherapy excreted an even lower level of urinary protein, 15.5 mg, compared to those that received monotherapy ($p < 0.01$, combination treatment vs. diabetic control; $p < 0.05$, combination treatment vs. valsartan or LMWH treatment).

3.2. Effect of valsartan, LMWH, and a combination of the two on renal histology

Figure 2 shows the histomorphological features

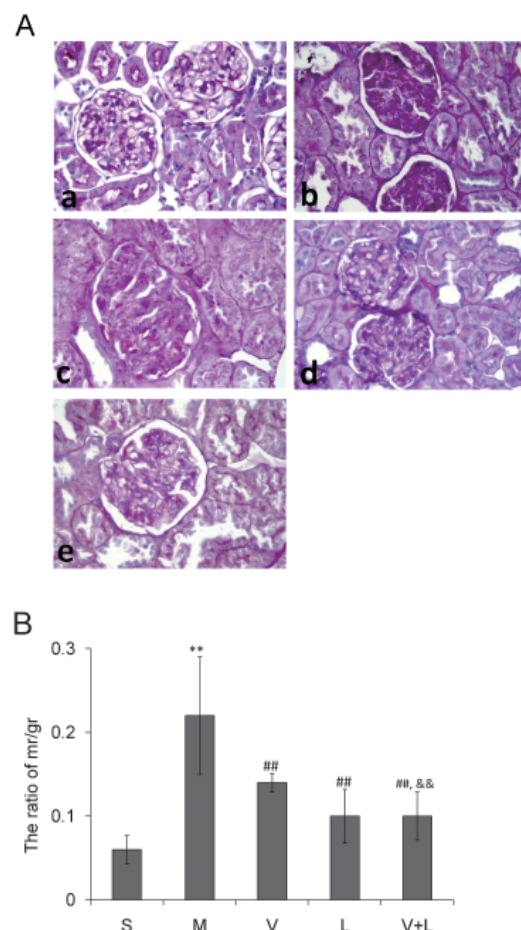


Figure 2. Renal histology (A) and the ratio of the area of the mesangial region (mr) with respect to the total area of renal glomeruli (rg) **(B)** for each group at the end of the study period (stained by PAS, $\times 400$). S, sham-operated rats; M, model rats (diabetic control rats); V, valsartan-treated rats (20 mg/kg/day); L, LMWH-treated rats (600 IU/kg/day); V + L, combination (valsartan + LMWH)-treated rats (10 mg/kg/day and 300 IU/kg/day). ** $p < 0.01$, vs. sham-operated group. ## $p < 0.01$ vs. model group. & $p < 0.01$ vs. valsartan group. & $p < 0.01$ vs. LMWH group.

of kidneys from rats receiving various treatments. Diabetic control rats (Figure 2Ab) had an enlarged area of the mesangial region and thicker GBM compared to sham-operated rats (Figure 2Aa). Valsartan or LMWH treatment alone improved glomerular pathology. A combination of both drugs at half the dose provided an equal or even greater benefit (Figures 2Ac-2Ae). The ratio of the mesangial region area with respect to the total area of renal glomeruli in each group is shown in Figure 2B. Diabetic control rats had a significantly larger ratio (0.22, $p < 0.01$) compared to sham-operated rats (0.06). Meanwhile, groups treated with valsartan or LMWH alone had a smaller ratio of the area of the mesangial region (0.14 and 0.10). The ratio for the combination treatment group was 0.10, which was significantly smaller than that for the valsartan treatment group and nearly equal to that for the LMWH treatment group ($p < 0.05$, combination treatment vs. valsartan treatment; $p > 0.05$, combination treatment vs. LMWH treatment).

The expression of ECM proteins Col-IV and LN in kidney tissues was examined immunohistochemically (Figure 3). The amount of Col-IV and LN in diabetic control rats had increased compared to the amount in sham-operated rats. Valsartan or LMWH treatment alone decreased the accumulation of these two proteins. The combination treatment was better at diminishing the expression of Col-IV and equivalent at reducing the expression of LN compared to sole drug treatment.

3.3. Effect of valsartan, LMWH, and a combination of the two on the serum TGF- β_1 level

The effect of drug treatment on the serum level of TGF- β_1 was also examined using an ELISA assay (Table 1). The mean serum concentration of TGF- β_1 in diabetic control rats was 266.4 pg/L and was higher than that (119.5 pg/L) in sham-operated rats. After 8 weeks of valsartan treatment at a dose of 20 mg/kg/day, rats exhibited significantly lower levels of TGF- β_1 ,

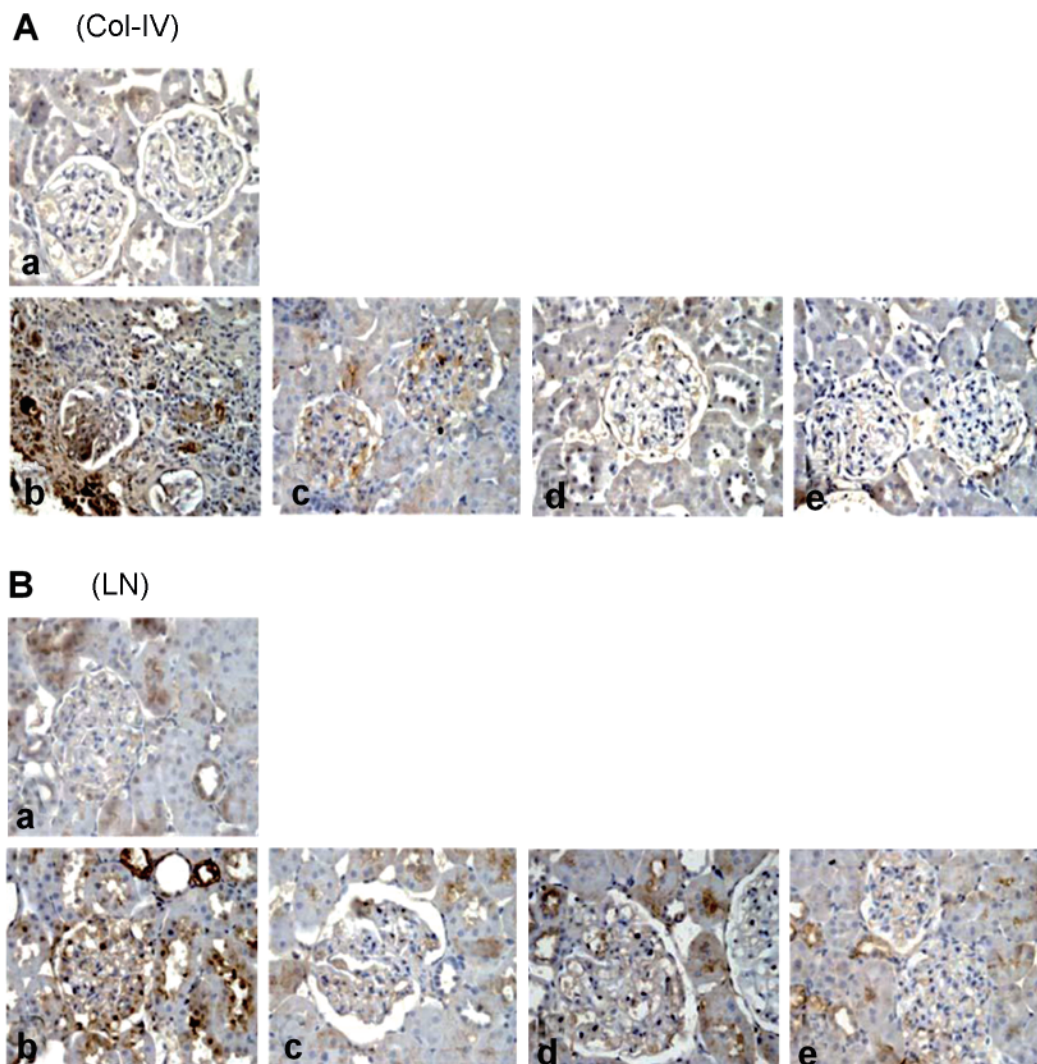


Figure 3. Immunohistochemical staining of Col-IV (A) and LN (B) in rat kidney tissues at the end of the study period. a, sham-operated rats; **b,** diabetic control rats; **c,** valsartan-treated rats (20 mg/kg/day); **d,** LMWH-treated rats (600 IU/kg/day); **e,** combination (valsartan + LMWH)-treated rats (10 mg/kg/day and 300 IU/kg/day).

Table 1. Rat serum TGF- β_1 concentrations in each group at the end of the study period

Group	Dosage	TGF- β_1 level (pg/L)
Sham-operated rats	–	119.5 \pm 23.8
Diabetic control rats	–	266.4 \pm 41.1**
Valsartan-treated rats	20 mg/kg	186.7 \pm 38.3 ^{###}
LMWH-treated rats	600 IU/kg	203.5 \pm 33.5 ^{###}
Combination (valsartan + LMWH)-treated rats	Valsartan, 10 mg/kg LMWH, 300 IU/kg	202.7 \pm 37.0 ^{###}

** $p < 0.01$, vs. sham-operated rats; ^{###} $p < 0.01$, vs. diabetic control rats.

186.7 pg/L on average, compared to diabetic control rats ($p < 0.01$). Rats treated with LMWH at a dose of 600 IU/kg/day also exhibited significantly lower levels of TGF- β_1 , *i.e.* 203.5 pg/L ($p < 0.01$) on average. In the combination treatment group, rats administered 10 mg/kg/day valsartan and 300 IU/kg/day LMWH had significantly lower levels of TGF- β_1 , 202.7 pg/L on average, compared to diabetic control rats ($p < 0.01$). However, no significance differences between the combination treatment group and valsartan or LMWH group were observed.

The present study investigated the renoprotective effects of valsartan, LMWH, and a low-dose combination of the two in rats with diabetic nephropathy induced by uninephrectomy and STZ. Valsartan, LMWH, or a low-dose combination of the two did not affect blood glucose levels in the rats. Treatment with valsartan or LMWH alone significantly decreased albuminuria, the abnormal thickness of the GBM, the ratio of the mesangial region area with respect to the total area of renal glomeruli, and the amount of ECM proteins Col-IV and LN that accumulated in kidney tissue. A combination therapy of valsartan and LMWH at half the dose used in monotherapy was better than monotherapy in terms of diminishing urine protein excretion and ameliorating renal histopathology and was equivalent to monotherapy with respect to reducing the level of serum TGF- β_1 . These findings implicate that a low-dose combination of valsartan and LMWH is better at improving glomerular membrane protein permeability in rats with diabetic nephropathy.

Kidney cells such as mesangial cells and podocytes are able to synthesize all of the components of RAS such as renin, the (pro)renin receptor, angiotensinogen, and Ang II receptors independently of the systemic RAS, thereby making the kidney capable of maintaining a high level of local Ang II (21,22). Hyperglycemia may activate the intrarenal RAS, leading to accumulation of Ang II in the kidney (22-24). Treatment of rat mesangial cells cultured *in vitro* with Ang II increased the expression of TGF- β_1 and ECM proteins while the competitive inhibitor of Ang II, saralasin, inhibited that expression (6). These results coincide with the current findings that blocking the Ang II pathway with valsartan decreased the serum level of TGF- β_1 in rats with diabetic

nephropathy. The current results are also consistent with findings from previous studies that LMWH significantly diminished the serum level of TGF- β_1 in diabetic rats. TGF- β_1 plays a key role in increasing glomerular permeability by stimulating ECM protein synthesis, increasing matrix protein receptors, and altering the protease/protease-inhibitor balance, thereby inhibiting matrix degradation (25). Thus, these results suggest that inhibiting TGF- β_1 expression with valsartan or LMWH is associated with ameliorated glomerular permeability.

The current study showed that a low-dose combination of valsartan and LMWH offered better renoprotection in terms of decreasing urine protein excretion, indicating that combination therapy is better at ameliorating glomerular permeability. Although combination therapy had the same level of inhibition of TGF- β_1 expression as did monotherapy, a low-dose combination of valsartan and LMWH resulted in additional inhibition of TGF- β_1 expression. Since lower dosages of valsartan and LMWH were employed in the combination therapy, adverse effects of these drugs might thus be reduced. Given these facts, the current study suggests that a low-dose combination of valsartan and LMWH is better at treating diabetic nephropathy. However, further studies are needed to clarify the mechanism underlying the augmented renoprotective effects of this combination therapy.

In conclusion, the current data demonstrated that a low-dose combination of valsartan and LMWH was better at ameliorating glomerular permeability than was monotherapy at high doses in rats with diabetic nephropathy. This study hints at the benefits of combining valsartan and LMWH when treating diabetic nephropathy.

References

1. Ritz E, Rychlik I, Locatelli F, Halimi S. End-stage renal failure in type 2 diabetes: A medical catastrophe of worldwide dimensions. *Am J Kidney Dis.* 1999; 34:795-808.
2. Gruden G, Perin PC, Camussi G. Insight on the pathogenesis of diabetic nephropathy from the study of podocyte and mesangial cell biology. *Curr Diabetes Rev.* 2005; 1:27-40.
3. Campbell KN, Raij L, Mundel P. Role of angiotensin II in the development of nephropathy and podocytopathy of diabetes. *Curr Diabetes Rev.* 2011; 7:3-7.
4. Chan JC, Ko GT, Leung DH, Cheung RC, Cheung MY, So WY, Swaminathan R, Nicholls MG, Critchley JA, Cockram CS. Long-term effects of angiotensin-converting enzyme inhibition and metabolic control in hypertensive type 2 diabetic patients. *Kidney Int.* 2000; 57:590-600.
5. Chen S, Iglesias-de la Cruz MC, Jim B, Hong SW, Isono M, Ziyadeh FN. Reversibility of established diabetic glomerulopathy by anti-TGF-beta antibodies in db/db mice. *Biochem Biophys Res Commun.* 2003; 300:16-22.
6. Kagami S, Border WA, Miller DE, Noble NA. Angiotensin II stimulates extracellular matrix protein

- synthesis through induction of transforming growth factor-beta expression in rat glomerular mesangial cells. *J Clin Invest.* 1994; 93:2431-2437.
7. Nakamura T, Fujiwara N, Sato E, Ueda Y, Sugaya T, Koide H. Renoprotective effects of various angiotensin II receptor blockers in patients with early-stage diabetic nephropathy. *Kidney Blood Press Res.* 2010; 33:213-220.
 8. Muller DN, Luft FC. Direct renin inhibition with aliskiren in hypertension and target organ damage. *Clin J Am Soc Nephrol.* 2006; 1:221-228.
 9. Yang SY, Hu ZY, Cao H, Yang T, Yu GH. Effect of angiotensin II receptor antagonist on renin-angiotensin system in main organs of spontaneously hypertensive rats. *Chinese Circulation Journal.* 2000; 15:56-58.
 10. Gambaro G, Cavazzana AO, Luzi P, Piccoli A, Borsatti A, Crepaldi G, Marchi E, Venturini AP, Baggio B. Glycosaminoglycans prevent morphological renal alterations and albuminuria in diabetic rats. *Kidney Int.* 1992; 42:285-291.
 11. Lewis EJ, Xu X. Abnormal glomerular permeability characteristics in diabetic nephropathy: Implications for the therapeutic use of low-molecular weight heparin. *Diabetes Care.* 2008; 31(Suppl 2):S202-S207.
 12. van der Pijl JW, van der Woude FJ, Geelhoed-Duijvestijn PH, Frolich M, van der Meer FJ, Lemkes HH, van Es LA. Danaparoid sodium lowers proteinuria in diabetic nephropathy. *J Am Soc Nephrol.* 1997; 8:456-462.
 13. Weigert C, Brodbeck K, Haring HU, Gambaro G, Schleicher ED. Low-molecular-weight heparin prevents high glucose- and phorbol ester-induced TGF-beta 1 gene activation. *Kidney Int.* 2001; 60:935-943.
 14. Saxena B. Anti-hyperlipidemic activity of *Withania coagulans* in streptozotocin-induced diabetes: A potent anti-atherosclerotic agent. *Drug Discov Ther.* 2010; 4:334-340.
 15. Srivastava S, Gupta A, Agarwal GG, Natu SM, Uma S, Goel MM, Srivastava AN. Correlation of serum vascular endothelial growth factor with clinicopathological parameters in cervical cancer. *BioSci Trends.* 2009; 3:144-150.
 16. Matsumoto-Takasaka A, Horie J, Sakai K, Furui Y, Sato R, Kawakami H, Toma K, Takayanagi A, Shimizu N, Fujita-Yamaguchi Y. Isolation and characterization of anti-T-antigen single chain antibodies from a phage library. *BioSci Trends.* 2009; 3:87-95.
 17. Nishi H, Inoue Y, Kageshita T, Takata M, Ihn H. The expression of human high molecular weight melanoma-associated antigen in acral lentiginous melanoma. *BioSci Trends.* 2010; 4:86-89.
 18. Santos GA, Cunha IW, Rocha RM, Mello CA, Guimaraes GC, Fregnani JH, Lopes A. Evaluation of estrogen receptor alpha, estrogen receptor beta, progesterone receptor, and cKIT expression in desmoids tumors and their role in determining treatment options. *BioSci Trends.* 2010; 4:25-30.
 19. Henry S, Bigler S, Wang J. High throughput analysis of neural progenitor cell proliferation in adult rodent hippocampus. *BioSci Trends.* 2009; 3:233-238.
 20. Amorim RF, Godoy GP, Galvao HC, Souza LB, Freitas RA. Immunohistochemical assessment of extracellular matrix components in syndrome and non-syndrome odontogenic keratocysts. *Oral Dis.* 2004; 10:265-270.
 21. Carey RM, Siragy HM. The intrarenal renin-angiotensin system and diabetic nephropathy. *Trends Endocrinol Metab.* 2003; 14:274-281.
 22. Liebau MC, Lang D, Bohm J, Endlich N, Bek MJ, Witherden I, Mathieson PW, Saleem MA, Pavenstadt H, Fischer KG. Functional expression of the renin-angiotensin system in human podocytes. *Am J Physiol Renal Physiol.* 2006; 290:F710-719.
 23. Yoo TH, Li JJ, Kim JJ, Jung DS, Kwak SJ, Ryu DR, Choi HY, Kim JS, Kim HJ, Han SH, Lee JE, Han DS, Kang SW. Activation of the renin-angiotensin system within podocytes in diabetes. *Kidney Int.* 2007; 71:1019-1027.
 24. Zhang Z, Sun L, Wang Y, Ning G, Minto AW, Kong J, Quigg RJ, Li YC. Renoprotective role of the vitamin D receptor in diabetic nephropathy. *Kidney Int.* 2008; 73:163-171.
 25. Border WA, Okuda S, Languino LR, Sporn MB, Ruoslahti E. Suppression of experimental glomerulonephritis by antiserum against transforming growth factor beta 1. *Nature.* 1990; 346:371-374.

(Received February 02, 2011; Revised February 20, 2011; Accepted February 24, 2010)

Hemocytes and humoral factors in silkworm blood are cooperatively involved in sheep erythrocyte aggregation

Katsutoshi Imamura, Kenichi Ishii, Hiroshi Hamamoto, Kazuhisa Sekimizu*

The Laboratory of Microbiology, Graduate School of Pharmaceutical Sciences, The University of Tokyo, Tokyo, Japan.

ABSTRACT: Sheep red blood cells (SRBCs) rapidly aggregated when injected into the blood (hemolymph) of living silkworms. SRBCs also rapidly aggregated when incubated with hemolymph *in vitro*. SRBCs did not aggregate when incubated with single hemolymph components, hemocytes and cell-free plasma separated by centrifugation, whereas incubation with the mixture of components induced SRBC aggregation, suggesting that both hemocytes and plasma are required for the reaction. Treatment of hemocytes with sodium azide inhibited SRBC aggregation. On the other hand, SRBCs pre-incubated with hemocytes aggregated in the plasma, even in the presence of sodium azide. SRBC aggregation was not observed when the SRBCs were physically separated from the hemocytes by a polycarbonate filter. These findings suggest that SRBCs are directly attacked by hemocytes and become sensitive to humoral factors that cause SRBC aggregation.

Keywords: Silkworm, SRBC, aggregation, innate immunity, hemocyte, humoral factor

1. Introduction

During evolution, multicellular organisms acquired immune systems to eliminate pathogenic invaders. Host immunity is classified as innate immunity or acquired immunity. In mammals, innate immunity acts as a primary defense against infectious agents and contributes to the successive activation of adaptive immunity. Invertebrates, on the other hand, lack antibody-producing organs and rely solely on innate immunity to eliminate foreign substances in the body (1). Therefore, investigations of defense mechanisms against pathogens

in invertebrate animals are useful toward understanding how hosts overcome infectious diseases by innate immune responses.

Pattern recognition receptors (PRRs), such as peptidoglycan recognition proteins, beta-glucan recognition proteins, and lectins, trigger various defensive responses in innate immunity (2-4). These PRRs exist in immune cells or in plasma as soluble proteins; those that reside in immune cells comprise membrane bound forms and cytoplasmic soluble receptors. Binding of PRRs to foreign substances activates humoral and cellular responses. The molecular mechanisms of humoral immune reactions include antimicrobial peptide production (5-7) and melanization (8-10). Cellular immunity involves several types of hemocyte-dependent reactions, such as phagocytosis (11), nodulation (12,13), and encapsulation (3,14). Nodulation is a lectin-mediated reaction that entraps a large number of bacteria in a clot formed by aggregating hemocytes (12,13). Similar to nodulation, encapsulation is a reaction in which hemocytes surround larger substances such as parasites and latex beads (14). We recently demonstrated that an insect cytokine, paralytic peptide, in silkworms activates both humoral and cellular immune responses, leading to host resistance against bacterial infection (15,16). Coordinative regulation of the humoral and cellular immune systems seems to be critical for host animals to efficiently remove pathogens. Immune reactions in which humoral and cellular immunity act in concert, however, are rarely studied, and their regulatory mechanisms remain elusive.

In vitro sheep red blood cell (SRBC) aggregation tests are widely applied to study antigen-antibody reactions in mammals (17) and lectin-mediated defense reactions in the hemolymph of insects (18). Komano and Natori observed that SRBCs formed aggregates and were eventually hemolyzed when injected into the blood of the flesh fly, *Sarcophaga peregrina* (18). Moreover, Suzuki and colleagues reported that SRBCs pre-treated with trypsin and glutaraldehyde underwent aggregation mediated by unidentified lectin-like factors in the silkworm hemolymph (19). The roles of humoral and cellular immune factors in the recognition and removal of SRBCs in the insect body, however,

*Address correspondence to:

Dr. Kazuhisa Sekimizu, The Laboratory of Microbiology, Graduate School of Pharmaceutical Sciences, The University of Tokyo, 7-3-1 Hongo, Bunkyo-ku, Tokyo 113-0033, Japan.
e-mail: sekimizu@mol.f.u-tokyo.ac.jp

are poorly understood. Here we show that hemocytes directly recognize and modify the surfaces of SRBCs, and then humoral factors induce SRBC aggregation in the silkworm hemolymph.

2. Materials and Methods

2.1. Insects

Silkworm eggs (*B. mori*, Hu·Yo × Tukuba·Ne) were purchased from Ehime Sanshu (Ehime, Japan). Silkworm larvae were reared on an artificial diet (Silkmate 2S, Nihon Nosan, Yokohama, Japan) at 27°C.

2.2. Reagents

SRBCs, beta-mercaptoethanol, and TC100 were purchased from Nippon Biotest Laboratories Inc., Nakalai Tesque, and AppliChem, respectively. Sodium azide and 4',6-diamidino-2-phenylindole (DAPI) were purchased from Wako Pure Chemical Industries and Dojindo Laboratories, respectively, and dissolved in saline (0.9% NaCl) before use.

2.3. Preparation of hemocytes and the plasma fraction

Hemolymph was collected into a tube (containing 1.25% of beta-mercaptoethanol to avoid melanization) after cutting the abdominal legs of two silkworm larvae (day 2 of 5th instar). To obtain hemocytes and plasma fractions, the hemolymph was first centrifuged at $300 \times g$ for 5 min. The precipitate was washed twice with phosphate-buffered saline (PBS, pH 8.0) and then suspended with insect cell culture medium TC100 containing 10% fetal bovine serum. The supernatant was further centrifuged at $9,000 \times g$ for 5 min to obtain the plasma fraction.

2.4. In vitro SRBCs aggregation assay

A 2-mL sample of SRBCs was washed twice with 50 mL of PBS and suspended in 2 mL of PBS. A SRBC suspension (2 μ L) was mixed with 100 μ L of each sample in a microtiter plate (non-treated 96-well round bottom, Iwaki, Japan). In some experiments, 200 mM sodium azide was added to kill the hemocytes. After incubation at 27°C for 2 h, SRBC aggregation was visually judged based on the attachment of cells to the bottom of the wells.

2.5. DAPI staining of hemocytes

The SRBCs were incubated with silkworm hemolymph at 27°C for 1 h. A 100- μ L aliquot of each sample was then mixed with 0.5 mL of 10 mg/mL DAPI and stained for 1 h. The remaining DAPI was washed in PBS three times. The morphology of cells and fluorescent nuclei was observed under an inverted fluorescence microscope (Leica, Tokyo, Japan).

3. Results

3.1. SRBC aggregation depends on both hemocytes and humoral factors in the silkworm hemolymph

Red-colored aggregates were observed in the silkworm hemolymph harvested 15 min after injecting the SRBCs (Figure 1B). We then tested whether SRBCs mixed with the silkworm hemolymph aggregated *in vitro*. When SRBCs suspended in PBS were applied to U-shaped wells and incubated for 2 h, the SRBCs precipitated to the center of the wells and appeared as spots (Figure 2A). In contrast, when the SRBCs were incubated with the silkworm hemolymph, they spread out and attached to the bottom of the wells to form aggregates (Figure 2B). Microscopic analysis revealed that when SRBCs were incubated alone in PBS, each cell remained separated from the other (Figure 2C), whereas those incubated in the hemolymph adhered together to form large clumps (Figure 2D). Based on the similar morphologic appearances of SRBC aggregates formed either *in vitro* or *in vivo*, further studies of the SRBC

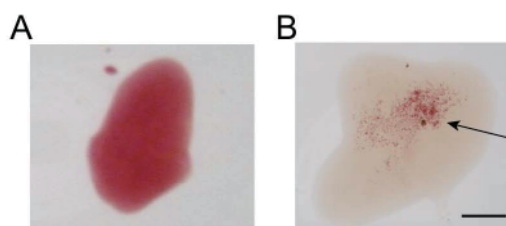


Figure 1. In vivo aggregation of SRBCs in the hemolymph of live silkworms. Silkworm hemolymph was collected immediately (A), or 15 min (B) after injecting SRBCs into the hemolymph and was observed under a microscope. Arrow indicates SRBC clumps. Bar; 5 mm.

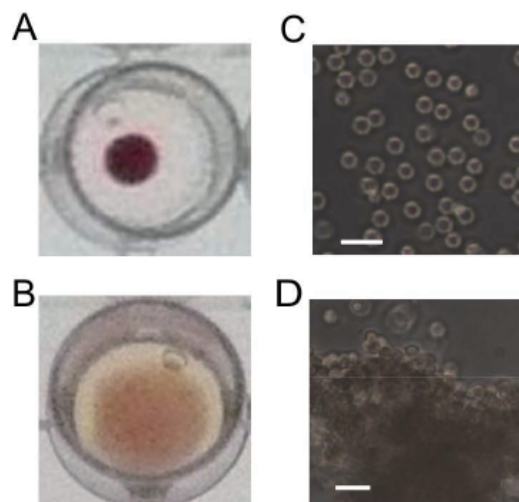


Figure 2. In vitro aggregation of SRBCs in the silkworm hemolymph. SRBCs in PBS (A, C) or silkworm hemolymph (B, D) were incubated at 27°C for 2 h in a microtiter plate. A and B; microscopic views of suspended samples of C and D, respectively. Bar; 10 μ m.

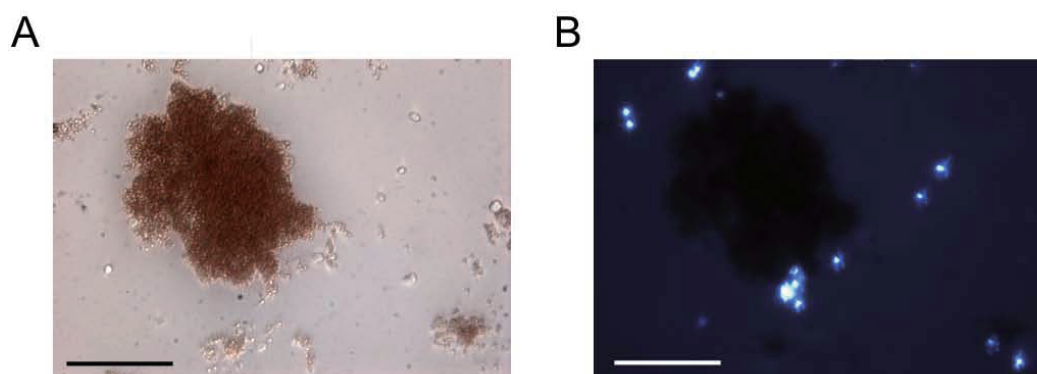


Figure 3. DAPI staining of hemocytes incorporated in clumps of SRBCs. Hemocytes were stained with DAPI. Clumps of SRBCs formed by incubation with silkworm hemolymph observed under a bright-field (A) or fluorescence (B) microscope. Bar; 100 μ m.

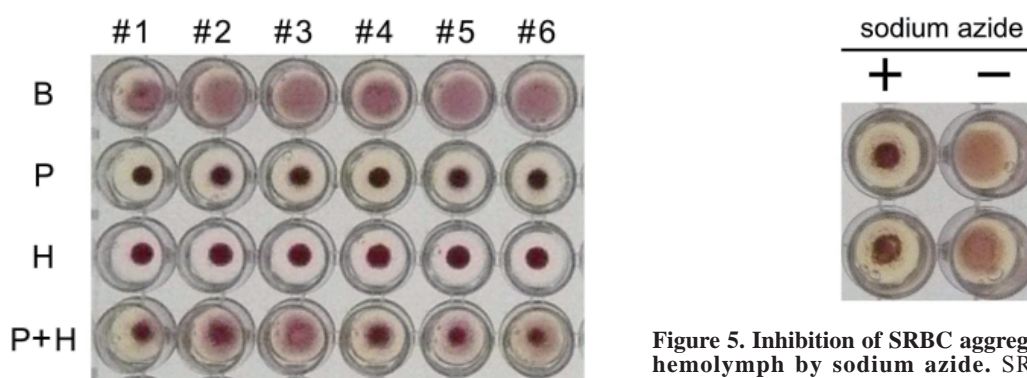


Figure 4. Aggregation of SRBCs depending on both hemocytes and humoral factors in the silkworm hemolymph. Hemolymph fractions from 6 independent silkworms were separated into hemocytes and plasma. Numbers indicate different batches of silkworms. SRBCs incubated with hemolymph (B), plasma (P), hemocytes (H), and mixtures of plasma and hemocytes (P + H).

aggregation reaction were performed *in vitro* using isolated hemolymph.

Encapsulation and nodulation are hemocyte-dependent aggregation reactions of foreign substances in insects (13,14). In these reactions, hemocytes surround non-self substances to form clots. To test whether hemocytes were incorporated into the clumps of SRBCs under our experimental conditions, we used DAPI to stain the hemocyte nuclei. Analysis under fluorescence microscopy revealed only a few DAPI-positive cells in the SRBC clumps that formed in the hemolymph (Figure 3). Therefore, we assumed that the aggregation of SRBCs induced by silkworm hemolymph was distinct from other cellular responses, such as encapsulation and nodulation in which hemocytes are present in the clots.

We then separated hemocytes and plasma from silkworm hemolymph by centrifugation to test their abilities to aggregate SRBCs *in vitro*. SRBCs incubated with either hemocytes or plasma alone did not aggregate, while those incubated in a mixture of hemocytes and plasma did aggregate (Figure 4). These results suggest that the aggregation of SRBCs in the silkworm hemolymph requires both hemocytes and plasma factors.

Figure 5. Inhibition of SRBC aggregation in the silkworm hemolymph by sodium azide. SRBCs incubated with hemolymph in the presence (+) or absence (-) of 200 mM sodium azide were observed from the top.

3.2. Requirement of direct interaction of hemocytes and SRBCs for the aggregation reaction

We further examined whether hemocyte viability was necessary for the SRBC aggregation. SRBC aggregation in the hemolymph was inhibited by the addition of sodium azide, a cytotoxic agent (Figure 5). When cells were stained with trypan blue, the addition of sodium azide reduced the ratio of trypan blue-negative cells from 100% to less than 10% (data not shown). These results indicate that viable hemocytes are required for the SRBC aggregation induced by silkworm hemolymph.

To elucidate the mechanism of the SRBC aggregation reactions mediated by both hemocytes and humoral factors, we tested the effect of pre-incubation of SRBCs with isolated hemocytes. When SRBCs were incubated with hemocytes prior to the addition of silkworm plasma, SRBC aggregation proceeded even when sodium azide was added. In contrast, SRBCs that were not pre-incubated with hemocytes did not form aggregates in the plasma (Figure 6). These findings suggest that SRBCs are initially attacked by hemocytes in the hemolymph and made vulnerable to humoral factors in plasma that induce the SRBC aggregation process.

We then tested whether direct interaction with hemocytes was needed for the SRBC aggregation.

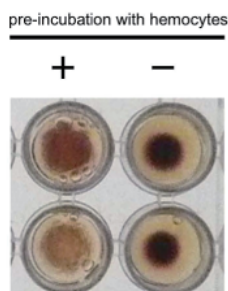


Figure 6. The effect of pre-incubation of SRBCs with hemocytes on SRBC aggregation in the presence of sodium azide. SRBCs pre-incubated with (+) or without (-) hemocytes were mixed with sodium azide-containing plasma, and incubated at 27°C for 2 h.

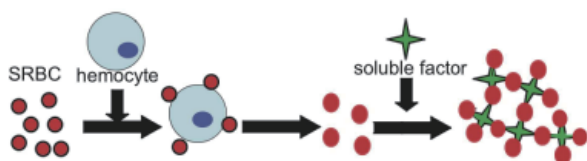


Figure 7. Proposed mechanism of SRBC aggregation in silkworm hemolymph.

Incubation of SRBCs in the plasma fraction that were physically separated from the hemocytes using a polycarbonate membrane filter that was permeable to soluble proteins did not lead to SRBC aggregation (data not shown). This result suggests that direct contact of hemocytes with SRBCs is required for SRBC aggregation in silkworm hemolymph.

4. Discussion

Here we describe a novel defense mechanism involving sequential contributions of hemocytes and soluble factors in the hemolymph plasma that were required for SRBC aggregation in silkworm hemolymph (Figure 7). This finding provides the first evidence that foreign substances are directly attacked by insect hemocytes, followed by clot formation induced by humoral factors.

Both cellular and humoral immunity are involved in the process of nodulation. Sato and colleagues reported that lectins in the hemolymph of silkworms bind to foreign substances, which are surrounded by an assembly of hemocytes to form nodules (12,20). Here we report that hemocytes first attacked the foreign substances, SRBCs, and then humoral factors aggregated the SRBCs. Furthermore, we showed that hemocytes were not incorporated into the clump of SRBCs formed in the hemolymph. Based on these findings, we consider that SRBC aggregation involving hemocytes and plasma factors is distinct from other self-defense reactions, such as nodulation and encapsulation.

Suzuki and Natori reported that lectin-like proteins in silkworm hemolymph aggregate trypsin- and glutaraldehyde-treated SRBCs (19). We assume that

the factors in the silkworm plasma that cooperate with hemocytes might be similar to the lectin-like proteins reported by Suzuki. Moreover, we found that direct interactions of SRBCs with hemocytes are necessary for the silkworm hemolymph to induce SRBC aggregation. Thus, the hemocyte attack on SRBCs might correspond to the trypsin and glutaraldehyde treatment of SRBCs required for the silkworm lectin-like proteins to induce SRBC aggregation (19).

Hemocytes circulating in silkworm hemolymph are classified into five subtypes, prohemocytes, plasmatocytes, granulocytes, spherulocytes, and oenocytoids (21,22). Among them, granulocytes are one of the major cell types responsible for defensive responses, and they attach to small foreign substances, such as SRBCs, by elongating their filopodia (23).

Thus, we speculate that granulocytes are a plausible candidate hemocyte subtype that directly interacts with SRBCs to form aggregates. Recently, Nakahara and colleagues established a fluorescence activated cell sorting-based method to separate each subtype of silkworm hemocyte from the hemolymph (22). Application of such methods will allow for the identification of the hemocyte subtypes involved in the aggregation of foreign substances.

Acknowledgements

This work was supported by Grant-in-aid for Young Scientists (B) 21790063 and Grant-in-aid for Japan Society for the Promotion of Science Fellows 2110519 from Japan Society for the Promotion of Science. We thank Kiyomi Kyougoku, Yumiko Matsuzawa, and Aya Yoshino for technical assistance.

References

1. Janeway CA Jr, Medzhitov R. Innate immune recognition. *Annu Rev Immunol.* 2002; 20:197-216.
2. Basbous N, Coste F, Leone P, Vincentelli R, Royet J, Kellenberger C, Roussel A. The *Drosophila* peptidoglycan-recognition protein LF interacts with peptidoglycan-recognition protein LC to downregulate the Imd pathway. *EMBO Rep.* 2011; 12:327-333.
3. Yang J, Wang L, Zhang H, Qiu L, Wang H, Song L. C-Type Lectin in *Chlamys farreri* (CfLec-1) mediating immunorecognition and opsonization. *PLoS One.* 2011; 6: e17089.
4. Goodridge HS, Wolf AJ, Underhill DM. Beta-glucan recognition by the innate immune system. *Immunol Rev.* 2009; 230:38-50.
5. Boman HG, Faye I, Gudmundsson GH, Lee JY, Lidholm DA. Cell-free immunity in *Cecropia*. A model system for antibacterial proteins. *Eur J Biochem.* 1991; 201:23-31.
6. Natori S, Shiraishi H, Hori S, Kobayashi A. The roles of *Sarcophaga* defense molecules in immunity and metamorphosis. *Dev Comp Immunol.* 1999; 23:317-328.
7. Okada M, Natori S. Purification and characterization of an antibacterial protein from haemolymph of *Sarcophaga peregrina* (flesh-fly) larvae. *Biochem J.*

- 1983; 211:727-734.
8. An C, Budd A, Kanost MR, Michel K. Characterization of a regulatory unit that controls melanization and affects longevity of mosquitoes. *Cell Mol Life Sci.* 2011; 68:1929-1939.
 9. Kan H, Kim CH, Kwon HM, Park JW, Roh KB, Lee H, Park BJ, Zhang R, Zhang J, Söderhäll K, Ha NC, Lee BL. Molecular control of phenoloxidase-induced melanin synthesis in an insect. *J Biol Chem.* 2008; 283:25316-25323.
 10. Ishii K, Hamamoto H, Imamura K, Adachi T, Shoji M, Nakayama K, Sekimizu K. *Porphyromonas gingivalis* peptidoglycans induce excessive activation of the innate immune system in silkworm larvae. *J Biol Chem.* 2010; 285:33338-33347.
 11. Hashimoto Y, Tabuchi Y, Sakurai K, Kutsuna M, Kurokawa K, Awasaki T, Sekimizu K, Nakanishi Y, Shiratsuchi A. Identification of lipoteichoic acid as a ligand for draper in the phagocytosis of *Staphylococcus aureus* by *Drosophila* hemocytes. *J Immunol.* 2009; 183:7451-7460.
 12. Watanabe A, Miyazawa S, Kitami M, Tabunoki H, Ueda K, Sato R. Characterization of a novel C-type lectin, *Bombyx mori* multibinding protein, from the *B. mori* hemolymph: Mechanism of wide-range microorganism recognition and role in immunity. *J Immunol.* 2006; 177:4594-4604.
 13. Koizumi N, Morozumi A, Imamura M, Tanaka E, Iwahana H, Sato R. Lipopolysaccharide-binding proteins and their involvement in the bacterial clearance from the hemolymph of the silkworm *Bombyx mori*. *Eur J Biochem.* 1997; 248:217-224.
 14. Ling E, Yu XQ. Cellular encapsulation and melanization are enhanced by immulectins, pattern recognition receptors from the tobacco hornworm *Manduca sexta*. *Dev Comp Immunol.* 2006; 30:289-299.
 15. Ishii K, Hamamoto H, Kamimura M, Sekimizu K. Activation of the silkworm cytokine by bacterial and fungal cell wall components *via* a reactive oxygen species-triggered mechanism. *J Biol Chem.* 2008; 283:2185-2191.
 16. Ishii K, Hamamoto H, Kamimura M, Nakamura Y, Noda H, Imamura K, Mita K, Sekimizu K. Insect cytokine paralytic peptide (PP) induces cellular and humoral immune responses in the silkworm *Bombyx mori*. *J Biol Chem.* 2010; 285:28635-28642.
 17. Licence ST, Binns RM. Analysis of a sheep anti-pig T lymphoblast serum with specificity for E rosette-forming lymphocytes. *Vet Immunol Immunopathol.* 1984; 7:255-273.
 18. Komano H, Natori S. Participation of *Sarcophaga peregrina* humoral lectin in the lysis of sheep red blood cells injected into the abdominal cavity of larvae. *Dev Comp Immunol.* 1985; 9:31-40.
 19. Suzuki T, Natori S. Identification of a protein having hemagglutinating activity in the hemolymph of the silkworm, *Bombyx mori*. *J Biochem.* 1983; 93:583-590.
 20. Koizumi N, Imai Y, Morozumi A, Imamura M, Kadotani T, Yaoi K, Iwahana H, Sato R. Lipopolysaccharide-binding protein of *Bombyx mori* participates in a hemocyte-mediated defense reaction against gram-negative bacteria. *J Insect Physiol.* 1999; 45:853-859.
 21. Beaulaton J. Hemocytes and hemocytopoiesis in Silkworms. *Biochimie.* 1979; 61:157-164.
 22. Nakahara Y, Shimura S, Ueno C, Kanamori Y, Mita K, Kiuchi M, Kamimura M. Purification and characterization of silkworm hemocytes by flow cytometry. *Dev Comp Immunol.* 2009; 33:439-448.
 23. Wago H. Humoral factors promoting the adhesive properties of the granular cells and plasmatocytes of the silkworm, *Bombyx mori*, and their possible role in the initial cellular reactions to foreignness. *Cell Immunol.* 1980; 54:155-169.

(Received April 27, 2011; Revised May 13, 2011; Accepted May 15, 2011)

Arabino-mycolates derived from cell-wall skeleton of *Mycobacterium bovis* BCG as a prominent structure for recognition by host immunity

Masanori Miyuchi^{1,*}, Masashi Murata¹, Keiko Shibuya¹, Erina Koga-Yamakawa¹, Yuko Uenishi², Naoto Kusunose¹, Makoto Sunagawa², Ikuya Yano³, Yasuo Kashiwazaki¹

¹ Drug Research Division, Dainippon Sumitomo Pharma Co., Ltd., Osaka, Japan;

² Technology Research & Development Division, Dainippon Sumitomo Pharma Co., Ltd., Osaka, Japan;

³ Japan BCG Central Laboratory, Tokyo, Japan.

ABSTRACT: Arabino-mycolates are components of the cell-wall skeleton of *Mycobacterium bovis* BCG (BCG-CWS). It is known that synthesized arabino-mycolates induce the production of tumor necrosis factor alpha (TNF- α) in murine macrophage cell lines at an intensity similar to that of BCG-CWS. However the immunological activity of natural arabino-mycolates isolated from BCG has not been investigated, probably due to the complexity of the molecule. In this paper, we investigated the immunostimulatory activity of arabino-mycolates isolated from BCG-CWS by acid hydrolysis. Arabino-mycolates obtained by acid hydrolysis from the originally prepared CWS (SMP-105) of *M. bovis* BCG Tokyo 172 strain consisted mainly of mono-arabinose mono-mycolate, penta-arabinose tetra-mycolate and hexa-arabinose tetra-mycolate fractions. Arabino-mycolates significantly induced TNF- α production with an intensity comparable to that of CWS and enhanced delayed type hypersensitivity (DTH) reactions against inactivated tumor cells. Arabino-mycolates-induced TNF- α production was completely dependent on TLR2 and MyD88 pathways. These findings indicate that isolated natural arabino-mycolates possess potent adjuvant immunostimulatory activity.

Keywords: Arabino-mycolates, TLR2, BCG-CWS, SMP-105

1. Introduction

The cell-wall skeleton (CWS) of *Mycobacterium bovis* BCG (BCG-CWS), a microbial adjuvant, has intensively been investigated for decades, and has consequently been shown to possess promising activity as a cancer immunotherapeutic agent (1-4). Toll-like receptors (TLRs) have been characterized as pattern-recognition receptors that recognize microbial components (5,6). Stimulation of macrophages and dendritic cells *via* TLRs induces production of cytokines and chemokines, and creates bridges to establish acquired immunity. Recent studies suggest that BCG-CWS induces cytokines and antitumor activity through TLR2 (7,8). However, due to the complexity of BCG-CWS, it is not clear which motif is essential for stimulating immunity or TLR2 agonistic activity.

BCG-CWS has a high molecular weight and is reported to be a mycoloyl-arabinogalactan-peptidoglycan complex. We have tried to shed light on the arabino-mycolate moiety of BCG-CWS and analyze its structure and biological activity. GC-MS and NMR of cell wall arabinogalactan oligosaccharide fragments revealed that the arabinogalactan contains a homogalactan segment of alternating 5-linked α -galactofuranosyl (Gal f) and 6-linked β -Gal f residues, and arabinan segments consisting of two major domains: a linear 5-linked arabinofuranosyl (α -Ara f) unit with branching introduced by 3,5- α -Ara f and branched oligosaccharides [β -Ara f -(1-2)-Ara f]₂-3,5- α -Ara f at the nonreducing termini (9). Separately, synthesized mycolic esters of the arabinan in the terminal lipo-arabinan motif have been shown to induce production of TNF- α (10). Although some glycolipids that do not constitute BCG-CWS, such as trehalose 6,6'-dimycolate (TDM), lipoarabinomannans, and phosphatidylinositol mannosides, have energetically been studied (11-15), arabino-mycolates that constitute BCG-CWS have not been investigated. We therefore were interested in isolating BCG-CWS arabino-mycolates and investigating their structural properties and immunostimulatory activity. Uenishi *et al.* have developed a unique method

*Address correspondence to:

Dr. Masanori Miyuchi, Drug Research Division, Dainippon Sumitomo Pharma Co., Ltd., 3-1-98, Kasugade-naka, Konohana-ku, Osaka-shi, Osaka, 554-0022, Japan.

e-mail: masanori-miyuchi@ds-pharma.co.jp

for isolation of arabino-mycolates derived from the cell-wall skeleton of *M. bovis* BCG Tokyo (SMP-105) (16). By making use of this method, particularly the isolated fraction consisting mainly of mono-arabinose mono-mycolate, tetra-arabinose tetra-mycolate, penta-arabinose tetra-mycolate and hexa-arabinose tetra-mycolate (Figure 1), we proceeded with our structural and biological investigation of BCG-CWS arabino-mycolates.

In this paper, we demonstrate that arabino-mycolates isolated from CWS activate macrophages *via* the TLR2-MyD88 pathway *in vitro* and have potent adjuvant activity *in vivo*. The mechanism of cell-mediated immunity activation by a giant insoluble BCG-CWS will be addressed in the context of digestive degradation reported in our previous paper (17).

2. Materials and Methods

2.1. Preparation of cell-wall skeleton (CWS) and arabinomycolates

CWS (SMP-105) was prepared from *M. bovis* BCG Tokyo 172 strain as previously described (18), and arabinomycolates were isolated as indicated elsewhere (16). In brief, a CWS suspension in toluene/0.1 mol/L hydrochloric acid (1:1, v/v) was heated at 100°C for about 1.5 hours. The toluene layer, taken as the portion containing the arabinomycolates was washed with water and then evaporated. The residual arabino-

mycolates were developed on silica gel HPTLC (Silica gel 60, 10 × 10 cm, Merck Ltd., Darmstadt, Germany) with a solvent containing chloroform/acetone/acetic acid/methanol (90:6:1:10, v/v) for further purification, which revealed multiple spots. The major spots, called A, B, B1, C and D, were deduced to be penta-arabinose tetra-mycolate, hexa-arabinose tetra-mycolate, mono-arabinose mono-mycolate, hepta-arabinose tetra-mycolate, and octa-arabinose tetra-mycolate, respectively. The A, B and B1 spots were selected as arabinomycolates for investigation of biological activity. The yield of refined arabinomycolates was approximately 17.9%.

2.2. Trehalose 6,6'-dimycolate (TDM)

TDM was prepared as described previously (4). In brief, lipids were extracted from heat-killed *M. bovis* BCG Tokyo 172 strain with chloroform/methanol (2:1, v/v). After the lower phase of two phases containing major glycolipids was collected, the solvent was evaporated in a rotary evaporator. Total lipids were then separated by thin-layer chromatography (TLC) on silica plates (Uniplate; Analtech, DE, USA), and TDM was recovered from the plate immediately after the iodine color had disappeared by passing through a small glass column. TDM was further purified by repeated TLC until a single spot was obtained.

2.3. Reagents

Pam3CSK4 was purchased from Calbiochem (Merck, Tokyo, Japan). *Escherichia coli* J5 lipopolysaccharide (LPS) was purchased from LIST Biological Laboratories (Campbell, CA, USA), and further purified using a phenol extraction method (19-21).

2.4. Animals

C57BL/6J female mice were purchased from Japan SLC (Shizuoka, Japan). TLR2 (22)-, TLR4 (23)- and MyD88 (24)-deficient mice were obtained from Oriental Bio Service (Kyoto, Japan). All mice were maintained under specific pathogen-free conditions. All animal experiments were conducted according to the guidelines of the Animal Care and Use Committee at Dainippon Sumitomo Pharma.

2.5. Cell lines

Murine macrophage cell line RAW264.7 was purchased from American Type Culture Collection (Manassas, VA, USA), and was maintained in DMEM (Sigma-Aldrich, MO, USA) supplemented with 10% FCS, 2 mM L-glutamine, 50 U/mL of penicillin, and 50 µg/mL of streptomycin. Lewis lung carcinoma (3LL) was obtained from the Cancer Institute for the Japanese

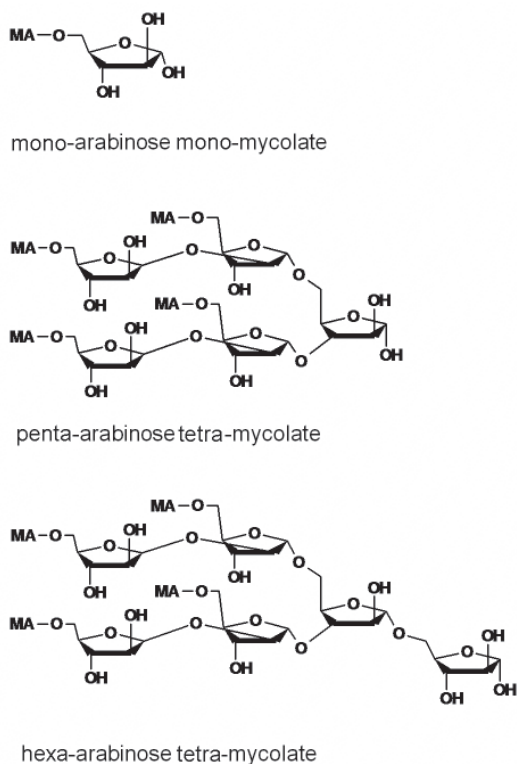


Figure 1. Structure of arabinomycolate fragments obtained from CWS of *M. bovis* BCG Tokyo 172. MA, mycolic acid.

Foundation for Cancer Research (Tokyo, Japan). 3LL cells were maintained in RPMI-1640 medium supplemented with 10% fetal calf serum (FCS), 50 µg/mL of streptomycin, and 50 U/mL of penicillin. To prepare inactivated 3LL, 3LL cells were incubated at 37°C for 20 min at 1×10^7 cells/mL in a culture medium containing 200 µg/mL of mitomycin C (Kyowa Hakko Kogyo, Tokyo, Japan), followed by repeated washing with sufficient culture medium.

2.6. Preparation of mouse peritoneal exudate cells

Thioglycollate-elicited peritoneal exudate cells (TG-PEC) were prepared from mice 5 days after intraperitoneal injection of 3% thioglycollate medium (Difco; Becton Dickinson Japan, Tokyo, Japan), and seeded at 5×10^5 cells/well in a 96-well plate. After removal of non-adherent cells by washing, adherent macrophages were treated with 1 ng/mL of recombinant mouse IFN-γ (R&D Systems, MN, USA) for 2 hours.

2.7. TNF-α induction assay

For experiments using RAW264.7 cells, CWS and arabino-mycolates were suspended in hexane/ethanol (9:1, v/v) and dispensed into 96-well polypropylene microplates before the solvent was evaporated in a clean bench. RAW264.7 cells were then seeded at 5×10^4 cells/well and cultured overnight.

For TG-PEC, a suspension of CWS or arabino-mycolates was prepared in saline containing 0.01% polysorbate 80 using a Potter-type homogenizer at 1,200 rpm for 5 min. TG-PEC was cultured overnight with the suspension of CWS or arabino-mycolates. The concentrations of TNF-α in the supernatants were determined by enzyme-linked immunosorbent assay (ELISA) (R&D Systems; Minneapolis, MN, USA).

2.8. Delayed type hypersensitivity (DTH) reaction

Inactivated 3LL cells (3×10^4 cells) in an oil-in-water emulsion of vehicle, CWS (12.5 µg), or arabino-mycolates (12.5 µg) were intradermally administered twice with a 7-day interval between injections into the left flank region of C57BL/6J mice.

Seven days after the second administration, inactivated 3LL cells (10^5 cells in 50 µL Hanks' Balanced Salt Solution) were inoculated into the left hind footpads of mice. Just before and 24 hours after inoculation, the thickness of the left footpad was measured using a dial gauge (Mitsutoyo Corp., Kanagawa, Japan). Percentage swelling of the footpad was calculated according to the following equation:

Footpad swelling (%) = $(\text{thickness of post-injected footpad (mm)} - \text{thickness of pre-injected footpad (mm)}) / \text{thickness of pre-injected footpad (mm)}$

The emulsion was prepared as follows; A four hundred micro liter aliquot of CWS or arabino-mycolates suspension dispersed in chloroform at 2 mg/mL was taken in a Potter-type homogenizer and 5.7 µL of squalane was added, followed by evaporation of the chloroform. Next, 0.66 mL of 5.1% (w/v) mannitol solution containing 1% (w/v) polysorbate 80 was added, and the mixture was homogenized at 2,000 rpm for 10 min with a Potter-type homogenizer. The composition of the vehicle was the same except for CWS or arabino-mycolates.

2.9. Statistical analysis

Results from all experiments are expressed as mean ± standard deviation (S.D.). Significant differences in DTH reaction were assessed using Dunnett's multiple comparison. Statistical analyses were carried out using SAS software (SAS Institute; Cary, NC, USA).

3. Results

3.1. Arabino-mycolates induce production of TNF-α in RAW264.7 cells

To confirm that arabino-mycolates activate macrophages, we investigated the ability of arabino-mycolates isolated from CWS to induce TNF-α production in RAW264.7 cells. Arabino-mycolates dose-dependently induced TNF-α production in RAW264.7 cells with an intensity similar to that of CWS (Figure 2a). This finding indicates

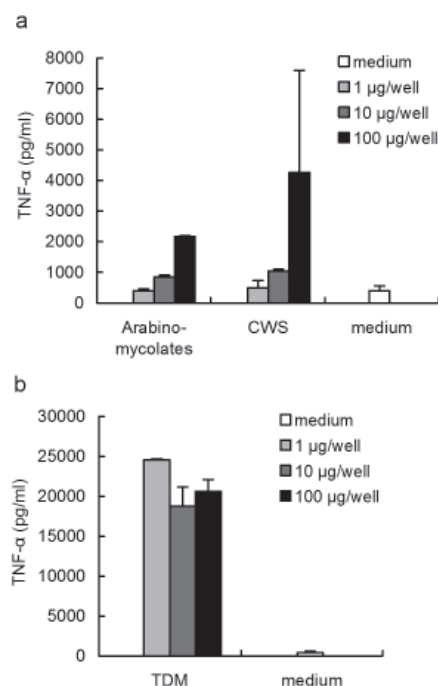


Figure 2. CWS and arabino-mycolates induced production of TNF-α in RAW264.7 cells. RAW264.7 cells were cultured in microplates absorbing CWS or arabino-mycolates (a) or TDM (b) overnight. TNF-α in the supernatant was determined by ELISA. Values are expressed as the means ± S.D. of triplicate determinations.

that arabino-mycolates stimulate innate immunity. Like CWS and arabino-mycolates, TDM, a mycolic ester of saccharides contained in the cell wall of mycobacteria, also induced TNF- α production in RAW264.7 cells (Figure 2b). The amount of TNF- α induced by TDM was greater than that induced by CWS or arabino-mycolates.

3.2. Arabino-mycolates activate TG-PEC in a TLR-2-dependent manner

To evaluate the effects of arabino-mycolates on TLRs, we next examined the ability of TG-PECs derived from TLR2, TLR4, or MyD88 knockout mice to induce TNF- α production. CWS and Pam3CSK4 (two TLR2 agonists), and LPS (a TLR4 agonist) were used as controls. As expected, CWS and Pam3CSK4 induced TNF- α production in TG-PEC derived from WT and TLR4 knockout mice, but not in TG-PEC derived from TLR2 or MyD88 knockout mice. LPS on the other hand induced TNF- α production in TG-PEC derived from WT and TLR2 knockout mice, but not in TG-PEC derived from TLR4 or MyD88 knockout mice. As in RAW264.7 cells, arabino-mycolates induced TNF- α production in TG-PEC derived from wild type mice, but not in TG-PEC derived from TLR2 or MyD88 knockout mice (Figure 3). Arabino-mycolates also induced TNF- α production in TG-PEC derived from TLR4 knockout mice with an intensity comparable to that found in wild type mice. These results indicate that the mycolyl-arabino structure activates TG-PEC in a TLR-2-/MyD88- dependent manner.

3.3. Arabino-mycolates enhance a DTH reaction

We next evaluated the ability of arabino-mycolates to stimulate innate immunity using a DTH reaction

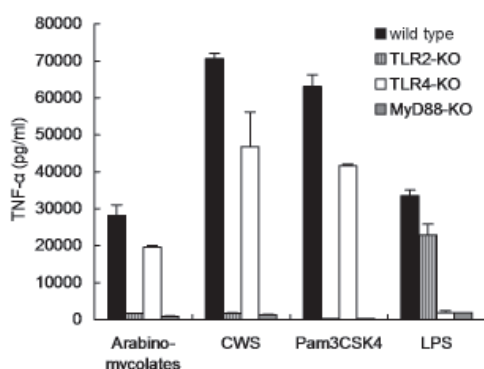


Figure 3. Arabino-mycolates induced production of TNF- α in TG-PEC derived from different mice. TG-PEC derived from wild type mice (black bar), TLR2 knockout (KO) mice (vertical stripes), TLR 4 KO mice (white bar), or MyD88 KO mice (gray bar) were cultured in the presence of 1 ng/mL of recombinant mouse interferon- γ with a medium control, CWS (100 μ g/mL), arabino-mycolates (100 μ g/mL), Pam3CSK4 (1 μ g/mL) or LPS (1 μ g/mL). After 18 hours, each supernatant was collected and the concentration of TNF- α was determined by ELISA. Values are expressed as the means \pm S.D. of triplicate determinations.

in mice. C57BL/6J mice were twice (once weekly) sensitized with mitomycin C treated 3LL tumor cells as antigen and CWS or arabino-mycolates as adjuvant. The mice were elicited one week after the 2nd sensitization by administration of the antigen only into the hind footpad. The DTH reaction was accessed by footpad swelling 24 hours after elicitation. CWS significantly enhanced the DTH reaction in mice (Figure 4). Arabino-mycolates on the other hand moderately enhanced DTH, which was significantly evoked with the vehicle. These findings indicate that arabino-mycolates induce establishment of T cell immunity. We think that the DTH results are consistent with the results of arabino-mycolates induction of TNF- α production *in vitro*.

4. Discussion

To our knowledge, this study is the first to demonstrate the immunostimulatory activity of arabino-mycolates isolated from CWS, although CWS itself has previously been reported to induce TNF- α in murine TG-PEC (8), and synthesized arabino-mycolates have been shown to induce TNF- α in RAW264.7 cells (10). Using a recently reported method for isolation of mycolic esters of arabinan (10,16), we isolated fractions containing the mono-arabinose mono-mycolate, penta-arabinose tetra-mycolate, and hexa-arabinose tetra-mycolate (Figure 1) and used them to investigate arabino-mycolates immunological activity. We found that arabino-mycolates activate macrophages *via* the TLR2-MyD88 pathway *in vitro*, and possess potent adjuvant activity in a DTH model.

Arabino-mycolates induced TNF- α production in RAW264.7 cells with an intensity similar to that of

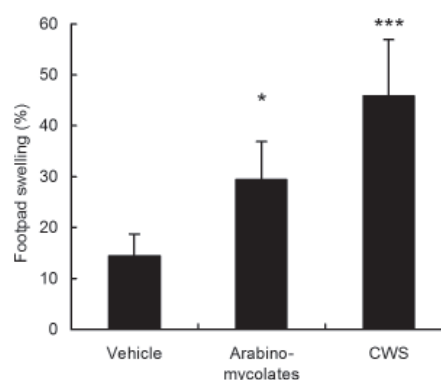


Figure 4. Effects of arabino-mycolates from CWS on delayed-type hypersensitivity reaction against 3LL tumor cells. Inactivated 3LL cells (3×10^4 cells) in an oil-in-water emulsion of vehicle, CWS (12.5 μ g) or arabino-mycolates (12.5 μ g) were intradermally administered twice with a 7-day interval between injections into the left flank region of C57BL/6J mice. Seven days after the second administration, inactivated 3LL cells (10^5 cells) were inoculated into the left footpads and swelling was monitored by measuring the thickness of the footpads 24 hours after inoculation, * $p < 0.05$; *** $p < 0.001$ (parametric Dunnett's test for multiple comparisons; compared to vehicle). Values are expressed as the means \pm S.D. of six mice.

CWS. This finding indicates that arabino-mycolates stimulate innate immunity (Figure 2a). Uenishi *et al.* have shown that CWS from *M. bovis* BCG Tokyo 172 contains 38.8% mycolic acid and 23.0% arabinose (18). Considering that the mycolate and arabinose constitute over half of the CWS, the amount of TNF- α produced by CWS seems to be consistent with the arabino-mycolate moiety.

We have previously reported that CWS activates the immune response in a TLR2-/MyD88- dependent manner (8). Accordingly, in this study arabino-mycolates induced TNF- α production in RAW264.7 cells as well as in TG-PEC derived from wild type mice, but not in TG-PEC derived from TLR2 or MyD88 knockout mice (Figure 3). In addition, and as expected, arabino-mycolates induced TNF- α production in TG-PEC derived from TLR4 knockout mice with an intensity comparable to that in wild type mice. Because neither mycolate nor arabinose can induce production of TNF- α (10), we postulate the mono-arabinose mono-mycolate as the smallest binding motif for TLR2. It is also likely that TLR2 dimerizes with different TLRs, *i.e.* TLR1 or TLR6, to recognize arabino-mycolates (25,26). Therefore, it is believed that the linkage region between mycolate- and arabinose-residues constitutes a crucial structure for binding to TLR2, which may render a plausible explanation as to why TDM is not recognized by TLR2 in spite of its similar structure to arabino-mycolates (27-29). Recently Ishikawa *et al.* have shown that macrophage inducible C-type lectin (Mincle) is an essential receptor for TDM in Mincle-deficient mice (30). Thus, the different signaling between arabino-mycolates and TDM can explain the difference of the amount of TNF- α induced (Figures 2a and 2b).

There is a commonly-held view that TLR agonists affect antigen-presenting cells by inducing an innate immune response and subsequently activating the adaptive immune system. In addition a number of studies have shown that stimulation of innate immunity with CWS and TDM leads to establishment of antigen-specific T cell immunity by the DTH reaction (17,31). We accessed in this study arabino-mycolate activity and used CWS as a control for the DTH reaction. Our results show that arabino-mycolates evoke significant swelling of the footpad (Figure 4). The swelling of footpad induced by CWS was also significant and almost comparable to that induced by arabino-mycolates. There is so far no report showing that isolated natural arabino-mycolates stimulate innate immunity *in vivo*, although synthesized arabino-mycolates have been shown to induce TNF- α production in RAW264.7 cells *in vitro* (10). In this study, we show for the first time that isolated natural arabino-mycolates stimulate innate immunity *in vivo*. This finding indicates that arabino-mycolate structure is important as it has a direct effect on adjuvant activity in CWS.

In this study, we show that arabino-mycolates stimulate macrophages to produce TNF- α and that this

effect is dependent on the TLR2-MyD88 pathway *in vitro*. We also show that arabino-mycolates enhance establishment of T cell-mediated immunity *in vivo*. We have previously reported that CWS is engulfed into dendritic cells and distributed in lysosomes, and that activation of dendritic cells is blocked by inhibition of phagocytosis, addressing digestive fragments of CWS that may function as TLR2 ligands (17). Now that we have shown that arabino-mycolate fragments prepared by acid hydrolysis can stimulate TLR2, it is highly likely that CWS is engulfed by phagocytosis and transferred into lysosomes that undergo acid hydrolysis by digestive enzymes to produce fragments capable of interacting with TLR2 directly.

In conclusion, arabino-mycolates produced by acid hydrolysis of BCG-CWS have been shown to have potent TLR2 ligand activity and to constitute an important antigen determinant of *M. bovis* BCG. Further investigation of other multilateral players in immunity would be applauded.

Acknowledgements

We thank Dr. Ichiro Azuma for his advice on the preparation of BCG-CWS. We also thank Dr. Nobuyoshi Chiba for his helpful discussion, and Ms. Yukari Ishitsubo for her assistance with the study experiments.

In conducting this study, all authors declare no potential conflicting interests. All authors are Dainippon Sumitomo Pharma employees, with the exception of Dr. Ikuya Yano who is working under a contract with Dainippon Sumitomo Pharma.

References

1. Kodama K, Higashiyama M, Takami K, Oda K, Okami J, Maeda J, Akazawa T, Matsumoto M, Seya T, Wada M, Toyoshima K. Innate immune therapy with a Bacillus Calmette-Guerin cell wall skeleton after radical surgery for non-small cell lung cancer: A case-control study. *Surg Today*. 2009; 39:194-200.
2. Azuma I, Ribic EE, Meyer TJ, Zbar B. Biologically active components from mycobacterial cell walls. I. Isolation and composition of cell wall skeleton and component P3. *J Natl Cancer Inst*. 1974; 52:95-101.
3. Matsumoto M, Seya T, Kikkawa S, *et al.* Interferon gamma-producing ability in blood lymphocytes of patients with lung cancer through activation of the innate immune system by BCG cell wall skeleton. *Int Immunopharmacol*. 2001; 1:1559-1569.
4. Hayashi D, Takii T, Fujiwara N, Fujita Y, Yano I, Yamamoto S, Kondo M, Yasuda E, Inagaki E, Kanai K, Fujiwara A, Kawarazaki A, Chiba T, Onozaki K. Comparable studies of immunostimulating activities *in vitro* among *Mycobacterium bovis* bacillus Calmette-Guerin (BCG) substrains. *FEMS Immunol Med Microbiol*. 2009; 56:116-128.
5. Akira S, Uematsu S, Takeuchi O. Pathogen recognition and innate immunity. *Cell*. 2006; 124:783-801.
6. Medzhitov R, Janeway CA, Jr. Innate immunity: The

- virtues of a nonclonal system of recognition. *Cell*. 1997; 91:295-298.
7. Tsuji S, Matsumoto M, Takeuchi O, Akira S, Azuma I, Hayashi A, Toyoshima K, Seya T. Maturation of human dendritic cells by cell wall skeleton of *Mycobacterium bovis* bacillus Calmette-Guerin: Involvement of toll-like receptors. *Infect Immun*. 2000; 68:6883-6890.
 8. Murata M. Activation of Toll-like receptor 2 by a novel preparation of cell wall skeleton from *Mycobacterium bovis* BCG Tokyo (SMP-105) sufficiently enhances immune responses against tumors. *Cancer Sci*. 2008; 99:1435-1440.
 9. Brennan PJ. Structure, function, and biogenesis of the cell wall of *Mycobacterium tuberculosis*. *Tuberculosis (Edinb)*. 2003; 83:91-97.
 10. Ishiwata A, Akao H, Ito Y, Sunagawa M, Kusunose N, Kashiwazaki Y. Synthesis and TNF-alpha inducing activities of mycoloyl-arabinin motif of mycobacterial cell wall components. *Bioorg Med Chem*. 2006; 14:3049-3061.
 11. Takimoto H, Maruyama H, Shimada KI, Yakabe R, Yano I, Kumazawa Y. Interferon-gamma independent formation of pulmonary granuloma in mice by injections with trehalose dimycolate (cord factor), lipoarabinomannan and phosphatidylinositol mannosides isolated from *Mycobacterium tuberculosis*. *Clin Exp Immunol*. 2006; 144:134-141.
 12. Sakaguchi I, Ikeda N, Nakayama M, Kato Y, Yano I, Kaneda K. Trehalose 6,6'-dimycolate (Cord factor) enhances neovascularization through vascular endothelial growth factor production by neutrophils and macrophages. *Infect Immun*. 2000; 68:2043-2052.
 13. Grand-Perret T, Lepoivre M, Petit JF, Lemaire G. Macrophage activation by trehalose dimycolate requirement for an expression signal *in vitro* for antitumoral activity; biochemical markers distinguishing primed and fully activated macrophages. *Eur J Immunol*. 1986; 16:332-338.
 14. Means TK, Wang S, Lien E, Yoshimura A, Golenbock DT, Fenton MJ. Human toll-like receptors mediate cellular activation by *Mycobacterium tuberculosis*. *J Immunol*. 1999; 163:3920-3927.
 15. Underhill DM, Ozinsky A, Hajjar AM, Stevens A, Wilson CB, Bassetti M, Aderem A. The Toll-like receptor 2 is recruited to macrophage phagosomes and discriminates between pathogens. *Nature*. 1999; 401:811-815.
 16. Uenishi Y, Kusunose N, Yano I, Sunagawa M. Isolation and identification of arabinose mycolates of cell wall skeleton (CWS) derived from *Mycobacterium bovis* BCG Tokyo 172 (SMP-105). *J Microbiol Methods*. 2010; 80:302-305.
 17. Miyauchi M, Murata M, Shibuya K, Koga-Yamakawa E, Yanagawa Y, Azuma I, Kashiwazaki Y. Phagocytosis plays a dual role in activating dendritic cells; digestive production of active Toll-like receptor ligands and cooperation with Toll-like receptor signaling. *Drug Discov Ther*. 2010; 4:135-143.
 18. Uenishi Y, Okada T, Okabe S, Sunagawa M. Study on the cell wall skeleton derived from *Mycobacterium bovis* BCG Tokyo 172 (SMP-105): Establishment of preparation and analytical methods. *Chem Pharm Bull (Tokyo)*. 2007; 55:843-852.
 19. Hirschfeld M, Ma Y, Weis JH, Vogel SN, Weis JJ. Cutting edge: Repurification of lipopolysaccharide eliminates signaling through both human and murine Toll-like receptor 2. *J Immunol*. 2000; 165:618-622.
 20. Manthey CL, Perera PY, Henricson BE, Hamilton TA, Qureshi N, Vogel SN. Endotoxin-induced early gene expression in C3H/HeJ (*Lpsd*) macrophages. *J Immunol*. 1994; 153:2653-2663.
 21. Manthey C, Vogel S. Elimination of trace endotoxin protein from rough chemotype LPS. *J Endotoxin Res*. 1994; 1:84-91.
 22. Takeuchi O, Hoshino K, Kawai T, Sanjo H, Takada H, Ogawa T, Takeda K, Akira S. Differential roles of TLR2 and TLR4 in recognition of gram-negative and gram-positive bacterial cell wall components. *Immunity*. 1999; 11:443-451.
 23. Hoshino K, Takeuchi O, Kawai T, Sanjo H, Ogawa T, Takeda Y, Takeda K, Akira S. Cutting edge: Toll-like receptor 4 (TLR4)-deficient mice are hyporesponsive to lipopolysaccharide: evidence for TLR4 as the *Lps* gene product. *J Immunol*. 1999; 162:3749-3752.
 24. Kawai T, Adachi O, Ogawa T, Takeda K, Akira S. Unresponsiveness of MyD88-deficient mice to endotoxin. *Immunity*. 1999; 11:115-122.
 25. Werninghaus K, Babiak A, Gross O, *et al*. Adjuvanticity of a synthetic cord factor analogue for subunit *Mycobacterium tuberculosis* vaccination requires FcRγ-Syk-Card9-dependent innate immune activation. *J Exp Med*. 2009; 206:89-97.
 26. Jin MS, Kim SE, Heo JY, Lee ME, Kim HM, Paik SG, Lee H, Lee JO. Crystal structure of the TLR1-TLR2 heterodimer induced by binding of a tri-acylated lipopeptide. *Cell*. 2007; 130:1071-1082.
 27. Gavin AL, Hoebe K, Duong B, Ota T, Martin C, Beutler B, Nemazee D. Adjuvant-enhanced antibody responses in the absence of toll-like receptor signaling. *Science*. 2006; 314:1936-1938.
 28. Geisel RE, Sakamoto K, Russell DG, Rhoades ER. *In vivo* activity of released cell wall lipids of *Mycobacterium bovis* bacillus Calmette-Guerin is due principally to trehalose mycolates. *J Immunol*. 2005; 174:5007-5015.
 29. Agger EM, Rosenkrands I, Hansen J, Brahimi K, Vandahl BS, Aagaard C, Werninghaus K, Kirschning C, Lang R, Christensen D, Theisen M, Follmann F, Andersen P. Cationic liposomes formulated with synthetic mycobacterial cordfactor (CAF01): A versatile adjuvant for vaccines with different immunological requirements. *PLoS One*. 2008; 3:e3116.
 30. Ishikawa E, Ishikawa T, Morita YS, Toyonaga K, Yamada H, Takeuchi O, Kinoshita T, Akira S, Yoshikai Y, Yamasaki S. Direct recognition of the mycobacterial glycolipid, trehalose dimycolate, by C-type lectin Mincle. *J Exp Med*. 2009; 206:2879-2888.
 31. Koike Y, Yoo YC, Mitobe M, Oka T, Okuma K, Tonooka S, Azuma I. Enhancing activity of mycobacterial cell-derived adjuvants on immunogenicity of recombinant human hepatitis B virus vaccine. *Vaccine*. 1998; 16:1982-1989.

(Received January 12, 2011; Revised May 26, 2011; Accepted June 12, 2011)

Mechanisms of vincristine-induced neurotoxicity: Possible reversal by erythropoietin

Lobna A. Kassem^{1,2,*}, Maha M. Gamal El-Din^{1,2}, Nadia A. Yassin^{1,2}

¹ Department of Physiology, Faculty of Medicine, Cairo University, Cairo, Egypt;

² Department of Physiology, Faculty of Pharmacy and Biotechnology, German University, Cairo, Egypt.

ABSTRACT: Vincristine (VCR) is a potent anticancer drug, but neurotoxicity is one of its most important dose-limiting toxicities. In this study, we investigated the neurotoxic effect of VCR, the possible mechanisms and the role of erythropoietin (EPO) in the protection against VCR-induced neurotoxicity in a rat model. The neurotoxicity of VCR and protective effect of EPO were examined using the tail flick test and by recording electrophysiological characteristics in isolated sciatic nerve. To elucidate the underlying mechanisms, mRNA expression of *N*-methyl-D-aspartate (NMDA) receptor, an index of glutamate excitotoxicity, and calcitonin gene-related peptide (CGRP), an important regulator of vascular tone, were measured in both spinal cord and sciatic nerves using an RT-PCR method. After intraperitoneal injection at a dose of 150 µg/kg three times weekly for five consecutive weeks, VCR significantly decreased the latency of tail withdrawal reflex, the amplitude of maximum compound action potential (MCAP) and chronaxie, and prolonged the duration of action potential (AP) and relative refractory period (RRP), but it had no effect on conduction velocity. VCR increased NMDA receptor expression and decreased CGRP expression. Forty µg/kg of EPO improved all VCR-induced changes, except chronaxie, while a higher dose of 80 µg/kg reversed all parameters and its effect was more prominent on tail flick test latency and NMDA receptor expression. These results suggested that VCR might cause increased nerve excitability and induce a state of glutamate excitotoxicity through enhancing NMDA receptor expression and diminishing CGRP expression, thus resulting in axonal degeneration. EPO had an obvious neuroprotective effect probably through decreasing NMDA receptor expression and

increasing CGRP expression both centrally and peripherally.

Keywords: Vincristine, action potential, *N*-methyl-D-aspartate receptor, Calcitonin gene-related peptide, erythropoietin

1. Introduction

Vincristine (VCR) is a chemotherapeutic agent that can be used in the treatment of many types of human cancer (1). It is a purified alkaloid extracted from the periwinkle plant *Vinca rosea* Linn. of the family Apocynaceae (2). However, like many chemotherapeutic drugs it is toxic to peripheral nerves, and the development of VCR-induced neuropathy seems to be dose-related and occurs in the early stage of treatment (2). Thus, the clinical use of VCR is limited by the predictable development of the neuropathy (3). If this effect could be prevented, it might be possible to use VCR more effectively in the treatment of malignant tumors at higher doses and for longer duration. Thus far, the mechanisms of VCR-induced neuropathy are poorly understood, which has hindered the development of protective measures against this toxic effect.

Erythropoietin (EPO), a well-established hematopoietic factor responsible for the production of red blood corpuscles, was discovered to have multiple functions outside the bone marrow. When it was found that recombinant human EPO crosses the blood-brain barrier (4), interest has focused on its function in the nervous system. Studies have shown that it reduces injury both centrally in acute ischemic stroke patients (5), as well as peripherally in sciatic nerve compression (6). Recently, EPO was also demonstrated to protect and reverse experimental diabetic neuropathy (7).

Thus, the aim of the present study was to clarify the alterations in VCR-induced peripheral neuropathy using a behavioral assay, the tail flick test, and neurophysiologic studies performed on the rat sciatic nerve. In addition,

*Address correspondence to:

Dr. Lobna A. Kassem, Department of Physiology, Faculty of Pharmacy and Biotechnology, German University in Cairo, Main Entrance Al Tagamoa Al Khames, New Cairo City, Egypt.
e-mail: Lobna.abdelaal@guc.edu.eg

some possible underlying mechanisms of the action of VCR were investigated by measuring *N*-methyl-D-aspartate (NMDA) receptor mRNA and calcitonin gene related peptide (CGRP) mRNA expression in both the spinal cord and sciatic nerves. Furthermore, we studied the potential beneficial role of EPO (at 2 different doses) in preventing VCR-induced peripheral neuropathy and whether it reversed the underlying pathology.

2. Materials and Methods

2.1. Animals

Forty male Sprague Dawley rats, weighing between 150-200 g, were purchased from the animal house of the National Research Center, Cairo University. They were given free access to water and food, and maintained on 12 h light/dark cycle. All experimental procedures were carried out in compliance with the guide for care and use of laboratory animals published by the US National Institutes of Health (NIH publication 85-23 revised 1985) and in compliance with the Local Animal Ethics Committee of Kasr Al Aini, Faculty of Medicine, Cairo University.

2.2. Experimental protocol

Rats were assigned into the following four equal groups: Group I (Control group), this group of rats received distilled water as a vehicle for 5 consecutive weeks; Group II (VCR-treated group, VCR group), vincristine sulfate (Korea United Pharm. Inc., Chungcheongnam-do, Korea; 1 mg/mL vial) was injected at a dose of 150 µg/kg, intraperitoneally, three times weekly for five consecutive weeks (8,9); Group III (EPO-treated group 1, EPO1 group), this group of rats was treated with VCR at the same dose and route of administration as in group II and concomitantly received human recombinant EPO (Egyptian International Pharmaceutical Industries Co., 10th of Ramadan City, Egypt; 10,000 IU/mL vial) at a dose of 40 µg/kg, intraperitoneally, three times weekly for five consecutive weeks (7); Group IV (EPO-treated group 2, EPO2 group), this group of rats was subjected to the same treatment protocol as in group III, but the EPO dose was doubled (80 µg/kg).

At the end of the experimental protocol, all groups were subjected to the tail flick test as a behavioral nociceptive reaction. Rats were then sacrificed by cervical dislocation followed by decapitation. Sciatic nerves of both limbs were exposed using a longitudinal skin incision in the hind legs. Each nerve was dissected free from the surrounding connective tissue and completely excised with the epineuria intact. One nerve was used for electrophysiological studies and the other one for assessment of gene expression of calcitonin gene-related peptide (CGRP) mRNA and *N*-methyl-D-aspartate (NMDA) receptor mRNA.

2.3. Electrophysiological recordings

The sciatic nerve was mounted in a nerve chamber (MLT012/B. AD Instruments) designed for the recording of action potentials from isolated nerves. It contains 15 stainless steel wire electrodes of 0.8 mm diameter spaced at intervals of 5 and 10 mm. Each end of the nerve was tied with short lengths of thread that were pushed into split silicone tubing at either end of the bath to help position the nerve without stretching it. The nerve was positioned over the electrodes and embedded in paraffin oil at 35°C to maximize signal amplitude and prevent drying. To record a monophasic action potential, the sciatic nerve was crushed with a forceps near its distal end.

The proximal part of the nerve was stimulated by 2 platinum stimulating hook electrodes. The recording electrodes were placed 1 to 2 cm apart from the stimulating ones.

The electrophysiological measurements were performed using an AD Instruments (Greenwich, CT) Power Lab 4/25 stimulator and a BioAMP amplifier followed by computer-assisted data analysis (Chart 5.0 and SCOPE 3.7; AD Instruments) and displayed at a sampling rate of 40 K/sec. Sciatic nerves were stimulated with square wave pulses of 0.2 msec duration at 1-10 volts for action potential, conduction velocity and refractory period measurements, and of 10-1,000 µsec at 50 µV-5 V for chronaxie. The parameters were assessed as follows.

2.3.1. Maximal compound action potential (MCAP) amplitude

The stimulating voltage was set to produce a maximal compound monophasic action potential using square wave pulses of supra-maximal strength and 0.2 msec in duration. The maximum amplitude was measured from the baseline to the peak of the action potential as shown in Figure 1 (10).

2.3.2. Duration of action potential

The time elapsed in milliseconds between the onset of depolarization to return to the base line was recorded (11).

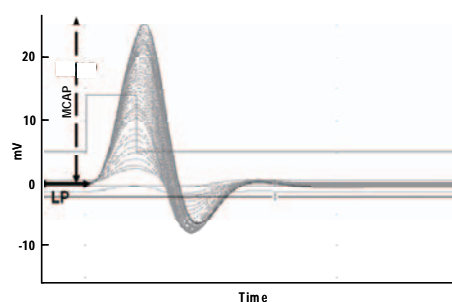


Figure 1. MCAP amplitude profile. MCAP amplitude was measured from the baseline to the peak of action potential. The latent period (LP) is the time elapsed between the application of the stimulus until the start of MCAP.

2.3.3. Relative refractory period (RRP)

Twin maximum pulse stimuli with stimulus interval of 2 msec were used to record 2 action potentials. Then, the stimulus interval was decreased gradually by 10 μ sec decrements. The interval when the amplitude of the second CAP decreases and reaches 75% of the first maximum CAP was recorded and taken as a standardized measure of refractoriness for comparison between groups (11).

2.3.4. Conduction velocity

This was measured by dividing the distance between the stimulating and the recording electrodes by the time elapsed between the application of the stimulus until the peak of the MCAP (12).

2.3.5. Chronaxie

The rheobase was measured as the threshold stimulus voltage for an active response with a long duration pulse. Chronaxie is the pulse width corresponding to twice the rheobase (12).

2.4. Behavioral assay

As a behavioral test, the tail flick (immersion) test is used to assess the nociceptive response to acute thermal pain stimulus. This measure was chosen because of the role small fiber dorsal root ganglia sensory neurons play in pain transmission (13). The animals were restrained in a restrainer cage with their tail hanging free and allowed to adapt for 30 min before testing. The lower 5 cm portion of the tail was marked. This part of the tail was immersed in a cup of freshly filled water of exactly 55°C. Within a few seconds, the rat reacted by withdrawing the tail. The latency of this tail withdrawal reflex was recorded using a stop watch in all animal groups (14).

2.5. Detection of NMDA receptor mRNA and CGRP expression mRNA by reverse transcriptase polymerase chain reaction (RT-PCR)

About 30 mg of nerve and spinal cord tissues were stored at -80°C in lysis buffer containing guanidium thiocyanate and β -mercaptoethanol for RNA extraction.

2.5.1. RNA extraction

Total RNA was extracted from both nerve and spinal cord after homogenization according to the manufacturer's instructions. The concentration of extracted RNA was measured spectrophotometrically at 260 nm.

2.5.2. RT-PCR

For amplification of the targets, reverse transcription

and PCR were run in two separate steps. Briefly, equal amounts of total RNA (6 μ g) were heat denatured and reverse transcribed by incubation at 42°C for 90 min with 12.5 U avian myeloblastosis virus reverse transcriptase (AMV) (Promega Corp., Madison, WI, USA), 20 U ribonuclease inhibitor RNasin (Promega Corp.), 200 nM deoxy-nucleoside 5'-triphosphate mixture, and 1 nM oligo-dT primer in a final volume of 30 μ L of 1 \times avian myeloblastosis virus reverse transcriptase buffer. The reactions were terminated by heating at 97°C for 5 min and cooling on ice. The cDNA samples were amplified in 50 μ L of 1 \times PCR buffer in the presence of 2.5 U Taq DNA polymerase (Promega Corp.), 200 nM deoxy-nucleoside 5'-triphosphate mixture, and the appropriate primer pairs (1 nM of each primer. These sets of primers of CGRP and NMDA were designed from GenBank (accession No. G35510 and 691379, respectively): forward primer, 5'-GAGATC AGGAGTTCAAGACC-3' and 5'-TCCAACTGGTCA CACCTCACT-3', respectively; reverse primer, 5'-TTGG CTCCTGCAACCTCC-3' and 5'-CAGCTTTGGTGAC AGCATCTCT-3', respectively.

PCR consisted of a first denaturing cycle at 97°C for 5 min, followed by a variable number of cycles of amplification defined by denaturation at 96°C for 1.5 min, annealing for 1.5 min, and extension at 72°C for 3 min. A final extension cycle of 72°C for 15 min was included. Annealing temperature was adjusted to 55°C (15).

2.5.3. Agarose gel electrophoresis

All PCR products were electrophoresed on 2% agarose stained with ethidium bromide and visualized with a UV transilluminator.

2.5.4. Semi-quantitative determination of PCR products

Semi-quantitation was performed using a gel documentation system (BioDO, Analyser) supplied by Biometra. According to the following amplification procedure, relative expression of each gene was calculated following the formula (15):

$$R = \text{Densitometrical units of each gene} / \text{Densitometrical units of } \beta\text{-actin}$$

β -actin primers were designed from GenBank (accession No. J00691).

2.6. Statistics

All data are expressed as means \pm S.E. Statistical analysis was performed using one way ANOVA (Microcal Origin Software, Inc., Version 5) followed by the Tukey test for multiple comparisons. A *p* value < 0.05 was considered statistically significant.

3. Results

3.1. Electrophysiological recordings

3.1.1. Sciatic nerve MCAP amplitude

Following VCR injection for 5 weeks, the mean MCAP was significantly reduced compared to the control group ($p < 0.05$) (Figure 2). Concomitant administration of EPO at the lower dose together with VCR in the EPO1 group completely reversed the effect of VCR and no significant difference in the amplitude of MCAP was measured compared to the control group. In the EPO2 group, however, the mean MCAP was significantly lower than in the control group, but still significantly higher than in the VCR group. There was a significantly lower mean MCAP in the EPO2 group compared to the EPO1 group ($p < 0.05$) (Figure 2).

3.1.2. Duration of action potential

The action potential duration was significantly prolonged in the VCR-treated group ($p < 0.05$) (Figure 3). In

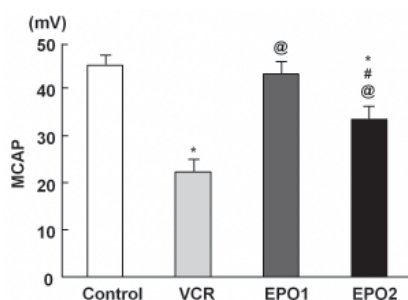


Figure 2. Maximum compound action potential amplitude produced by supramaximal stimulation of the sciatic nerve. Values are expressed as mean \pm S.E., * $p < 0.05$ significant vs. control, @ $p < 0.05$ vs. VCR group, # $p < 0.05$ vs. EPO1 group ($n = 10$ rats/group). EPO1 group received 40 $\mu\text{g}/\text{kg}$, three times weekly for five consecutive weeks. EPO2 group received 80 $\mu\text{g}/\text{kg}$, three times weekly for five consecutive weeks.

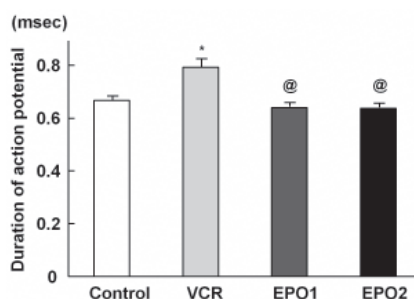


Figure 3. Duration of action potential in VCR, EPO1, and EPO2 groups. Duration of action potential showed a significant prolongation in the VCR group with complete reversal back to control by both doses of EPO. Values are expressed as mean \pm S.E., * $p < 0.05$ significant vs. control, @ $p < 0.05$ vs. VCR group, # $p < 0.05$ vs. EPO1 group ($n = 10$ rats/group). EPO1 group received 40 $\mu\text{g}/\text{kg}$, three times weekly for five consecutive weeks. EPO2 group received 80 $\mu\text{g}/\text{kg}$, three times weekly for five consecutive weeks.

the EPO1 and EPO2 groups, this prolongation was completely abolished and the action potential duration showed no significant change compared to the control group.

3.1.3. RRP

With regard to the RRP, it was found to be significantly prolonged in the VCR group compared to the control group ($p < 0.05$) (Figure 4). Again, this effect of VCR was completely abolished by the concomitant administration of the two doses of EPO, so that the RRP in the EPO1 and EPO2 groups was not significantly different from the values of the control group.

3.1.4. Conduction velocity

The conduction velocity was not significantly altered in any of the tested groups compared to the control group ($p > 0.05$) (Figure 5).

3.1.5. Chronaxie

In the VCR group, chronaxie was significantly shortened

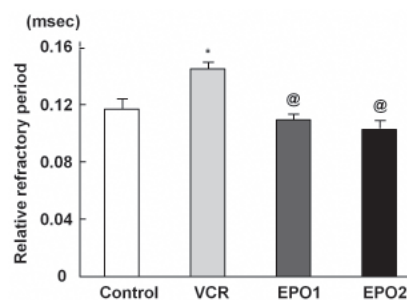


Figure 4. Relative refractory period in VCR, EPO1, and EPO2 groups. RRP was significantly increased after 5 weeks of treatment with VCR and was totally declined with any of the doses used of EPO. Values are expressed as mean \pm S.E., * $p < 0.05$ significant vs. control, @ $p < 0.05$ vs. VCR group, # $p < 0.05$ vs. EPO1 group ($n = 10$ rats/group). EPO1 group received 40 $\mu\text{g}/\text{kg}$, three times weekly for five consecutive weeks. EPO2 group received 80 $\mu\text{g}/\text{kg}$, three times weekly for five consecutive weeks.

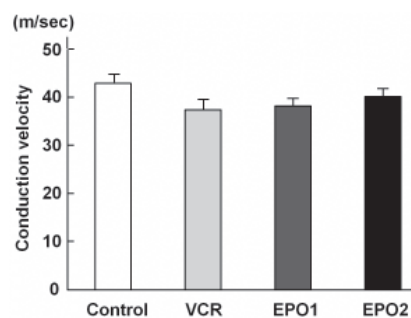


Figure 5. Sciatic nerve conduction velocity in VCR, EPO1, and EPO2 groups. Sciatic nerve conduction velocity measurements showed no significant changes in any of the studied groups. Values are expressed as mean \pm S.E. ($n = 10$ rats/group).

Table 1. Results of chronaxie and tail flick test as indices of nerve excitability in the different experimental groups

	Groups*			
	Control	VCR	EPO1	EPO2
Chronaxie (μ sec)	89.3 \pm 2.0	77.5 \pm 3.8 ^a	79.2 \pm 3.3 ^a	92.3 \pm 1.2 ^{b,c}
Tail flick test (sec)	14.9 \pm 0.6	7.8 \pm 0.6 ^a	10.6 \pm 1.1 ^{a,b}	14.6 \pm 0.4 ^{b,c}

* VCR group, vincristine-treated group; EPO1 group, erythropoietin-treated group 1; EPO2 group, erythropoietin-treated group 2. EPO1 and EPO2 groups received 40 μ g/kg and 80 μ g/kg of EPO, respectively, three times weekly for five consecutive weeks. Values are expressed as mean \pm S.E. ($n = 10$ rats/group). ^a $p < 0.05$ vs. control group; ^b $p < 0.05$ vs. VCR group; ^c $p < 0.05$ vs. EPO1 group.

($p < 0.05$) compared to the control group (Table 1). The lower dose of EPO in the EPO1 group was not able to reverse this effect. The EPO2 group, however, showed a significantly prolonged chronaxie compared to the VCR group ($p < 0.05$), and it was not significantly different from the control (Table 1).

3.2. Behavioral assay (tail flick test)

The latency of tail withdrawal reflex in response to immersion of the tail in warm water was significantly shortened in the VCR group compared to the control group ($p < 0.05$) (Table 1). In the EPO1 group, the latency was significantly lower than that of the control group, but significantly higher than in the VCR group ($p < 0.05$) (Table 1). In the EPO2 group, the higher dose of EPO completely reversed the effect of VCR in the tail flick test, so that there was no significant difference between the EPO2 group and control, while the latency was significantly longer than in the VCR and EPO1 groups ($p < 0.05$) (Table 1).

3.3. NMDA receptor and CGRP gene expression

Gene expressions of NMDA receptor and CGRP were evaluated using RT-PCR and agarose gel electrophoresis (Figure 6). As shown in Table 2, NMDA receptor expression was significantly increased in the VCR group ($p < 0.05$) in both the spinal cord and sciatic nerves. In the EPO1 group, concomitant administration of EPO at the lower dose with VCR, resulted in a significant decrease in the expression of NMDA receptors compared to the VCR group ($p < 0.05$), but it was still significantly higher than in the control group ($p < 0.05$) in the spinal cord and sciatic nerves. With the higher dose of EPO, the EPO2 group showed a complete reversal of the effect of VCR in the sciatic nerves, as NMDA receptor expression was not significantly different than that of the control group ($p > 0.05$). In the spinal cord, however, the expression of NMDA receptors was significantly lower in the EPO2 group, but it remained higher than in the control group ($p < 0.05$).

With regard to the expression of CGRP, the VCR group showed significantly reduced expression in the spinal cord and sciatic nerves compared to the control group ($p < 0.05$) (Table 2). In the EPO1 and EPO2 groups there was a significant increase of the expression of

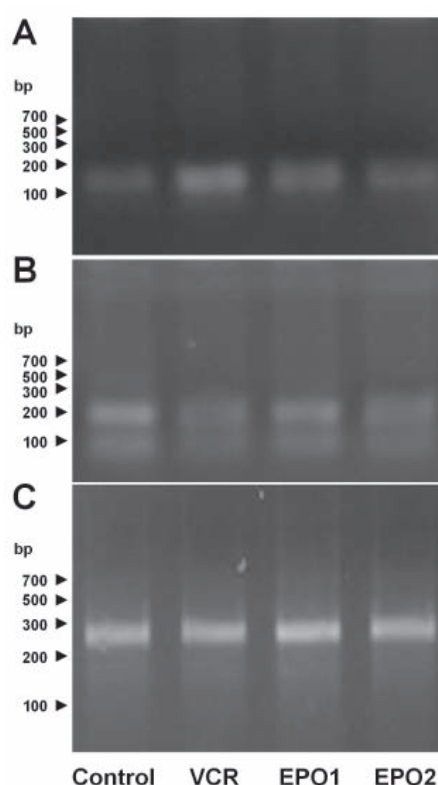


Figure 6. Agarose gel electrophoresis profiles showing PCR products of various genes tested in sciatic nerve. (A) PCR products of NMDA gene (105 bp). **(B)** PCR products of CGRP gene (210 bp). **(C)** PCR products of β -actin gene (256 bp). Lane 1, Control group; Lane 2, VCR group; Lane 3, EPO1 group; Lane 4, EPO2 group.

CGRP in sciatic nerves compared to the VCR group, but it was still significantly lower than in the control group ($p < 0.05$). In the spinal cord, however, CGRP expression in both EPO1 and EPO2 groups was significantly increased compared to the VCR and the control group ($p < 0.05$).

4. Discussion

In the present study, VCR-induced neurotoxicity was tested by electrophysiological measurements. We observed that the amplitude of the MCAP was significantly decreased, while its duration was significantly prolonged in the VCR group. This suggests that a significant number of sensory and motor fibers are affected by the drug as confirmed by reported histological studies, which showed VCR-induced axonal degeneration as well as disorganization of the axonal microtubule cytoskeleton

Table 2. NMDA receptor and CGRP gene expression (in sciatic nerves and spinal cord) in the different experimental groups

	Groups*			
	Control	VCR	EPO1	EPO2
NMDA receptor expression				
In sciatic nerves	1.21 ± 0.09	3.55 ± 0.27 ^a	2.19 ± 0.10 ^{a,b}	1.51 ± 0.14 ^{b,c}
In spinal cord	0.02 ± 0.06	1.67 ± 0.21 ^a	0.56 ± 0.12 ^{a,b}	0.51 ± 0.03 ^{a,b}
CGRP expression				
In sciatic nerves	4.99 ± 0.29	2.38 ± 0.16 ^a	3.91 ± 0.21 ^{a,b}	4.15 ± 0.12 ^{a,b}
In spinal cord	4.63 ± 0.18	1.46 ± 0.19 ^a	6.16 ± 0.15 ^{a,b}	6.78 ± 0.26 ^{a,b}

* VCR group, vincristine-treated group; EPO1 group, erythropoietin-treated group 1; EPO2 group, erythropoietin-treated group 2. EPO1 and EPO2 groups received 40 µg/kg and 80 µg/kg of EPO, respectively, three times weekly for five consecutive weeks. Values are expressed as mean ± S.E. (n = 10 rats/group). ^ap < 0.05 vs. control group; ^bp < 0.05 vs. VCR group; ^cp < 0.05 vs. EPO1 group. Abbreviations: NMDA, N-methyl-D-aspartate; CGRP, calcitonin gene related peptide.

and increase in the caliber of unmyelinated sensory axons (9,16). On the other hand, no significant change was observed in conduction velocity. The preservation of conduction velocity, despite a reduced amplitude and prolonged duration of action potential, may reflect that axonal degeneration may have been too mild and too early to show an effect on nerve conduction and suggests an early stage of myelin disruption.

In the present study, the RRP was found to be significantly prolonged in the VCR group. RRP measurement is more sensitive than routine measures of nerve conduction in detection of axonal disorders (17) and early neurotoxicity (18). To our knowledge, no other study has investigated the effect of VCR on RRP. However, another study, using Oxaliplatin (a chemotherapeutic drug) observed a prolonged RRP (19). It proposed that this might be mediated through an effect on axonal voltage-gated transient Na⁺ channels, which is involved in the subsequent process of axonal degeneration.

In this study, VCR induced shortening of chronaxie, suggesting increased nerve excitability. This is further evidenced by the results of the tail-flick test which showed significant shortening of the reaction time, indicating a decreased nociceptive threshold to thermal stimuli. The observed increased excitability suggests the presence of an excitotoxicity. Glutamate mediates excitatory synaptic transmission through the activation of ionotropic glutamate receptors that are sensitive to NMDA, amino-3-hydroxy-5-methyl-4-isoxazolepropionic acid (AMPA), or kainate. Excess and sustained activation of these receptors causes fulminant neuronal death, namely, glutamate excitotoxicity (20). The Ca²⁺ influx through NMDA receptors mediates the rapidly-triggered NMDA neurotoxicity, while Na⁺ influx contributes to the swelling of the neuronal cell body (21). Therefore, we studied the expression of NMDA receptors in this study both in sciatic nerves and spinal cord. A significant increase was detected in VCR group. Our results are consistent with another study that showed that NMDA receptor antagonist decreased VCR-induced hyperalgesia (22). However, it has been reported that NMDA receptor-mediated signaling pathways were not involved in VCR-induced neuropathic pain in an *in vitro* study on primary

cerebellar granule neurons (23). This discrepancy might be due to the differences between the *in vivo* and *in vitro* studies as well as the differential vulnerability of neurons to the NMDA antagonist.

Current results showed that VCR resulted in significant reduction of CGRP expression in sciatic nerves and spinal cord. It was reported that epineurial peptidergic terminals mediate a vasodilatory response through CGRP that increases blood flow in the downstream endoneurial compartment (24). Thus, it may be suggested that VCR by decreasing CGRP decreases the blood flow to the nerves producing ischemia. Won *et al.* (20) showed that ischemia induces excitotoxicity. Therefore, VCR-induced excitotoxicity in our study may not only be due to increase in expression of NMDA receptors, but may also be due to ischemia. It appears that VCR mediated its effects at the level of both spinal cord and peripheral nerves.

In the present study, EPO1 reversed most of VCR-induced changes in all electrophysiological parameters measured, except chronaxie. It also shortened the latency of the tail flick test. EPO2 had a similar effect to EPO1, but was also able to reverse the decreased chronaxie induced by VCR. It was also more potent than EPO1 with regard to tail flick test. From these results we could suggest that the higher dose of EPO has a more pronounced effect on both C and A-alpha or A-beta fibers but this needs further investigation. Unexpectedly, EPO2 proved to be less effective on MCAP. This could not be due to a toxic effect of the high dose of EPO as the other electrophysiological recordings were completely reversed. Further studies are recommended.

In the present study, the increase in NMDA receptor expression by VCR was also significantly reduced by both doses of EPO in spinal cord and sciatic nerves. Yet, the higher dose of EPO in the EPO2 group produced a complete reversal of VCR-induced changes at the peripheral nerve level. This clearly indicates that one of the mechanisms of action of EPO as a neuroprotective agent is mediated through decreasing excitotoxicity. It also seems that the higher dose was more capable of preventing excitotoxicity as it had a more prominent effect not only on NMDA receptor expression, but also on improving the latency of the tail flick test and

chronaxie, which are both indicators of excitability. An inhibitory effect of EPO on excitotoxicity was reported in several neurotoxic models (25,26). Furthermore, Yazihan *et al.* (27) showed that the neuroprotective effect of EPO was abolished *via* NMDA receptor antagonist. Other previous studies suggested that EPO could ameliorate or prevent neuronal injury by other mechanisms such as antiapoptotic, antioxidant and anti-inflammatory effects (28,29).

In the current study, the reduction in CGRP expression observed in the spinal cord and sciatic nerves with VCR administration was reversed by EPO. At the level of the spinal cord, both doses of EPO even increased CGRP expression to higher levels than normal. Similarly, Toth *et al.* (30) reported that EPO increased the density and intensity of CGRP expression within outgrowing axons after crush injury. Thus, it seems that another mechanism for improvement of VCR-induced neurotoxicity by EPO may be *via* restoration of blood flow in central and peripheral nervous tissue by increasing CGRP.

It can be concluded that VCR caused electrophysiological changes indicating axonal degeneration. This study was the first to demonstrate that VCR caused a state of glutamate excitotoxicity both centrally and peripherally. It could also decrease endoneural blood flow and induce vascular neurotoxicity but this needs further investigation to prove it. The higher dose of EPO was more effective in improving VCR-induced neurotoxicity. There may exist several mechanisms of action of EPO, but we were able to detect that EPO decreased NMDA receptor expression and increased CGRP expression, thus decreasing the excitotoxicity caused by VCR.

References

- Gidding CE, Kellie SJ, Kamps WA, de Graaf SS. Vincristine revisited. *Crit Rev Oncol Hematol.* 1999; 29:267-287.
- Pal PK. Clinical and electrophysiological studies in vincristine induced neuropathy. *Electromyogr Clin Neurophysiol.* 1999; 39:323-330.
- Le Quesne PM, Fowler CJ, Harding AE. A study of the acute effect of isaxone on vincristine-induced peripheral neuropathy in man and regeneration following peripheral nerve crush in the rat. *J Neurol Neurosurg Psychiatry.* 1985; 48:933-935.
- Brines ML, Ghezzi P, Keenan S, Agnello D, de Lanerolle NC, Cerami C, Itri LM, Cerami A. Erythropoietin crosses the blood-brain barrier to protect against experimental brain injury. *Proc Natl Acad Sci U S A.* 2000; 97:10526-10531.
- Ehrenreich H, Hasselblatt M, Dembowski C, *et al.* Erythropoietin therapy for acute stroke is both safe and beneficial. *Mol Med.* 2002; 8:495-505.
- Erbayraktar S, Grasso G, Sfacteria A, *et al.* Asialoerythropoietin is a nonerythropoietic cytokine with broad neuroprotective activity *in vivo*. *Proc Natl Acad Sci U S A.* 2003; 100:6741-6746.
- Bianchi R, Buyukakilli B, Brines M, Savino C, Cavaletti G, Oggioni N, Lauria G, Borgna M, Lombardi R, Cimen B, Comelekoglu U, Kanik A, Tataroglu C, Cerami A, Ghezzi P. Erythropoietin both protects from and reverses experimental diabetic neuropathy. *Proc Natl Acad Sci U S A.* 2004; 101:823-828.
- Authier N, Gillet JP, Eschalier A, Coudore F. A new animal model of vincristine-induced nociceptive peripheral neuropathy. *Neurotoxicology.* 2003; 24:797-805.
- Ja'afar FM, Hamdan FB, Mohammed FH. Vincristine-induced neuropathy in rat: Electrophysiological and histological study. *Exp Brain Res.* 2006; 173:334-345.
- Potocnik I, Tomsic M, Sketelj J, Bajrovic FF. Articaine is more effective than lidocaine or mepivacaine in rat sensory nerve conduction block *in vitro*. *J Dent Res.* 2006; 85:162-166.
- Anderson RJ. Alterations in nerve and muscle compound action potentials after acute acrylamide administration. *Environ Health Perspect.* 1982; 44:153-157.
- Leal-Cardoso JH, Matos-Brito BG, Lopes-Junior JE, Viana-Cardoso KV, Sampaio-Freitas AB, Brasil RO, Coelho-De-Souza AN, Albuquerque AA. Effects of estragole on the compound action potential of the rat sciatic nerve. *Braz J Med Biol Res.* 2004; 37:1193-1198.
- Schratberger P, Walter D, Rittig K, Bahlmann F, Pola R, Curry C, Silver M, Krainin JG, Weinberg DH, Ropper AH, Isner JM. Reversal of experimental diabetic neuropathy by VEGF gene transfer. *J Clin Invest.* 2001; 107:1083-1092.
- Ramabadran K, Bansinath M, Turndorf H, Puig MM. Tail immersion test for the evaluation of a nociceptive reaction in mice. *J Pharmacol Meth.* 1989; 21:21-31.
- Chomczynski P, Sacchi N. Single-step method of RNA isolation by acid guanidinium thiocyanate-phenol-chloroform extraction. *Anal Biochem.* 1987; 162:156-159.
- Ravula SK, Wang MS, McClain MA, Asress SA, Frazier B, Glass JD. Spatiotemporal localization of injury potentials in DRG neurons during vincristine-induced axonal degeneration. *Neurosci Lett.* 2007; 415:34-39.
- Boërio D, Hogrel JY, Créange A, Lefaucheur JP. Methods and clinical value of peripheral nerve refractory period measurement in man. *Neurophysiol Clin.* 2004; 34:279-291.
- Anderson RJ. Relative refractory period as a measure of peripheral nerve neurotoxicity. *Toxicol Appl Pharmacol.* 1983; 71:391-397.
- Krishnan AV, Goldstein D, Friedlander M, Kiernan MC. Oxaliplatin and axonal Na⁺ channel function *in vivo*. *Clin Cancer Res.* 2006; 12:4481-4484.
- Won SJ, Kim DY, Gwag BJ. Cellular and molecular pathways of ischemic neuronal death. *J Biochem Mol Biol.* 2002; 35:67-86.
- Choi DW. Ionic dependence of glutamate neurotoxicity. *J Neurosci.* 1987; 7:369-379.
- Zhu CZ, Wilson SG, Mikusa JP, Wismer CT, Gauvin DM, Lynch JJ. Assessing the role of metabotropic glutamate receptor 5 in multiple nociceptive modalities. *Eur J Pharmacol.* 2004; 506:107-118.
- Wick A, Wick W, Hirrlinger J, Gerhardt E, Dringen R, Dichgans J. Chemotherapy-induced cell death in primary cerebellar granule neurons but not in astrocytes; *in vitro* paradigm of differential neurotoxicity. *J Neurochem.* 2004; 91:1067-1074.
- Zochodne DW, Ho LT. Influence of perivascular peptides in endoneurial blood flow and microvascular resistance in the sciatic nerve of the rat. *J Physiol.* 1991; 444:615-630.

25. Keller M, Yang J, Griesmaier E, Gorna A, Sarkozy G, Urbanek M, Gressens P, Simbruner G. Erythropoietin is neuroprotective against NMDA-receptor-mediated excitotoxic brain injury in newborn mice. *Neurobiol Dis.* 2006; 24:357-366.
26. Montero M, Poulsen FR, Noraberg J, Kirkeby A, vanBeek J, Leist M, Zimmer J. Comparison of neuroprotective effects of erythropoietin (EPO) and carbamylerythropoietin (CEPO) against ischemia-like oxygen-glucose deprivation (OGD) and NMDA excitotoxicity in mouse hippocampal slice. *Exp Neurol.* 2007; 204:106-117.
27. Yazihan N, Uzuner K, Salman B, Vural M, Koken T, Arslantas A. Erythropoietin improves oxidative stress following spinal cord trauma in rats. *Injury.* 2008; 39:1408-1413.
28. Ranchon Cole I, Bonhomme B, Doly M. Pre-treatment of adult rats with high doses of erythropoietin induces caspase-9 but prevents light-induced retinal injury. *Exp Eye Res.* 2007; 85:782-789.
29. Agnello D, Bigini P, Villa P, Mennini T, Cerami A, Brines ML, Ghezzi P. Erythropoietin exerts an anti-inflammatory effect on the CNS in a model of experimental autoimmune encephalomyelitis. *Brain Res.* 2002; 952:128-134.
30. Toth C, Martinez JA, Liu WQ, Diggle J, Guo GF, Ramji N, Mi R, Hoke A, Zochodne DW. Local erythropoietin signaling enhances regeneration in peripheral axons. *Neuroscience.* 2008; 154:767-783.

(Received October 20, 2010; Revised November 29, 2010; Re-revised April 13, 2011; Accepted May 19, 2011)

Antityrosinase and antioxidant activities of essential oils of edible Thai plants

Kiattisak Saeio, Wantida Chaiyana, Siriporn Okonogi*

Faculty of Pharmacy, Chiang Mai University, Chiang Mai, Thailand.

ABSTRACT: This work was undertaken to explore antityrosinase and antioxidant activities of twenty essential oils of edible Thai plants. Antityrosinase activity against mushroom tyrosinase was examined by means of the dopachrome method using L-dopa as an enzymatic substrate. The essential oil of *Cymbopogon citratus* had the highest level of antityrosinase activity, followed by that of *Ocimum canum* with enzymatic inhibition of 69 ± 4 and $66 \pm 3\%$. GC-MS revealed that geranial and neral were the two most abundant components of their chemical compositions. Antioxidant activity was gauged by the free radical scavenging activity test and ferric reducing/antioxidant power assay. The essential oil of *Ocimum sanctum* had the highest level of antioxidant activity, followed by the essential oil of *Ocimum gratissimum*. These results led to the conclusions that the essential oils of edible Thai plants exhibit important biological activities and are a promising choice as natural active ingredients because of their antityrosinase and antioxidant activities.

Keywords: Essential oil, antityrosinase, antioxidant, geranial, neral

1. Introduction

Plants have been used in cooking, cosmetics, perfumery, and medicine since ancient times (1). Certain parts of edible plants are added to the diet because they can produce flavors and enhance the palatability of food. Many natural compounds extracted from plants exhibit important biological activities. Among the diverse natural compounds, essential oils extracted from aromatic plants are attracting particular attention. Essential oils are complex natural mixtures of volatile secondary metabolites, isolated from different

parts of plants, and are also responsible for the fragrant and biological properties of medicinal plants (2). The multi-component systems in the essential oils consist mainly of low molecular weight terpenoids (3). These small compounds allow easy transport across cell membranes to induce different biological activities (4). The essential oils are recognized as having several therapeutic applications and have vast pharmacological effects (5,6). Recently, essential oils from edible plants have attracted greater interest due to their availability, fewer side effects or toxicity, and biodegradability (2). However, a comparative study of important activities of edible plants has yet to be conducted. The aim of the present study was to investigate and compare antioxidant and antityrosinase activities of essential oils extracted from several often consumed edible Thai plants. The chemical profile of the potential oils was also determined in order to analyze the constituents existing in the oils.

2. Materials and Methods

2.1. Plant materials

Eighteen edible plants, *Centella asiatica* Urban., *Polyscias fruticosa* Harms., *Eupatorium odoratum* Linn., *Cymbopogon citratus* Stapf., *Ocimum sanctum* Linn., *Ocimum canum* Sims., *Ocimum gratissimum* Linn., *Melissa officinalis* L., *Ocimum basilicum* Linn., *Cinnamomum bejolghota* (Buch. Ham.) Sweet, *Piper sarmentosum* Roxb., *Polygonum odoratum* Lour., *Citrus hystrix* DC., *Citrus aurantifolia* Swing., *Citrus maxima*, *Alpinia galanga* (Linn.) Swartz., *Zingiber officinale* Roscoe, and *Zingiber cassumunar* Roxb., were collected from local farms located in Chiang Mai, Thailand in January 2010. All plants were authenticated and their voucher specimens were deposited in the Herbarium of the Faculty of Pharmacy, Chiang Mai University, Thailand.

2.2. Chemicals and enzymes

Trolox, 2,2'-azinobis(3-ethylbenzothiazoline-6-sulfonic acid) diammonium salt (ABTS), 2,4,6-tri(2-pyridyl)-s-

*Address correspondence to:

Dr. Siriporn Okonogi, Faculty of Pharmacy, Chiang Mai University, Chiang Mai 50200, Thailand.
e-mail: sirioko@chiangmai.ac.th

triazine (TPTZ), anhydrous sodium sulphate (Na_2SO_4), sodium carbonate (Na_2CO_3), potassium persulfate ($\text{K}_2\text{S}_2\text{O}_8$), ferrous sulfate ($\text{FeSO}_4 \cdot 7\text{H}_2\text{O}$), and ferric chloride ($\text{FeCl}_3 \cdot 6\text{H}_2\text{O}$) were purchased from Sigma-Aldrich (St. Louis, MO, USA). Mushroom tyrosinase and L-dopa were purchased from Fluka Chemical Co. (Japan). Sodium dihydrogen orthophosphate dehydrate, sodium chloride, and calcium chloride were obtained from Fisher Chemicals (Loughborough, UK). Di-Sodium hydrogen orthophosphate dehydrate was obtained from Ajax Finechem (NSW, Australia). Methanol and ethanol were of analytical grade and obtained from Merck (Darmstadt, Germany).

2.3. Distillation of essential oils

The essential oils from a total of twenty plant samples were obtained by hydrodistillation for 3 h using a Clevenger-type apparatus. The yield of each essential oil was determined. These oils were dried over anhydrous sodium sulphate and kept in light-protected containers at 4°C until analysis. The density of each essential oil was analyzed using a pycnometer.

2.4. GC-MS

The essential oils isolated were analyzed using GC-MS. The GC-MS analysis was performed on Agilent 6890 gas chromatograph in electron impact (EI, 70 eV) mode coupled to an HP 5973 mass selective detector and fitted with a fused silica capillary column (HP-5MS) supplied by HP, USA (30.0 m \times 250 mm i.d., 0.25 mm film thickness). The analytical conditions were: carrier gas, helium (ca. 1.0 mL/min); injector temperature, 260°C; oven temperature, 3 min isothermal at 100°C (no peaks before 100°C after first injection), 3 °C/min to 188°C, and then 20 °C/min to 280°C (3 min isothermal); and detector temperature, 280°C. Programmed-temperature Kováts retention indices (RI) were obtained by GC-MS analysis of an aliquot of the volatile oil spiked with an n-alkanes mixture containing each homologue from n-C11 to n-C27. Identification of the compounds was based on a comparison with a mass spectra database (WILEY&NIST) and spectroscopic data. The percentage of each component was calculated based on the total area of all peaks obtained from the oil.

2.5. Antityrosinase activity test

The antityrosinase activity of the oils was determined using the modified dopachrome method with L-dopa as a substrate (7). Assays were conducted in a 96-well microtiter plate. Test samples were dissolved in 50% DMSO. Each well contained 40 μL of sample, 80 μL of phosphate buffer solution (PBS) (0.1 M, pH 6.8), 40 μL of tyrosinase (200 units/mL), and 40 μL of L-dopa (2 μM). The microplate reader was read at absorbance of

450 nm. Each sample was accompanied by a blank that had all of the components except L-dopa. Results were compared with a control consisting of 50% DMSO in place of the sample. The percentage tyrosinase inhibition was calculated as follows:

$$\text{Tyrosinase inhibition (\%)} = 100 \times (\Delta A_{\text{Control}} - \Delta A_{\text{Sample}}) / \Delta A_{\text{Control}}$$

2.6. Free radical scavenging activity test

A free radical scavenging activity test or ABTS assay was performed according to the method described by Tachakittirungrod *et al.* (8) with some modifications. An ABTS free radical solution was prepared by mixing 7 mM ABTS with 2.45 mM potassium persulphate ($\text{K}_2\text{S}_2\text{O}_8$) in a ratio of two to three. After incubation in the dark for 16 h, the ABTS free radical solution was then diluted with 20-fold ethanol to obtain absorbance of 0.7 ± 0.1 units at 750 nm. The ABTS free radical solution (180 μL) was mixed with 20 μL of each sample. The disappearance of ABTS free radicals was determined by measuring the decrease in absorbance at 750 nm at the end of 5 min using a 96-well microplate reader. Solutions of Trolox with known concentrations were used to construct a calibration curve. Each sample was measured at 4 concentrations to plot % inhibition *versus* concentration. The results were expressed in terms of Trolox equivalent antioxidant activity (TEAC).

2.7. Ferric reducing/antioxidant power assay

The ferric reducing/antioxidant power (FRAP) assay was carried out according to the method described by Okonogi *et al.* (9). This assay measures the reducing properties of antioxidants based on the reduction of ferric ion. Therefore, ferrous sulfate (FeSO_4) was used for calibration. Briefly, a freshly prepared FRAP solution contained 50 mL of 0.3 M acetate buffer (pH 3.6) plus 5 mL of 10 mM TPTZ solution in 40 mM HCl (previously prepared) and 5 mL of 20 mM ferric chloride. After mixing 180 μL of FRAP solution with 20 μL of each sample, the ferric reducing ability was measured using a 96-well microplate reader at the end of 5 min at an absorbance of 595 nm. The results were reported as equivalent capacity (EC) indicating the ability to reduce ferric ions, expressed as mM FeSO_4 equivalents per mg of the oil. Each experiment was done in triplicate.

2.8. Statistical analysis

The experiments were done in the triplicate and all data are indicated as mean \pm standard deviation. The antityrosinase activity is presented as % enzymatic inhibition. Antioxidant activity in the form of free radical scavenging and ferric reducing/antioxidant

power is presented in terms of TEAC and EC values, respectively. Individual differences were evaluated by one-way ANOVA (post-hoc test). In all cases, $p < 0.05$ indicated a significant difference.

3. Results and Discussion

3.1. Yield and density of essential oils

The essential oils obtained were clear liquids with a light yellow color except *C. asiatica* and *E. odoratum*, which had no color. The yield of essential oils ranged from 0.005% to 1.393% (w/w), as shown in Figure 1. The highest content was obtained from the leaves of *C. hystrix*. The whole *C. asiatica* plant had the lowest oil content and this might be because of its nature as a succulent. The density of each essential oil analyzed by the conventional method ranged from 0.761 to 0.941 g/mL, as shown in Table 1.

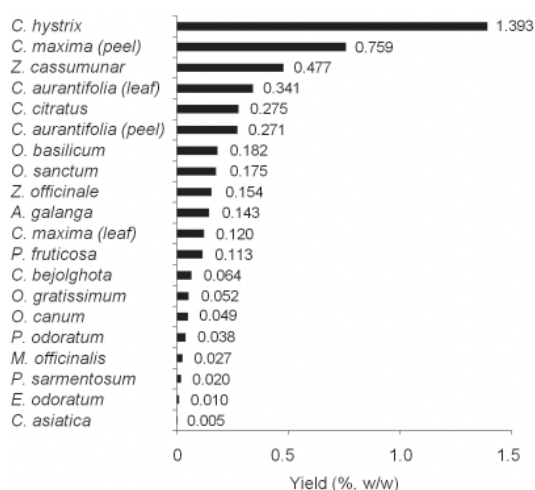


Figure 1. Yield (% w/w) of essential oils.

Table 1. Density of essential oils of plants used in this study

Plant species	Family	Plant part	Density (g/mL)
<i>Centella asiatica</i> Urban.	Apiaceae	Whole plant	0.920
<i>Polyscias fruticosum</i> Harms.	Araliaceae	Leaf	0.808
<i>Eupatorium odoratum</i> Linn.	Asteraceae	Whole plant	0.900
<i>Cymbopogon citratus</i> Stapf.	Gramineae	Stem	0.886
<i>Ocimum sanctum</i> Linn.	Lamiaceae	Leaf	0.941
<i>Ocimum canum</i> Sims.	Lamiaceae	Whole plant	0.810
<i>Ocimum gratissimum</i> Linn.	Lamiaceae	Leaf	0.833
<i>Melissa officinalis</i> Linn.	Lamiaceae	Leaf	0.883
<i>Ocimum basilicum</i> Linn.	Lamiaceae	Leaf	0.910
<i>Cinnamomum bejolghota</i> (Buch. Ham.) Sweet	Lauraceae	Leaf	0.795
<i>Piper sarmentosum</i> Roxb.	Piperaceae	Leaf	0.813
<i>Polygonum odoratum</i> Lour.	Polygonaceae	Whole plant	0.761
<i>Citrus hystrix</i> DC.	Rutaceae	Leaf	0.823
<i>Citrus aurantifolia</i> Swing.	Rutaceae	Leaf	0.812
		Fruit peel	0.840
<i>Citrus maxima</i> (Burm.) Merr.	Rutaceae	Leaf	0.826
		Fruit peel	0.835
<i>Alpinia galanga</i> (Linn.) Swartz.	Zingiberaceae	Rhizome	0.887
<i>Zingiber officinale</i> Roscoe.	Zingiberaceae	Rhizome	0.856
<i>Zingiber cassumunar</i> Roxb.	Zingiberaceae	Rhizome	0.900

3.2. Antityrosinase activity test

Tyrosinase, also known as polyphenol oxidase, is a copper-containing enzyme widely distributed in microorganisms, animals, and plants. This enzyme is mainly implicated in two distinct reactions of melanin biosynthesis, including monophenolase and diphenolase activity. After L-tyrosine (monophenol) is hydroxylated by catalysis of tyrosinase, the hydroxylation product named L-dopa (diphenol) is further oxidized into the corresponding *o*-quinone by catalysis of the same enzyme (10,11). Tyrosinase catalyzes melanin biosynthesis in human skin, resulting in epidermal hyperpigmentation that leads to various dermatological disorders such as melasma, freckles, and age spots (12). Because they inhibit enzymatic oxidation, tyrosinase inhibitors have become increasingly important in medicines (11) and cosmetics (13) to prevent hyperpigmentation. The antityrosinase activities of twenty essential oils are shown in Figure 2. The highest level of inhibitory activity, $69 \pm 4\%$, was from the essential oil of *C. citratus*, which was followed closely by the inhibitory activity, $66 \pm 3\%$, of the essential oil of *O. canum*.

The chemical composition of these two oils was further investigated by GC-MS and the results are shown in Table 2. Twelve volatiles were identified in the *C. citratus* oil, comprising 89.5% of the total composition. Most of this oil was monoterpene, which comprised up to 85.2% of the oil. The most abundant compositions were geranial (42.0%) and neral (32.1%). These results are in accordance with previously published data on *C. citratus* essential oils (14,15). For *O. canum*, thirteen volatiles representing 94.7% of the total oil were identified. Geranial (35.1%) and neral (27.4%) were the major components of this oil. The

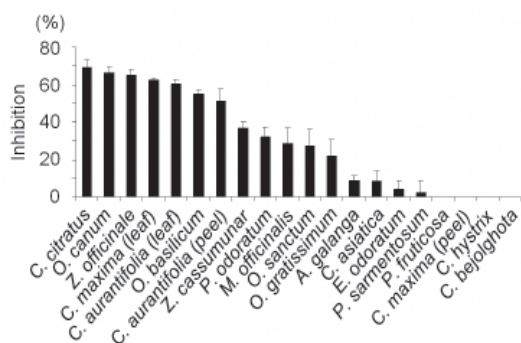


Figure 2. Tyrosinase inhibitory activities of essential oils.

Table 2. Chemical composition of the essential oil of *C. citratus* and *O. canum*

Retention time (min)	Component	Component percentage	
		<i>C. citratus</i>	<i>O. canum</i>
3.48	<i>trans</i> -beta-ocimene	0.58	
4.07	<i>n</i> -undecene	1.4	
4.26	linalool		5.51
5.32	D-camphor	0.49	
5.75	(+)-borneol	0.35	
6.24	alpha-terpineol		0.94
7.09	nerol		4.16
7.25	neral	32.07	27.35
7.55	geraniol	5.21	3.69
8.13	geranial	42.01	35.08
11.05	eugenol		3.09
11.38	piperitenone oxide	2.25	
11.53	decanoic acid	0.79	
11.72	alpha-copaene	1.4	
13.25	caryophyllene		4.87
13.71	alpha- <i>trans</i> -bergamotene		1.57
14.41	alpha-humulene		1.29
15.37	germacrene D		1.92
17.51	<i>cis</i> -alpha-bisabolene		4.58
18.97	caryophyllene oxide		0.64
20.66	beta-maaliene	0.94	
21.02	alpha-cadinol	2.04	
	Total	89.53	94.69

components of linalool (5.5%), caryophyllene (4.9%), *cis*-alpha-bisabolene (4.6%), and nerol (4.2%) were also present. Of 13 volatiles, monoterpene compounds accounted for most of the *O. canum* oil, comprising 79.9%. The essential oil of *O. canum* has been reported to have a good lemony flavor and high citral content (16-18).

3.3. Antioxidant activities

Multiple reactions and mechanisms are reportedly involved in antioxidant processes (19), e.g. free radical scavenging and reducing activity. ABTS and FRAP assays are tests based on different mechanisms of antioxidant action. ABTS indicates the ability of natural antioxidants to scavenge free radicals and is expressed as the TEAC value while FRAP determines the total reducing capacity of the test compound and is expressed as the EC value. Therefore, these two

methods were used to investigate the mechanism of antioxidant action of the test samples.

The ABTS test was first introduced in 1993 (20) to test biological samples and was then widely used to test the antioxidant activity of other samples. The principle of this method is to monitor the decay of the radical-cation (ABTS^{•+}) resulting from the oxidation of ABTS. Since ABTS^{•+} is soluble in both aqueous and organic solvents and is not affected by ionic strength, this method was widely used to indicate the antioxidant activity of samples (21). The quantity of ABTS^{•+} consumed due to the reaction is expressed as the TEAC value although TEAC of an individual antioxidant is really the number of the ABTS^{•+} consumed per molecule of antioxidant. The TEAC values of twenty essential oils are shown in Figure 3A. Essential oils obtained from different plant species and plant parts were found to have different potentials. The two highest TEAC values were 1.06 ± 0.01 mM/mL and 1.05 ± 0.01 mM/mL and were from the essential oils of *O. sanctum* and *O. gratissimum*, respectively.

The ferric reducing/antioxidant power (FRAP) assay was originally developed in 1996 (22) to measure reducing power in plasma, but the assay has also subsequently been adapted and used to assay antioxidants in many botanicals. This method is based on the ability of the test sample to reduce Fe(III) to Fe(II). In the presence of TPTZ, this reduction is accompanied by the formation of a colored complex with Fe(II). The reducing power of twenty essential oils is shown in Figure 3B in terms of EC. The two highest EC values were 3.74 ± 0.01 mM/mL and 3.26 ± 0.01 mM/mL and were from essential oils of *O. sanctum* and *O. gratissimum*, respectively.

These results clearly indicate that the essential oils of both *O. sanctum* and *O. gratissimum* possess antioxidant activity with respect to mechanisms of both free radical scavenging and reducing activities. Other essential oils were further investigated for these mechanisms. The correlation between TEAC and EC values was plotted and the results are shown in Figure 4. A strong correlation ($R^2 = 0.964$) was obtained, indicating that most of the essential oils possessed antioxidant mechanisms in the form of both free radical scavenging and reducing power. This result coincided with that of previous studies indicating that the antioxidant compounds from plants generally possess both mechanisms of action (21). A study by Nantitanon *et al.* (23) found a strong correlation (R^2 of 0.894) between the free radical scavenging activity and reducing power of guava leaf extracts. In addition, Khonkarn *et al.* (24) revealed that there was a linear relationship ($R^2 = 0.979$) between TEAC and EC values of the different fractionated extracts of peels from the three fruits of rambutan, mangosteen, and coconut.

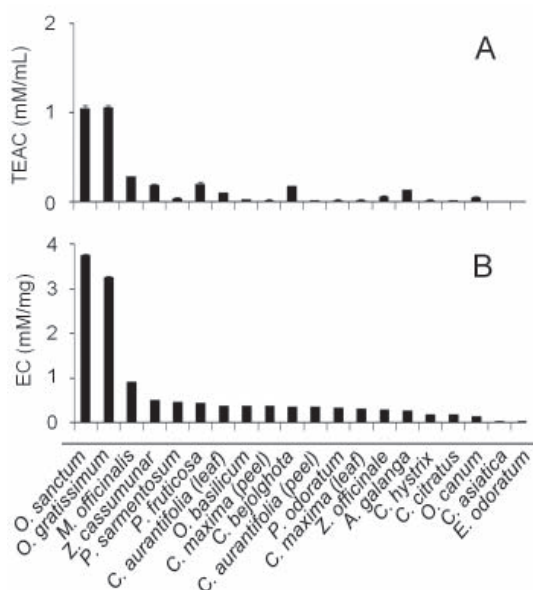


Figure 3. Free radical scavenging activity (A) and ferric reducing/antioxidant power (B) of essential oils.

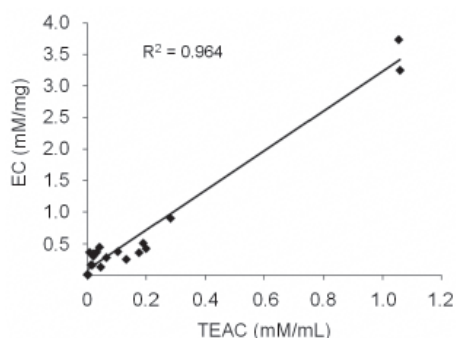


Figure 4. Correlation between free radical scavenging activity and reducing power of essential oils ($R^2 = 0.964$).

4. Conclusion

Among 20 essential oils from edible Thai plants, the essential oil of *C. citratus* had the highest level of antityrosinase activity, followed by that of *O. canum* with enzymatic inhibition of 69 ± 4 and $66 \pm 3\%$. GC-MS revealed that geranial and neral were the two most abundant components of their chemical compositions. Antioxidant activity was gauged by the free radical scavenging activity test and ferric reducing/antioxidant power assay. The essential oil of *O. sanctum* had the highest level of antioxidant activity, followed by the essential oil of *O. gratissimum*. These results led to the conclusions that the essential oils of several edible plants exhibit important biological activities and are a promising choice as natural active ingredients because of their antityrosinase and antioxidant activities.

Acknowledgements

The authors are grateful for financial support received

from the Thailand Research Fund through Research Grant No. IUG5080012 and the Royal Golden Jubilee PhD Program. The authors also wish to thank the Graduate School of Chiang Mai University for its support.

References

1. Low Dog T. A reason to season: The therapeutic benefits of spices and culinary herbs. *Explore* (NY). 2006; 2:446-449.
2. Vagionas K, Ngassapa O, Runyoro D, Graikou K, Gortzi O, Chinou I. Chemical analysis of edible aromatic plants growing in Tanzania. *Food Chem*. 2007; 105:1711-1717.
3. Edris AE. Pharmaceutical and therapeutic potentials of essential oils and their individual volatile constituents: A review. *Phytother Res*. 2007; 21:308-323.
4. Loizzo MR, Menichini F, Conforti F, Tundis R, Bonesi M, Saab AM, Statti GA, Cindio B, Houghton PJ, Menichini F, Giuseppe Frega N. Chemical analysis, antioxidant, antiinflammatory and anticholinesterase activities of *Origanum ehrenbergii* Boiss and *Origanum syriacum* L. essential oils. *Food Chem*. 2009; 117:174-180.
5. Savelev S, Okello E, Perry NS, Wilkins RM, Perry EK. Synergistic and antagonistic interactions of anticholinesterase terpenoids in *Salvia lavandulaefolia* essential oil. *Pharmacol Biochem Behav*. 2003; 75:661-668.
6. Liang CH, Chou TH, Ding HY. Inhibition of melanogenesis by a novel origanoside from *Origanum vulgare*. *J Dermatol Sci*. 2010; 57:170-177.
7. Chan EWC, Lim YY, Wong LF, Lianto FS, Wong SK, Lim KK, Joe CE, Lim TY. Antioxidant and tyrosinase inhibition properties of leaves and rhizomes of ginger species. *Food Chem*. 2008; 109:477-483.
8. Tachakittirungrod S, Okonogi S, Chowwanapoonpohn S. Study on antioxidant activity of certain plants in Thailand: Mechanism of antioxidant action of guava leaf extract. *Food Chem*. 2007; 103:381-388.
9. Okonogi S, Duangrat C, Anuchpreeda S, Tachakittirungrod S, Chowwanapoonpohn S. Comparison of antioxidant capacities and cytotoxicities of certain fruit peels. *Food Chem*. 2007; 103:839-846.
10. Hsu CK, Chang CT, Lu HY, Chung YC. Inhibitory effects of the water extracts of *Lavendula* sp. on mushroom tyrosinase activity. *Food Chem*. 2007; 105:1099-1105.
11. Seo SY, Sharma VK, Sharma N. Mushroom tyrosinase: Recent prospects. *J Agri Food Chem*. 2003; 51:2837-2853.
12. Kim YJ, Uyama H. Tyrosinase inhibitors from natural and synthetic sources: Structure, inhibition mechanism and perspective for the future. *Cell Mol Life Sci*. 2005; 62:1707-1723.
13. Kubo I, Kinoshita H, Yokokawa Y. Tyrosinase inhibitors from *Anacardium occidentale* fruits. *J Nat Prod*. 1994; 57:545-551.
14. Blanco MM, Costa CA, Freire AO, Santos JG Jr, Costa M. Neurobehavioral effect of essential oil of *Cymbopogon citratus* in mice. *Phytomedicine*. 2009; 16:265-270.
15. Tzortzakis NG, Economakis CD. Antifungal activity of lemongrass (*Cymbopogon citratus* L.) essential oil against key postharvest pathogens. *Inn Food Sci Emerg Technol*. 2007; 8:253-258.
16. Morales MR, Charles DJ, Simon JE. New aromatic

- lemon basil germplasm. New crops Wiley, New York, USA, 1993; pp. 632-635.
17. Telci I, Bayram E, Yilmaz G, Avcı B. Variability in essential oil composition of Turkish basil (*Ocimum basilicum* L.). *Biochem System Ecol.* 2006; 34:489-497.
 18. Choudhary R, Kharya MD, Dixit VK, Varma KC. Role of phytohormone on the cultivar and essential oil of *Ocimum canum* Sims. A potential source of citral. *Indian Perfum.* 1989; 33:224-227.
 19. Chu YH, Chang CL, Hsu HF. Flavonoid content of several vegetables and their antioxidant activity. *J Sci Food Agri.* 2000; 80:561-566.
 20. Miller NJ, Rice-Evans C, Davies MJ, Copinathan V, Milner A. A novel method for measuring antioxidant capacity and its application to monitoring the antioxidant status in premature neonants. *Clin Sci (Lond).* 1993; 84:407-412.
 21. Prior RL, Wu X, Schaichs K. Standardized methods for the determination of antioxidant capacity and phenolics in foods and dietary supplements. *J Agri Food Chem.* 2005; 53:4290-4302.
 22. Benzie IF, Strain JJ. The Ferric reducing ability of plasma (FRAP) as a measure of "antioxidant power": The FRAP assay. *Anal Biochem.* 1996; 239:70-76.
 23. Nantitanon W, Yotsawimonwat S, Okonogi S. Factors influencing antioxidant activities and total phenolic content of guava leaf extract. *LWT-Food Sci Technol.* 2010; 43:1095-1103.
 24. Khonkarn R, Okonogi S, Ampasavate C, Anuchapreeda S. Investigation of fruit peel extracts as sources for compounds with antioxidant and antiproliferative activities against human cell lines. *Food Chem Toxicol.* 2010; 48:2122-2129.

(Received February 22, 2011; Revised May 07, 2010; Accepted May 10, 2010)

Emulsions and rectal formulations containing myrrh essential oil for better patient compliance

Mohamed Etman¹, Mohamed Amin¹, Aly H. Nada^{2,*}, Mohamed Shams-Eldin¹, Osama Salama³

¹ Department of Pharmaceutics, Faculty of Pharmacy, Alexandria University, Alexandria, Egypt;

² Department of Pharmaceutics, Faculty of Pharmacy, Kuwait University, Kuwait;

³ Faculty of Pharmaceutical Sciences and Pharmaceutical Industries, Future University, Cairo, Egypt.

ABSTRACT: Myrrh has long been used for its circulatory, disinfectant, analgesic, antirheumatic, antidiabetic, and schistosomicidal properties. Myrrh essential oil (MEO) was extracted from the oleo-gum resin of *Commiphora molmol* and formulated into emulsions and suppositories to mask/avoid its bitter taste. Three oil-in-water emulsions (E1-E3) were formulated and taste was evaluated by 10 volunteers. Particle size distribution was measured and correlated with excipients and the method of preparation. Physical and chemical stability testing was carried out for the optimum formulation (E2). Seven suppository formulations were investigated (F1-F7). Suppocire AML (F1) and Suppocire CM (F2) were chosen as fatty bases, and polyethylene glycol (PEG) 1500 (F3), PEG 4000 (F4), and a PEG blend (50% PEG 6000 + 30% PEG 1500 + 20% PEG 400) (F5) were chosen as water-soluble bases. A blend of PEG 1500 and Suppocire CM was also used (F7). Camphor (5%) was added to PEG 1500 (F6). Disintegration time, release rate, DSC, fracture points, and weight uniformity were evaluated. The overall average bitterness for formulations E1, E2, and E3 was 6.44, 4.15, and 3.45, respectively. Suppositories containing Suppocire AML had the fastest disintegration time (1.5 min) with dissolution efficiency (DE) of 56.8%. F3 containing PEG 1500 had a fast disintegration time of 2.5 min and maximum DE of 93.5%. The PEG blend had satisfactory release: (DE = 90.9%). A mixed fatty and water-soluble base (F7) had a disintegration time of 5 min and low DE (33.4%). A stable MEO emulsion with acceptable taste was formulated to improve patient acceptance and compliance. F3 suppositories yielded satisfactory results, while formulations containing fat-soluble bases exhibited poor release.

Keywords: Myrrh essential oil, emulsions, taste masking, suppositories, release, stability

*Address correspondence to:

Dr. Aly H. Nada, Department of Pharmaceutics, Faculty of Pharmacy, Kuwait University, Kuwait, POB 24923 Safat, 13110 Kuwait.
e-mail:alynada@hsc.edu.kw

1. Introduction

Myrrh (Arabian or Somali Myrrh) is an oleo-gum resin, obtained from the stem of various species of *Commiphora*, Family Burseraceae, growing in north-east Africa and Arabia (1). The chief source is *Commiphora molmol*. The volatile oil obtained from *C. molmol* is thick and pale yellow (2). The constituents of the essential oil include cadinene, elemol, eugenol, cuminaldehyde, furanosesquiterpenes, furandiene, furanodienone, curzerenone, lindestrene, and furanoeudesma-1,3-diene (1,3,4). The oil has been used to treat sore throats, canker sores and gingivitis, acne, boils, and arthritis (5).

An extract of myrrh (gum) effectively decreased the absolute increment of blood glucose above the fasting concentration at all times in an oral glucose tolerance test with both normal and diabetic rats (6). Myrrh is also used in cosmetic preparations to treat the hair and scalp (7). In addition, myrrh has anti-inflammatory activity, antipyretic activity (8), anti-ulcerogenic activity, and offers protection against mucosal damage caused by indomethacin (9). Myrrh is not recommended during pregnancy as it is a uterine stimulant and excessive oral doses (2-4 g) may lead to diarrhea, heart rate changes, and kidney irritation. Myrrh has been found to have cytotoxic and antitumor activity equivalent to that of the standard cytotoxic drug cyclophosphamide (10).

Myrrh could be used therapeutically to chelate toxic metals, thus potentially reducing their toxicity and tissue damage (11). The sesquiterpene fractions of myrrh have antibacterial and antifungal activity against standard pathogenic strains of *Escherichia coli*, *Staphylococcus aureus*, and *Pseudomonas aeruginosa* (12).

In the last few years, a myrrh extract purified using methyl alcohol has been formulated and marketed as soft gelatin capsules (MIRAZID[®]) to treat *Schistosoma mansoni* and *Schistosoma haematobium* (13). Recently, the efficacy of this new anti-schistosomiasis drug was questioned by several research articles describing the administration of MIRAZID[®] as having a very limited antischistosomal effect (14,15). More recently, Nomicos reported on the numerous uses of myrrh from antiquity to the present (16).

Emulsions can be designed for oral administration. An oil-in-water (O/W) emulsion is a convenient means of orally administering water-insoluble liquids, especially when the dispersed phase has an unpleasant taste, *e.g.* a cod liver oil emulsion (17). More significant in contemporary pharmacy is the observation that some oil-soluble compounds, such as some vitamins, are absorbed more completely when emulsified than when administered as an oily solution.

Rectal delivery is an alternative to the oral route because it can decrease gastrointestinal side effects, avoid undesirable effects of meals on drug absorption, and is also useful when vomiting is present – a situation particularly relevant to young children. However, the choice of a suppository base is paramount since drug release from a suppository base is often the rate-determining step in the absorption process and, consequently, the onset of drug action (18).

In this study, various O/W emulsion and suppository formulations were prepared to mask/avoid the unpleasant taste of myrrh essential oil (MEO) serving as the active ingredient. Two types of suppository bases, fatty bases and water-soluble bases, were used in addition to a blend of a water-soluble and a fatty base.

2. Materials and Methods

2.1. Materials

Aspartame, butylated hydroxyanisole (BHA), butylated hydroxytoluene (BHT), and EDTA were from Jebsen & Jessen, Hamburg, Germany. Anise oil and peppermint oil were supplied by Burnet, Italy. Cremophore RH40 and polyethylene glycols (PEGs) were procured from BASF, Schwarzheide, Germany. Myrrh (oleogum resin; Somali origin) was supplied by Emiga, Gardanne, France. Xanthan gum was from Red Carnation Gums Ltd., Basildon, UK. Methyl and propyl paraben were from Suntin MediPharma Co. Ltd., Shenzhen, China. Petroleum ether 40-60 and camphor were from El-Nasr Pharmaceuticals, Alexandria, Egypt. Propylene glycol was from Lyondell, France. Citric acid was from Jungunzlauer, Basel, Switzerland. Suppocire CM and Suppocire AML were supplied by Gattefosse, Lyon, France.

2.2. Preparation of MEO

The particle size of oleogum resin was reduced in the following two steps: trituration using a mortar and pestle followed by further refining using a small scale electric grinder. Subsequently, percolation was performed using 1 L petroleum ether 40-60 as a solvent for each kg of oleogum resin (19). The solvent was left overnight before collection and the procedure was repeated 3 times in succession in an attempt to ensure the complete extraction of the late-eluting fractions of the oil. The three crops of the percolate were added together and the

oil was separated from petroleum ether using a rotary evaporator at 50°C. The resulting oil was a pale yellow viscous liquid.

2.3. Preparation of MEO Emulsions

MEO emulsions were prepared according to the formulations shown in Table 1. The emulsifier Cremophore RH40 was subjected to slight warming on a water bath before the oil mixture (the flavoring agents anise, peppermint oil, and myrrh) was added, and the result was sonicated for a few minutes. Water containing citric acid was warmed until its temperature slightly exceeded the cremophore/oil mixture before it was added to the oily phase, and the result was homogenized at a fixed speed of 6,500 rpm (Ultraturrax T25, IKA Labor Technik, Staufen, Germany). Preliminary trials using various homogenizing speeds revealed this to be the optimum speed. Xanthan gum (viscosity imparting agent), which was left in a closed container overnight at room temperature for optimum hydration, was added to the formed emulsion along with the prepared simple syrup. BHA (antioxidant) and methyl and propyl parabens (preservatives) were incorporated after dissolution in the ethanol/propylene glycol mixture. Finally, EDTA (chelating agent) was added to the water in order to bring the emulsion to its final volume and produce a creamy white liquid product.

2.4. Physicochemical evaluation of emulsions

2.4.1. Taste

A study was carried out to evaluate the taste of three formulations using a taste panel (ten volunteers). The test was performed as previously reported in the literature (20) with a modification: the taste panel was asked to report

Table 1. Percent (w/w) of the individual ingredients used for preparation of the proposed emulsion formulations

Components	Formulations		
	E1	E2	E3
Cremophore RH40	2.00	2.00	2.00
Myrrh Essential oil	3.60	3.60	3.60
Citric acid	0.01	0.01	0.01
Aspartame	0.40	0.40	0.40
Xanthan gum	0.15	0.15	0.15
Sucrose	40.00	40.00	40.00
Ethanol	5.00	5.00	5.00
Propylene glycol	2.00	2.00	2.00
Methyl paraben	0.06	0.06	0.06
Propyl paraben	0.06	0.06	0.06
BHA	0.02	0.02	0.02
EDTA	0.10	0.10	0.10
Anise oil	–	0.10	0.10
Peppermint oil	–	0.10	0.10
Glycerol	–	–	30.00
Water	to 100	to 100	to 100

initial bitterness (1st round) and sustained bitterness (2nd round) instead of a single round of testing. The average bitterness was calculated from these 2 rounds and taste was rated on a scale where 1 was acceptable and 10 was completely unacceptable. The taste panel was allowed to rinse their mouths out with water and wait 10 min before tasting the next formulation. The three formulations were tested in random order.

2.4.2. Particle size determination

A laser particle size analyzer (Model 1064; CILAS, Orleans, France) was used to determine the size of oil droplets (21) in the range of 0.04-500 μm . Particle size distribution was correlated with the effect of excipients and method used for emulsion preparation.

2.4.3. Physical stability

A temperature cycling method was used in which the emulsion was stored at an elevated temperature (45°C) for 48 h and then refrigerated (4°C) for 48 h (22). The effect of centrifugal force on the stability of the prepared emulsions was evaluated at the following two speed levels (16): *i*) high speed, 4,000 rpm for 2 min and *ii*) low speed, 2,000 rpm for 6 min.

2.4.4. Chemical stability

The E2 emulsion was evaluated in terms of the stability of MEO content over three months at 25°C and 4°C. A colorimetric method was used to determine MEO in the emulsion (19). The calibration curve was constructed using a stock standard solution of MEO (5 mg/mL) in methanol. Aliquots of the stock standard solution ranging from 400-2,000 μL were transferred to 2 mL screw-capped test tubes. To each tube, 5 mL of 1% (w/v) vanillin solution and 1 mL of methanol were successively added. The tubes were capped and heated in a water bath at 60°C for 60 min, allowed to cool for 30 min, and then the contents were transferred to 50 mL volumetric flasks and brought to final volume with methanol. The absorbance of the developed violet color was measured against a reagent blank at 518 nm (Helios alpha UV-Visible spectrophotometer, Thermo Spectronic, Cambridge, UK). A 7 mL volume of the well mixed oral emulsion, equivalent to 252 mg of MEO, was transferred to a 50 mL-volumetric flask, dissolved in methanol, and then brought to final volume with methanol. Aliquots of this solution (1,000 μL) were treated using the above described procedure prior to spectrophotometric analysis at 518 nm.

A placebo formulation was tested using the same procedure of determining MEO to ensure no interference from any of the excipients used. A characteristic violet color should not develop in the absence of the active component.

2.5. Suppository formulations

Seven different suppository formulations (F1-F7) were prepared using the fusion method and employing different bases (Table 2). Suppocire CM and AML were chosen as fatty bases while PEG 1500, PEG 4000, and a PEG blend (50% PEG 6000 + 30% PEG 1500 + 20% PEG 400) were used as water-soluble suppository bases. A blend consisting of 70% PEG 1500 and 30% Suppocire CM was also investigated. Camphor (5%) was added to PEG 1500-based suppositories (F6). BHT was included in all formulation (0.4%) as an antioxidant. MEO was added to the melted base (180 mg MEO/supp) and the resulting mixture was then poured into a metal mold and allowed to cool. The prepared suppositories were stored at 4°C until use.

2.6. Physicochemical evaluation

The displacement values of MEO in each suppository base are shown in Table 2. Uniformity of weight was evaluated using 20 suppositories of each formulation and the average and standard deviation were calculated.

Differential scanning calorimetry (DSC) thermograms were obtained (DSC 6, Perkin-Elmer, Waltham, MA, USA) for the pure base and final formulation. Samples (20 mg) were heated in aluminum pans at a rate of 2 °C/min over a temperature range of 25 to 125°C. The values for the transitions were derived from the computed extrapolated peak maximum and onset and end of melting, and the enthalpy values (ΔH) were calculated from the area under the melting peak.

Disintegration was tested using a tablet disintegration tester (QC-21; Hanson Research, Chatsworth, CA, USA) and suppositories stored for 24 h at room temperature. Water (37 \pm 0.5°C) was used as the immersion fluid and the time required for each suppository to completely melt or dissolve was measured.

Fragility of suppositories was determined using a fracture point apparatus (Model SBT; Erweka GmbH, Heusenstamm, Germany) equipped with a double-walled chamber to maintain the desired temperature at 25°C. Each suppository was subjected to an initial load of 0.6 kg. After 1 min, a metallic disc weighing 0.2 kg was

Table 2. Displacement values of MEO in each suppository base used

Formulations	Suppository base (each containing 180 mg MEO)	D.V.*
F1	Suppocire AML	1.22
F2	Suppocire CM	0.94
F3	PEG 1500	1.00
F4	PEG 4000	0.92
F5	PEG mixture (50% PEG 6000, 30% PEG 1500, 20% PEG 400)	1.05
F6	PEG 1500 containing 5% camphor	1.00
F7	70% PEG 1500 + 30% Suppocire CM	1.30

* Displacement value of the suppository base.

added and the process continued until the suppository collapsed. If breaking occurred within the first 20 sec after application of the additional disc, only the sum of the previous weights was considered. If it collapsed in 20-40 sec, only half the value of the additional weight was added to the sum. If breaking occurred after 40 sec, the additional weight was fully considered.

An *in vitro* drug release test was carried out using Dissolution Tester USP-25, apparatus 1 (Model TDT-O6N; Electrolab, Mumbai, India). The medium consisted of 450 mL phosphate buffer, pH 7.4, with 3% sodium lauryl sulphate maintained at $37 \pm 0.5^\circ\text{C}$ and the paddles were rotated at 100 rpm. Aliquots were withdrawn at 5, 10, 15, 20, 30, 45, and 60 min. Samples were then suitably diluted and the amount of MEO was determined by reaction with freshly prepared vanillin sulfuric acid followed by spectrophotometric measurement at 518 nm using an appropriate blank. Details of this method have been previously described (19). The data presented are the average of three determinations.

3. Results and Discussion

3.1. Emulsions

3.1.1. Taste

To evaluate the improved taste and lack of bitterness of formulations, the taste of the prepared emulsions was evaluated. Table 3 shows the results of a taste evaluation by ten volunteers. The overall average bitterness for formulations E1, E2, and E3 was 6.5 ± 0.8 , 4.2 ± 1.3 , and 3.5 ± 0.6 , respectively. The simple use of natural and synthetic sweetening agents such as sucrose and aspartame (E1) was not sufficient to make a product containing a drug with a particularly unpleasant taste,

Table 3. Taste evaluation of the prepared emulsions by a panel of ten volunteers

Evaluation	Formulations		
	E1	E2	E3
1st round	4.8 ± 1.4	3.6 ± 1.6	2.7 ± 1.1
2nd round	8.1 ± 0.5	4.7 ± 2.4	4.2 ± 1.4
Average	6.5 ± 0.8	4.2 ± 1.3	3.5 ± 0.6

Data are shown as means \pm S.D. ($n = 10$).

Table 4. Effect of emulsion composition and stirring rate on particle size distribution

Formulation	Diameter at 10% (μm)*	Diameter at 50% (μm)*	Diameter at 90% (μm)*	Mean diameter (μm)
E2, 6,500 rpm	0.09	1.23	84.9	24.3
E2, 9,500 rpm	0.92	69.8	130	64.7
E2, 13,500 rpm	1.00	70.9	129	65.3
E2, magnetic stirrer	0.22	7.12	117	40.7
E2, Xanthan gum only	2.65	270	456	245
E3, 6,500 rpm	0.10	34.9	369	93.9
Emulsifier and oily ingredients	7.51	19.9	36.9	21.3

* Particle size corresponding to cumulative frequency distribution data.

such as myrrh, more palatable. The use of an anise/peppermint oil mixture in E2 increased the formulation's acceptance by volunteers. Anise and peppermint oils are common ingredients in pediatric formulations. This may be particularly useful in improving patient compliance. Moreover, anise and peppermint have proven to be particularly useful in masking a bitter taste in comparison to other flavors (23). The use of glycerol in E3 further increased acceptance by volunteers. This could be due to the additional sweetening effect of glycerol. However, formulation E3 containing glycerol had less physical stability than E2 that lacked glycerol, as evidenced by the greater particle size distribution of E3 in comparison to E2 (Table 4).

3.1.2. Particle size analysis

The particle size distribution of the prepared emulsions was evaluated in an attempt to examine the effect of emulsion composition on globule size since this may affect emulsion stability and appearance. Aliquots from each emulsion were appropriately diluted by the aqueous phase to a droplet concentration of approximately 0.0005% to avoid the effects of multiple scattering (21). The results of particle size analysis are summarized in Table 4. Incorporation of glycerol in E3 increased the particle size dramatically in comparison to E2.

With a formulation containing cremophore/anise/peppermint and MEO and no other excipients, none of the oil droplets exceeded $100 \mu\text{m}$ (the maximum diameter for oil droplets was $71 \mu\text{m}$) and the diameter at 50% was $19.9 \mu\text{m}$ (Table 4).

The homogenization used to formulate emulsions yielded more satisfactory results than did the direct use of a magnetic stirrer. Homogenization produced particles with a diameter of $1.23 \mu\text{m}$ at 50% cumulative value and a maximum diameter of $140 \mu\text{m}$ compared to a diameter of $7.12 \mu\text{m}$ at 50% cumulative value and a maximum diameter of $240 \mu\text{m}$ when a magnetic stirrer was used (Table 4). Increasing the speed of homogenization above 6,500 rpm failed to improve the particle size distribution (Table 4). The adverse effect of increasing the homogenization speed on the droplet size distribution could be attributed to the partial breakdown of the structure formed by the emulsion stabilizer

xanthan gum (24). This structure is thought to be responsible for arresting oil droplets in place, preventing their adherence, coalescence, and hence growth in size.

3.1.3. Physical stability

The stability of the prepared emulsions (F1, F2, and F3) was determined by exposure to highly elevated and reduced temperatures in cycles. An elevated temperature (45°C) and a refrigeration temperature (4°C) were used for evaluation.

No changes were observed for up to 5 cycles of the elevated and refrigeration temperatures (data not shown). A centrifugation test was performed to examine the physical stability of the formulation; separation of a layer was deemed to indicate a product with a poor design and poor physical stability. No signs of creaming were observed after centrifugation at high (4,000 rpm) or low (2,000 rpm) speeds of centrifugation (data not shown). These results could be useful indicators of the stability of future formulations.

3.1.4. Chemical stability

Liquid dosage forms are known to be far less stable than solid or semisolid products. Therefore, the chemical stability of the emulsion of choice (Formulation E2) was monitored by analysis of its MEO content at the time of preparation (baseline) and 1, 2, and 3 months after emulsion preparation. The results of chemical analysis are shown in Table 5. The results clearly show that the emulsion maintained its oil quality over the period of examination when stored both on the shelf and in the refrigerator. However, UV spectrophotometric methods are not suitable for indicating chemical stability. Thus, the test used in this study only serves as a preliminary

Table 5. Percent of remaining MEO in formulation E2 during storage at various temperatures

Storage period	Remaining MEO in E2 (%)	
	25°C	4°C
Baseline	100.0	100.0
1 month	100.0	97.6
2 month	98.3	99.0
3 month	98.0	98.3

indication of the produced formulation's chemical stability. These results along with the results of physical stability indicate the suitability of the composition and method of its preparation to produce emulsions with acceptable properties.

3.2. Suppositories

3.2.1. Uniformity of weight

All of the prepared suppositories had acceptable results with regard to the uniformity of weight described in BP 2004 (25) (data not shown). No more than two of the individual weights deviated from the average weight by more than 5% and none deviated by twice that percentage; the standard deviations of the prepared formulations ranged from ± 0.01 to ± 0.06 . The BP does not require uniformity of content for suppositories containing more than 2 mg or 2% of the total mass; drug content in the investigated suppositories was 3.6%.

3.2.2. Differential scanning calorimetry (DSC)

The data derived from DSC thermograms of the prepared suppositories are summarized in Table 6. A decrease in the melting points of the suppositories was observed with all formulations in comparison to the respective base. This could be explained by the liquid nature of MEO. Mixing camphor with PEG 1500 led to a slight reduction in the melting point of the base; melting points were 49.3 and 50.8°C, respectively. On the other hand, inclusion of the oil (MEO) in camphor suppositories containing PEG 1500 led to an increase in the melting point from 49.3 to 59.3°C. This increase may be explained by the interaction between PEG and some of the components of MEO, which resulted in higher molecular weight compounds. This may be a consequence of ether formation by the free -OH groups of PEG and free -OH groups of elemol and eugenol present in MEO and the formation of high molecular weight compounds, which are expected to have higher melting points. Similar interactions involving transesterification of PEG with aspirin (26) and pancreatin (27) have previously been reported in the literature.

Table 6. Parameters obtained from DSC thermograms of suppository bases before (A) and after (B) the incorporation of MEO

Parameters	F1		F2		F3		F4		F5		F6		F7	
	A	B	A	B	A	B	A	B	A	B	A	B	A	B
Peak (°C)	38.9	35.7	40.6	37.6	50.8	46.7	63.4	60.6	58.4	55.7	49.3	59.3	49.5	35.4
Peak Height (MW)	12.2	7.5	14.9	9.8	26.6	14.8	32.5	20.5	13.1	8.8	22.1	16.4	21.4	7.0
Area (MJ)	5,894	3,797	4,934	5,048	5,954	5,081	6,442	6,284	5,964	5,226	8,682	4,502	5,699.5	4,477
Delta H (J/G)	294.7	189.8	246.7	252.4	297.7	254.0	322.1	314.2	298.2	261.3	434.1	225.1	284.9	223.9
End (°C)	40.8	37.8	42.6	39.6	53.0	48.7	66.4	62.5	60.5	57.5	51.5	61.1	51.6	37.8
Onset (°C)	35.7	25.1	38.1	32.3	47.1	37.9	60.5	58.2	54.8	50.0	46.2	56.2	46.9	28.0

The lowest melting points were observed with Suppocire fatty bases, *i.e.* 35.7 and 37.6°C for Suppocire AML (F1) and Suppocire CM (F2), respectively. The melting point of a Suppocire AML-based suppository (F1) was sufficient to allow melting at body temperature shortly after insertion. Suppositories prepared using PEG bases had melting points ranging from 46.7 to 60.6°C (F3 to F6). A mixed base suppository formulation (F7) had a lower melting point of 35.4°C.

3.2.3. Disintegration time

According to BP 2004 (25), suppositories of water-soluble bases are supposed to dissolve within 60 min and those of fatty bases should soften and melt in no more than 30 min. The results of the disintegration experiments are shown in Table 7. Results revealed that fatty bases (Suppocire AML and Suppocire CM) (F1 and F2, respectively) typically had faster disintegration times than water-soluble bases. Of water-soluble bases, PEG 1500/camphor-based suppositories (F6) had the fastest disintegration time while PEG 4000 (F4) had the slowest disintegration time, *i.e.* 2 and 15 min for F6 and F4, respectively.

3.2.4. In vitro drug release

The percentage of drug released after 30 min was chosen for comparison of the *in vitro* drug release from various suppository bases (Figure 1). Moreover, the percentage dissolution efficiency (DE%) values obtained from the dissolution profiles of the drug from different suppository bases have been calculated using the following equation:

$$DE\% = (\text{Area under dissolution curve to a certain time}) / (\text{Area of the rectangle of 100\% dissolution in the same time}) \times 100$$

The areas under the dissolution profiles (Figure 1) were calculated using the trapezoidal principle and the respective dissolution efficiencies are shown in Table 7.

The fastest release was observed with suppositories based only on PEG 1500 (F3), and this formulation had the highest drug release in 30 min along with a DE% of 93.5%. This was followed by suppositories with a blend of PEGs (F5), which had a DE% of 90.9%. The high release rate of MEO from PEG suppository bases (F3 and F5) may be the result of the opposite natures of the aqueous base and the fatty nature of the active material. However, users may experience slight irritation when using PEG-based suppositories.

Slow and incomplete release in 30 min was observed with Suppocire fatty bases, *i.e.* DE% of 56.8% with Suppocire AML (F1) and DE% of 12.5% with Suppocire CM (F2). The slow and incomplete release

Table 7. Disintegration time, percentage dissolution efficiency, and fracture points of different suppositories

Formulations	Disintegration time (min)	Dissolution efficiency (%)	Fracture point (kg)
F1	1.5	56.8	0.7
F2	2.0	12.5	0.9
F3	2.5	93.5	2.4
F4	15.0	85.6	3.0
F5	7.0	90.9	3.2
F6	2.0	85.5	1.7
F7	5.0	33.4	1.0

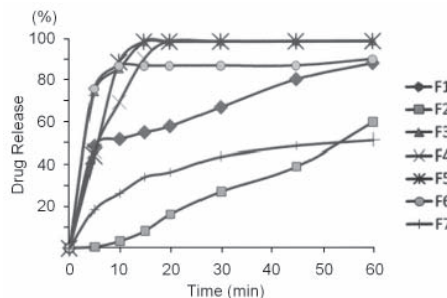


Figure 1. Mean drug release from different suppository formulations (F1-F7). Drug release was examined in phosphate buffer, pH 7.4, with 3% sodium lauryl sulphate maintained at $37 \pm 0.5^\circ\text{C}$ ($n = 3$).

of the MEO from Suppocire-based suppositories F1 and F2, despite their quick disintegration time, may be attributed to the high affinity of the oily active material for the fatty base, presumably hindering its release (18).

A mixed fatty/water-soluble suppository base containing 70% PEG 1500 and 30% Suppocire CM produced poor results, which may be attributed to the entrapment of MEO in the fatty Suppocire component. In a previous study, drugs such as Etodolac produced good results with this base (28). This may be explained by the state in which the drug is dispersed in the base. MEO is a hydrophobic liquid and therefore may undergo quick and extensive distribution in the fatty Suppocire component. This would hinder its departure from the suppository base and entry into the dissolution medium.

4. Conclusion

A stable MEO emulsion with an acceptable taste was formulated using Cremophore as an emulsifier and a combination of anise oil, peppermint oil, and glycerol as flavoring agents. Masking of the bitter and disagreeable taste of MEO will improve patient acceptance and compliance. Suppositories prepared from PEG 1500 (F3) yielded satisfactory results as evidenced by more than 90% release after 30 min.

Suppository formulations containing fat-soluble Suppocire AML and CM had poor release properties. Suppositories with mixed water and fat-soluble bases (PEG 1500:Suppocire CM; 70 and 30%) had inferior release properties in comparison to those based only on PEGs.

References

- Evans WC. Trease and Evans Pharmacognosy. 15th ed., WB Saunders, Edinburgh, UK, 2002; pp. 285-286.
- Wallis TE. Textbook of Pharmacognosy. 5th ed., J. and W. Churchill Ltd., London, UK, 1967; pp. 497-500.
- Brieskorn CH, Noble P. Constituents of the essential oil of myrrh. *Planta Med.* 1982; 44:87-90.
- Brieskorn CH, Noble P. Two furanoeudesmanes from the essential oil of myrrh. *Phytochemistry.* 1983; 22:187-189.
- Chevallier A. The Encyclopedia of Medicinal Plants. 4th ed., DK Publisher, New York, NY, USA, 1996; p. 84.
- Al Awadi FM, Gumaa KA. Studies on the activity of the individual plants of an antidiabetic plant mixture. *Acta Diabetol Lat.* 1987; 24:37-41.
- Kubec F, Knap J, Juchelka J. Czech Cs Patent: 244387; CA 109, 236732, 1998.
- Qureshi S, al-Harbi MM, Ahmed MM, Raza MM, Giangero AB, Shah AH. Evaluation of the genotoxic, cytotoxic and antitumor properties of *Commiphora molmol* using normal and Ehrlich ascites carcinoma cell bearing swiss albino mice. *Cancer Chemother Pharmacol.* 1993; 33:130-138.
- Atta AH, Alkotahi A. Anti-nociceptive and anti-inflammatory effects of some Jordanian medical plant extracts. *J Ethnopharmacol.* 1998; 60:117-124.
- Al Harbi MM, Qureshi S, Raza M, Ahmed MM. Effect of *Commiphora molmol* in rats. *J Ethnopharmacol.* 1997; 55:141-150.
- El-Ashmawy IM, Ashry KM, El-Nahas AF, Salama OM. Protection by Turmeric and Myrrh against liver oxidative damage and genotoxicity induced by lead acetate in mice. *Basic Clin Pharmacol Toxicol.* 2006; 98:32-37.
- Dolara P, Corte B, Ghelardini C, Pugliese AM, Cerbai E, Menichetti S, Lo Nostro A. Local anaesthetic, antibacterial and antifungal properties of sesquiterpenes from myrrh. *Planta Med.* 2000; 66:356-358.
- Sheir Z, Nasr AA, Massoud A, Salama O, Badra GA, El-Shennawy H, Hassan N, Hammad SM. A safe, effective, herbal antischistosomal therapy derived from myrrh. *Am J Trop Med Hyg.* 2001; 65:700-704.
- Barakat R, Elmorshedy H, Fenwick A. Efficacy of myrrh in the treatment of human *Schistosomiasis mansoni*. *Am J Trop Med Hyg.* 2005; 73:365-367.
- Botros S, Sayed H, El-Dusoki H, Sabry H, Rabie I, El-Ghannam M, Hassanein M, El-Wahab YA, Engels D. Efficacy of mirazid in comparison with praziquantel in Egyptian *Schistosoma mansoni*-infected school children and households. *Am J Trop Med Hyg.* 2005; 72:119-123.
- Nomicos EY. Myrrh: Medical marvel or myth of the Magi? *Holist Nurs Pract.* 2007; 21:308-323.
- Banker GS, Rhodes CT. Modern Pharmaceutics. 2nd ed., Marcel Dekker Inc., New York, NY, USA, 1989; pp. 347-351.
- Florence AT, Attwood D. Physicochemical Principles of Pharmacy. 3rd ed., Macmillan Press Ltd., London, UK, 1998; pp. 442-446.
- Abdel-Hay MH, Saleh A, El-Ashry ESH, Rashed N, Salama O. Colorimetric determination of crude powdered myrrh, purified myrrh extract, oily fraction, and its different pharmaceutical dosage forms. *Spectrosc Lett.* 2002; 35:183-197.
- Suzuki H, Onishi H, Takahashi Y, Iwata M, Machida Y. Development of oral acetaminophen chewable tablets with inhibited bitter taste. *Int J Pharm.* 2003; 251:123-132.
- Ogawa S, Decker EA, Mc Clements DJ. Production and characterization of O/W emulsions containing cationic droplets stabilized by lecithin-chitosan membranes. *J Agric Food Chem.* 2003; 51:2806-2812.
- Lachman L, Lieberman HA, Kanig JL. The Theory and Practice of Industrial Pharmacy. 3rd ed., Lea and Febiger, Philadelphia, PA, USA, 1986.
- Aulton ME. The Design and Manufacture of Medicines. 3rd ed., Churchill Livingstone, Edinburgh, UK, 2007; pp. 369-370.
- Martin A, Bustamente P. Physical Pharmacy: Physical Chemical Principles in the Pharmaceutical Sciences. 4th ed., Lea & Febiger, Philadelphia, PA, USA, 1993; pp. 486-502.
- British Pharmacopoeia 2004, British Pharmacopoeia Commission, UK, pp. 2138.
- Jun HW, Whitworth CW, Luzzi LA. Decomposition of aspirin in polyethylene glycols. *J Pharm Sci.* 1972; 61:1160-1162.
- Graf E, Sakr A, Nada A. Studies on direct compression of pharmaceuticals: 5. Pancreatin, c) Evaluation of some lubricants and their effects on amylase and lipase activities. *Pharm Ind.* 1981; 43:282-286.
- Salama RO. Formulation and Evaluation of Various Dosage Forms of Etodolac as a Nonsteroidal Anti-inflammatory Drug. Thesis, Department of Pharmaceutics, Faculty of Pharmacy, Alexandria University, Alexandria, Egypt, 2003; pp. 59-76.

(Received January 12, 2011; Revised February 24, 2011; Re-revised May 18, 2011; Accepted May 23, 2011)

Guide for Authors

1. Scope of Articles

Drug Discoveries & Therapeutics welcomes contributions in all fields of pharmaceutical and therapeutic research such as medicinal chemistry, pharmacology, pharmaceutical analysis, pharmaceuticals, pharmaceutical administration, and experimental and clinical studies of effects, mechanisms, or uses of various treatments. Studies in drug-related fields such as biology, biochemistry, physiology, microbiology, and immunology are also within the scope of this journal.

2. Submission Types

Original Articles should be well-documented, novel, and significant to the field as a whole. An Original Article should be arranged into the following sections: Title page, Abstract, Introduction, Materials and Methods, Results, Discussion, Acknowledgments, and References. Original articles should not exceed 5,000 words in length (excluding references) and should be limited to a maximum of 50 references. Articles may contain a maximum of 10 figures and/or tables.

Brief Reports definitively documenting either experimental results or informative clinical observations will be considered for publication in this category. Brief Reports are not intended for publication of incomplete or preliminary findings. Brief Reports should not exceed 3,000 words in length (excluding references) and should be limited to a maximum of 4 figures and/or tables and 30 references. A Brief Report contains the same sections as an Original Article, but the Results and Discussion sections should be combined.

Reviews should present a full and up-to-date account of recent developments within an area of research. Normally, reviews should not exceed 8,000 words in length (excluding references) and should be limited to a maximum of 100 references. Mini reviews are also accepted.

Policy Forum articles discuss research and policy issues in areas related to life science such as public health, the medical care system, and social science and may address governmental issues at district, national, and international levels of discourse. Policy Forum articles should not exceed 2,000 words in length (excluding references).

Case Reports should be detailed reports of the symptoms, signs, diagnosis, treatment, and follow-up of an individual patient. Case reports may contain a demographic profile of the patient but usually describe an unusual or novel occurrence. Unreported or unusual side effects or adverse interactions involving medications will also be considered. Case

Reports should not exceed 3,000 words in length (excluding references).

News articles should report the latest events in health sciences and medical research from around the world. News should not exceed 500 words in length.

Letters should present considered opinions in response to articles published in Drug Discoveries & Therapeutics in the last 6 months or issues of general interest. Letters should not exceed 800 words in length and may contain a maximum of 10 references.

3. Editorial Policies

Ethics: Drug Discoveries & Therapeutics requires that authors of reports of investigations in humans or animals indicate that those studies were formally approved by a relevant ethics committee or review board.

Conflict of Interest: All authors are required to disclose any actual or potential conflict of interest including financial interests or relationships with other people or organizations that might raise questions of bias in the work reported. If no conflict of interest exists for each author, please state "There is no conflict of interest to disclose".

Submission Declaration: When a manuscript is considered for submission to Drug Discoveries & Therapeutics, the authors should confirm that 1) no part of this manuscript is currently under consideration for publication elsewhere; 2) this manuscript does not contain the same information in whole or in part as manuscripts that have been published, accepted, or are under review elsewhere, except in the form of an abstract, a letter to the editor, or part of a published lecture or academic thesis; 3) authorization for publication has been obtained from the authors' employer or institution; and 4) all contributing authors have agreed to submit this manuscript.

Cover Letter: The manuscript must be accompanied by a cover letter signed by the corresponding author on behalf of all authors. The letter should indicate the basic findings of the work and their significance. The letter should also include a statement affirming that all authors concur with the submission and that the material submitted for publication has not been published previously or is not under consideration for publication elsewhere. The cover letter should be submitted in PDF format. For example of Cover Letter, please visit <http://www.ddtjournal.com/downloadcentre.php> (Download Centre).

Copyright: A signed JOURNAL PUBLISHING AGREEMENT (JPA) must be provided by post, fax, or as a scanned file before acceptance of the article. Only forms with a hand-written signature are accepted. This copyright will ensure the widest possible dissemination of information. A form facilitating transfer of copyright can be downloaded by clicking the appropriate link and can be returned to the e-mail address or fax number noted on the form (Please visit

Download Centre). Please note that your manuscript will not proceed to the next step in publication until the JPA form is received. In addition, if excerpts from other copyrighted works are included, the author(s) must obtain written permission from the copyright owners and credit the source(s) in the article.

Suggested Reviewers: A list of up to 3 reviewers who are qualified to assess the scientific merit of the study is welcomed. Reviewer information including names, affiliations, addresses, and e-mail should be provided at the same time the manuscript is submitted online. Please do not suggest reviewers with known conflicts of interest, including participants or anyone with a stake in the proposed research; anyone from the same institution; former students, advisors, or research collaborators (within the last three years); or close personal contacts. Please note that the Editor-in-Chief may accept one or more of the proposed reviewers or may request a review by other qualified persons.

Language Editing: Manuscripts prepared by authors whose native language is not English should have their work proofread by a native English speaker before submission. If not, this might delay the publication of your manuscript in Drug Discoveries & Therapeutics.

The Editing Support Organization can provide English proofreading, Japanese-English translation, and Chinese-English translation services to authors who want to publish in Drug Discoveries & Therapeutics and need assistance before submitting a manuscript. Authors can visit this organization directly at <http://www.iacmhr.com/iac-eso/support.php?lang=en>. IAC-ESO was established to facilitate manuscript preparation by researchers whose native language is not English and to help edit works intended for international academic journals.

4. Manuscript Preparation

Manuscripts should be written in clear, grammatically correct English and submitted as a Microsoft Word file in a single-column format. Manuscripts must be paginated and typed in 12-point Times New Roman font with 24-point line spacing. Please do not embed figures in the text. Abbreviations should be used as little as possible and should be explained at first mention unless the term is a well-known abbreviation (*e.g.* DNA). Single words should not be abbreviated.

Title page: The title page must include 1) the title of the paper (Please note the title should be short, informative, and contain the major key words); 2) full name(s) and affiliation(s) of the author(s); 3) abbreviated names of the author(s); 4) full name, mailing address, telephone/fax numbers, and e-mail address of the corresponding author; and 5) conflicts of interest (if you have an actual or potential conflict of interest to disclose, it must be included as a footnote on the title page of the manuscript; if no conflict of interest exists for each author, please state "There is no conflict of interest to disclose"). Please visit [Download Centre](#) and refer to the title page of the manuscript sample.

Abstract: A one-paragraph abstract consisting of no more than 250 words must be included. The abstract should briefly state the purpose of the study, methods, main findings, and conclusions. Abbreviations must be kept to a minimum and non-standard abbreviations explained in brackets at first mention. References should be avoided in the abstract. Key words or phrases that do not occur in the title should be included in the Abstract page.

Introduction: The introduction should be a concise statement of the basis for the study and its scientific context.

Materials and Methods: The description should be brief but with sufficient detail to enable others to reproduce the experiments. Procedures that have been published previously should not be described in detail but appropriate references should simply be cited. Only new and significant modifications of previously published procedures require complete description. Names of products and manufacturers with their locations (city and state/country) should be given and sources of animals and cell lines should always be indicated. All clinical investigations must have been conducted in accordance with Declaration of Helsinki principles. All human and animal studies must have been approved by the appropriate institutional review board(s) and a specific declaration of approval must be made within this section.

Results: The description of the experimental results should be succinct but in sufficient detail to allow the experiments to be analyzed and interpreted by an independent reader. If necessary, subheadings may be used for an orderly presentation. All figures and tables must be referred to in the text.

Discussion: The data should be interpreted concisely without repeating material already presented in the Results section. Speculation is permissible, but it must be well-founded, and discussion of the wider implications of the findings is encouraged. Conclusions derived from the study should be included in this section.

Acknowledgments: All funding sources should be credited in the Acknowledgments section. In addition, people who contributed to the work but who do not meet the criteria for authors should be listed along with their contributions.

References: References should be numbered in the order in which they appear in the text. Citing of unpublished results, personal communications, conference abstracts, and theses in the reference list is not recommended but these sources may be mentioned in the text. In the reference list, cite the names of all authors when there are fifteen or fewer authors; if there are sixteen or more authors, list the first three followed by *et al.* Names of journals should be abbreviated in the style used in PubMed. Authors are responsible for the accuracy of the references. Examples are given below:

Example 1 (Sample journal reference):
Nakata M, Tang W. Japan-China Joint Medical Workshop on Drug Discoveries and Therapeutics 2008: The need of Asian pharmaceutical researchers' cooperation. *Drug Discov Ther.* 2008; 2:262-263.

Example 2 (Sample journal reference with more than 15 authors):
Darby S, Hill D, Auvinen A, *et al.* Radon in homes and risk of lung cancer: Collaborative analysis of individual data from 13 European case-control studies. *BMJ.* 2005; 330:223.

Example 3 (Sample book reference):
Shalev AY. Post-traumatic stress disorder: diagnosis, history and life course. In: *Post-traumatic Stress Disorder, Diagnosis, Management and Treatment* (Nutt DJ, Davidson JR, Zohar J, eds.). Martin Dunitz, London, UK, 2000; pp. 1-15.

Example 4 (Sample web page reference):
World Health Organization. The World Health Report 2008 – primary health care: Now more than ever. http://www.who.int/whr/2008/whr08_en.pdf (accessed September 23, 2010).

Tables: All tables should be prepared in Microsoft Word or Excel and should be arranged at the end of the manuscript after the References section. Please note that tables should not be in image format. All tables should have a concise title and should be numbered consecutively with Arabic numerals. If necessary, additional information should be given below the table.

Figure Legend: The figure legend should be typed on a separate page of the main manuscript and should include a short title and explanation. The legend should be concise but comprehensive and should be understood without referring to the text. Symbols used in figures must be explained.

Figure Preparation: All figures should be clear and cited in numerical order in the text. Figures must fit a one- or two-column format on the journal page: 8.3 cm (3.3 in.) wide for a single column, 17.3 cm (6.8 in.) wide for a double column; maximum height: 24.0 cm (9.5 in.). Please make sure that artwork files are in an acceptable format (TIFF or JPEG) at minimum resolution (600 dpi for illustrations, graphs, and annotated artwork, and 300 dpi for micrographs and photographs). Please provide all figures as separate files. Please note that low-resolution images are one of the leading causes of article resubmission and schedule delays. All color figures will be reproduced in full color in the online edition of the journal at no cost to authors.

Units and Symbols: Units and symbols conforming to the International System of Units (SI) should be used for physicochemical quantities. Solidus notation (*e.g.* mg/kg, mg/mL, mol/mm²/min) should be used. Please refer to the SI Guide www.bipm.org/en/si/ for standard units.

Supplemental data: Supplemental data might be useful for supporting and enhancing your scientific research and

Drug Discoveries & Therapeutics accepts the submission of these materials which will be only published online alongside the electronic version of your article. Supplemental files (figures, tables, and other text materials) should be prepared according to the above guidelines, numbered in Arabic numerals (*e.g.*, Figure S1, Figure S2, and Table S1, Table S2) and referred to in the text. All figures and tables should have titles and legends. All figure legends, tables and supplemental text materials should be placed at the end of the paper. Please note all of these supplemental data should be provided at the time of initial submission and note that the editors reserve the right to limit the size and length of Supplemental Data.

5. Submission Checklist

The Submission Checklist will be useful during the final checking of a manuscript prior to sending it to Drug Discoveries & Therapeutics for review. Please visit [Download Centre](#) and download the Submission Checklist file.

6. Online submission

Manuscripts should be submitted to Drug Discoveries & Therapeutics online at <http://www.ddtjournal.com>. The manuscript file should be smaller than 5 MB in size. If for any reason you are unable to submit a file online, please contact the Editorial Office by e-mail at office@ddtjournal.com

7. Accepted manuscripts

Proofs: Galley proofs in PDF format will be sent to the corresponding author *via* e-mail. Corrections must be returned to the editor (proof-editing@ddtjournal.com) within 3 working days.

Offprints: Authors will be provided with electronic offprints of their article. Paper offprints can be ordered at prices quoted on the order form that accompanies the proofs.

Page Charge: A page charge of \$140 will be assessed for each printed page of an accepted manuscript. The charge for printing color figures is \$340 for each page. The total charge may be reduced or waived in accordance with conditions in the country where the study took place.

(Revised February 2011)

Editorial and Head Office:

Pearl City Koishikawa 603
2-4-5 Kasuga, Bunkyo-ku
Tokyo 112-0003
Japan
Tel: +81-3-5840-9697
Fax: +81-3-5840-9698
E-mail: office@ddtjournal.com

JOURNAL PUBLISHING AGREEMENT (JPA)

Manuscript No:

Title:

Corresponding author:

The International Advancement Center for Medicine & Health Research Co., Ltd. (IACMHR Co., Ltd.) is pleased to accept the above article for publication in Drug Discoveries & Therapeutics. The International Research and Cooperation Association for Bio & Socio-Sciences Advancement (IRCA-BSSA) reserves all rights to the published article. Your written acceptance of this JOURNAL PUBLISHING AGREEMENT is required before the article can be published. Please read this form carefully and sign it if you agree to its terms. The signed JOURNAL PUBLISHING AGREEMENT should be sent to the Drug Discoveries & Therapeutics office (Pearl City Koishikawa 603, 2-4-5 Kasuga, Bunkyo-ku, Tokyo 112-0003, Japan; E-mail: office@ddtjournal.com; Tel: +81-3-5840-9697; Fax: +81-3-5840-9698).

1. Authorship Criteria

As the corresponding author, I certify on behalf of all of the authors that:

- 1) The article is an original work and does not involve fraud, fabrication, or plagiarism.
- 2) The article has not been published previously and is not currently under consideration for publication elsewhere. If accepted by Drug Discoveries & Therapeutics, the article will not be submitted for publication to any other journal.
- 3) The article contains no libelous or other unlawful statements and does not contain any materials that infringes upon individual privacy or proprietary rights or any statutory copyright.
- 4) I have obtained written permission from copyright owners for any excerpts from copyrighted works that are included and have credited the sources in my article.
- 5) All authors have made significant contributions to the study including the conception and design of this work, the analysis of the data, and the writing of the manuscript.
- 6) All authors have reviewed this manuscript and take responsibility for its content and approve its publication.
- 7) I have informed all of the authors of the terms of this publishing agreement and I am signing on their behalf as their agent.

2. Copyright Transfer Agreement

I hereby assign and transfer to IACMHR Co., Ltd. all exclusive rights of copyright ownership to the above work in the journal Drug Discoveries & Therapeutics, including but not limited to the right 1) to publish, republish, derivate, distribute, transmit, sell, and otherwise use the work and other related material worldwide, in whole or in part, in all languages, in electronic, printed, or any other forms of media now known or hereafter developed and the right 2) to authorize or license third parties to do any of the above.

I understand that these exclusive rights will become the property of IACMHR Co., Ltd., from the date the article is accepted for publication in the journal Drug Discoveries & Therapeutics. I also understand that IACMHR Co., Ltd. as a copyright owner has sole authority to license and permit reproductions of the article.

I understand that except for copyright, other proprietary rights related to the Work (e.g. patent or other rights to any process or procedure) shall be retained by the authors. To reproduce any text, figures, tables, or illustrations from this Work in future works of their own, the authors must obtain written permission from IACMHR Co., Ltd.; such permission cannot be unreasonably withheld by IACMHR Co., Ltd.

3. Conflict of Interest Disclosure

I confirm that all funding sources supporting the work and all institutions or people who contributed to the work but who do not meet the criteria for authors are acknowledged. I also confirm that all commercial affiliations, stock ownership, equity interests, or patent-licensing arrangements that could be considered to pose a financial conflict of interest in connection with the article have been disclosed.

Corresponding Author's Name (Signature):

Date:

